

---

Theses and Dissertations

---

Spring 2016

# Hydroxylated and sulfated metabolites of lower chlorinated PCBs bind with high affinity to human serum albumin and exhibit selective toxicity to neuronal cells

Eric Alberto Rodriguez  
*University of Iowa*

Copyright 2016 Eric Alberto Rodriguez

This dissertation is available at Iowa Research Online: <http://ir.uiowa.edu/etd/3175>

---

## Recommended Citation

Rodriguez, Eric Alberto. "Hydroxylated and sulfated metabolites of lower chlorinated PCBs bind with high affinity to human serum albumin and exhibit selective toxicity to neuronal cells." PhD (Doctor of Philosophy) thesis, University of Iowa, 2016.  
<http://ir.uiowa.edu/etd/3175>.

---

Follow this and additional works at: <http://ir.uiowa.edu/etd>

 Part of the [Pharmacy and Pharmaceutical Sciences Commons](#)

Hydroxylated and Sulfated Metabolites of Lower Chlorinated PCBs Bind with High Affinity to Human Serum Albumin and Exhibit Selective Toxicity to Neuronal Cells

by

Eric Alberto Rodriguez

A thesis submitted in partial fulfillment  
of the requirements for the Doctor of  
Philosophy degree in Pharmacy (Medicinal & Natural Products Chemistry)  
in the Graduate College of  
The University of Iowa

May 2016

Thesis Supervisor: Professor Michael W. Duffel

Graduate College  
The University of Iowa  
Iowa City, Iowa

CERTIFICATE OF APPROVAL

---

PH.D. THESIS

---

This is to certify that the Ph.D. thesis of

Eric Alberto Rodriguez

has been approved by the Examining Committee  
for the thesis requirement for the Doctor of Philosophy  
degree in Pharmacy (Medicinal & Natural Products Chemistry)  
at the May 2016 graduation.

Thesis Committee: \_\_\_\_\_  
Michael W. Duffel, Thesis Supervisor

\_\_\_\_\_  
Robert J. Kerns

\_\_\_\_\_  
Jonathan A. Doorn

\_\_\_\_\_  
David L. Roman

\_\_\_\_\_  
Larry W. Robertson

For my mother

DON'T PANIC

-Douglas Adams

The Hitchhiker's Guide to the Galaxy

## ACKNOWLEDGMENTS

I would like to acknowledge the people in my life that have contributed to the successful completion and realization of this thesis, which without their support might not have come to fruition.

I would first like to acknowledge and thank my graduate advisor Michael W. Duffel for the rigorous training I received under his tutelage. Thank you for your patience and support throughout my time in your lab. I have learned a great deal from you about science, and integrity, and being a good, fair, and just person. I hope to represent you well in my professional and scientific endeavors.

To my dissertation committee, Drs. Michael Duffel, Jonathan Doorn, Robert Kerns, David Roman, and Larry Robertson, I would like to extend my gratitude for their support in the completion of my thesis. I am grateful for your insights and the many things I have learned from all of you, both inside and outside of the classroom setting. I would also like to acknowledge the collaborative works that have come out of my relationships with Dr. Doorn, and Dr. Robertson, both of which have contributed to my burgeoning publication record!

My time spent at the University of Iowa and in Iowa City was made much easier, and a bit more fun and exciting because of the people that I was lucky to meet here. In particular, my very good and dear friends, Ioana Cracium and Brigitte Vanle have been such a luxury in my life. Thank you both so much for being there for me and feigning amusement at my hacky jokes and ridiculousness, you both have made me feel loved and important. I hope that we can all remain friends until we're too old to remember why this all even started.

To my boyfriend, Justin De Guzman, I thank you for standing next to me these past six years and never faltering when I needed you. You have made my life much easier and much more enjoyable in our time spent together. Thank you for putting up

with my wild moods and neurotic ways and for always making me laugh, I love you very much.

I also extend my gratitude to my friends and family who have always been there to support me. My support system has been vital to me and I thank my dad Tomas, my aunt and uncles, my cousins, Adriana, Tomas Jr., and my best-friend Carlos! I hope to be able to extend the same sentiments to you all throughout my life. I would like to especially acknowledge my Grandma Maria Elena and my Tio Rafa and Tia Terry. Thank you so much for the love you've shown to me and for your constant concern about my well-being and the realization of my goals. I would also like to acknowledge my brother Ismael and my sister Isela who have come up directly beside me from the desert mounds of Polvoron, El Paso, Texas. You are both great life-companions and I am so happy to be tethered to you. I hope that these small accomplishments can show the babies Eva, Iris, Lucas, and Angel that it is okay (and necessary) to extend yourself beyond from where you think you belong.

Finally I would like to thank the most important people in my life, my mother Lorena Garcia and my grandmother Berta Cerros. I was given a decent start to this life and it is because of both of you and your dedication. Thank you for encouraging me to read and think, dance, sing, crochet, laugh and make jokes. My accomplishments are possible because of the hard work throughout both of your lives and I love you very much.

Thank you all!

## PUBLIC ABSTRACT

The harmful effects that polychlorinated biphenyls (PCBs) exert on biological and environmental systems is a great concern for our planet. Exposure to these agents has been associated with various human disorders and diseases, some of which involve the development and function of the brain. Although overall PCB levels have decreased worldwide in the last few decades, PCBs with lower numbers of chlorine atoms (LC-PCBs) have garnered increasing interest due to their prevalence in indoor and outdoor air. These types of PCBs undergo metabolic changes in the body, and one metabolic pathway results in the formation of hydroxylated and sulfated derivatives. A sulfate group may make the PCB more readily excreted, but it may also enable its transport to tissues through binding to the most abundant protein in serum, human serum albumin (HSA). The binding of LC-PCBs and hydroxylated (OH-LC-PCBs) and sulfated metabolites to HSA is reported here. It was found that generally, PCB sulfates bound to HSA with a comparable or higher affinity than the LC-PCBs or the OH-LC-PCBs. Furthermore, the neurotoxic activity of these metabolites was assessed by measuring their effect on cell viability in neuronal cells and comparing the results to hepatic cells. OH-LC-PCBs were more toxic to the former than the latter, and one PCB sulfate exhibited toxicity similar to the OH-LC-PCBs. The studies reported in this thesis contribute to further understanding the neurotoxicity of LC-PCB and hydroxylated and sulfated metabolites, and the role that binding to serum proteins may play in it.



## ABSTRACT

Polychlorinated biphenyls (PCBs) are a class of persistent organic pollutants that have been associated with a myriad of negative human health effects. These man-made compounds were used throughout most of the 20<sup>th</sup> century and although their intentional production has since been banned and their use limited to closed systems, their prevalence in the environment remains a factor in disease states for exposed populations. The worldwide levels of PCBs has been declining, however, there is evidence for renewed sources of these compounds. The presence of PCBs have been verified as unintentional byproducts in paints and pigments, the decomposition of PCB waste, or the recycling or disposal attempts of PCB-laden materials. While exposure to the higher chlorinated congeners (>4 chlorine atoms, HC-PCBs) is often attributed to the consumption of contaminated water or fatty animal meat, a significant route of exposure to airborne lower chlorinated congeners ( $\leq 4$  chlorine atoms, LC-PCBs) is through inhalation. These semi-volatile compounds have been detected in high quantities in both indoor and outdoor air in urban and rural communities, and their presence is pronounced in older buildings (e.g., homes and schools). When compared to HC-PCBs, LC-PCBs are more highly susceptible to metabolic transformations, and recently their sulfated metabolites have gained much interest. Although the sulfation of xenobiotics often is considered a route for their removal from the body, a previous study of Sprague-Dawley rats treated with 4-chlorobiphenyl (PCB 3) resulted in the substantial formation of sulfated metabolites (i.e., hydroxylation followed by sulfation of the LC-PCB). This metabolic route accounted for more than half of the treatment dose. Furthermore, LC-PCB sulfates have been shown to bind to the human serum protein, transthyretin, *in vitro*.

Of the health effects associated with PCB exposure, neurotoxicity has been well established through various laboratory and epidemiological studies. It is proposed that the dopaminergic system lies at the core of the observed cognitive, motor, and intellectual

dysfunction observed in exposed populations, especially in children exposed perinatally. Interestingly, PCB exposure has been linked to Parkinson's disease (PD) etiology, which is marked by a substantial loss of dopaminergic neurons.

This thesis describes studies on the binding of selected LC-PCBs and their hydroxylated and sulfated metabolites to human serum albumin (HSA), the most abundant protein in human serum. The displacement of fluorescent probes, selective for the two major drug binding sites of HSA, indicated that LC-PCB sulfates generally bound to HSA with such affinity that is equal to or greater than that for the LC-PCBs or OH-LC-PCBs. This work also included a study of the selective toxicity of these compounds to dopaminergic neuronal cells. The selective toxicity of these compounds was studied in a series of immortalized cell lines (i.e., two neuronal cell lines: the rat midbrain-derived N27 cell line, the human neuroblastoma-derived SH-SY5Y cell line, and the human liver-derived HepG2 cell line). The assessment of toxicity by MTT reduction and LDH release in these cellular models indicated that hydroxylated and sulfated metabolites of LC-PCBs exhibited toxicity that was selective to neuronal cells and, in most cases, selective for the dopaminergic neuronal cells. Furthermore, HPLC analysis of the distribution of the compounds from the extracellular medium into the cellular milieu indicated that the observed toxicity may be due in some cases to selective transport and further metabolism. This work contributes to understanding the neurotoxicity of LC-PCB hydroxylated and sulfated metabolites and the role that binding to serum proteins may play in it. Furthermore, it emphasizes the need for future studies on the effects that metabolism, particularly sulfation, may play in the disposition of LC-PCB congeners as it pertains to their metabolism, retention, and toxic effects.

## TABLE OF CONTENTS

LIST OF TABLES .....	xi
LIST OF FIGURES .....	xii
LIST OF ABBREVIATIONS.....	xxi
CHAPTER 1: INTRODUCTION.....	1
Polychlorinated Biphenyls (PCBs).....	1
Background.....	1
Environmental distribution of PCBs .....	2
PCBs and human health.....	5
Lower Chlorinated PCBs (LC-PCBs).....	7
Airborne PCBs.....	7
Metabolism of LC-PCBs .....	9
PCB sulfates .....	11
Human Serum Albumin (HSA).....	11
Synthesis, distribution, and function .....	11
Binding to HSA .....	13
Neurotoxic effects of PCB exposure .....	15
Epidemiological studies.....	15
In vitro and in vivo studies .....	16
Dopaminergic system as a target for PCB induced toxicity.....	16
CHAPTER 2: STATEMENT OF THE PROBLEM.....	19
CHAPTER 3: THE BINDING OF LC-PCB METABOLITES TO HSA .....	23
HSA properties .....	23
HSA binding sites.....	24
Binding assays .....	25
PCB-HSA binding .....	26
Approach.....	28
Results and discussion .....	28
Displacement of probes from HSA by PCBs, OH-PCBs, and PCB Sulfates .....	28
Recovery of PCB sulfates following incubation with HSA .....	32
Binding of the monochlorinated PCB 3 and its hydroxylated and sulfated metabolites to HSA.....	33
Binding of dichlorinated PCB congeners and their metabolites to HSA .....	35
Binding of tri-, tetra-, and penta- PCB congeners and their metabolites to HSA.....	36
Discussion and conclusions .....	37
CHAPTER 4: THE NEUROTOXICITY OF LC-PCB METABOLITES.....	40
Persistent organic pollutants and neurotoxicity.....	40
PCBs and neurotoxicity .....	41
The dopaminergic system as a target for PCB induced neurotoxicity.....	41
PCBs and Parkinson's disease.....	42
PCB metabolites and neurotoxicity .....	43
Neuronal cellular models.....	44

N27 cells.....	44
SH-SY5Y cells .....	45
HepG2 cells .....	45
Determining cell viability.....	46
Approach.....	46
Results and discussion .....	48
Cell viability by MTT reduction - results.....	48
Cell viability by LDH release - results .....	54
The effects of serum on neurotoxicity - results .....	60
Intracellular and extracellular distribution of OH-LC-PCBs and LC-PCB sulfates .....	62
Conclusions.....	72
CHAPTER 5: CONCLUSIONS .....	75
CHAPTER 6: MATERIALS AND METHODS .....	79
HSA binding experiments.....	79
Materials .....	79
Human Serum Albumin (HSA) binding assay .....	79
HPLC analysis of recovery and reversibility in the binding of PCB sulfates to HSA.....	80
Neurotoxicity experiments.....	81
Materials .....	81
Cell lines and culture conditions .....	82
Neurotoxicity studies .....	83
APPENDIX.....	87
REFERENCES .....	120

## LIST OF TABLES

Table 4-1 A comparison of MTT-reduction $EC_{50}$ values across three cell lines (N27, SH-SY5Y, HepG2) after exposure to LC-PCBs or their hydroxylated or sulfated metabolites in serum free media for 24h.....	54
Table 4-2 A comparison of LDH-release $EC_{50}$ values across three cell lines (N27, SH-SY5Y, HepG2) after exposure to LC-PCBs or their hydroxylated or sulfated metabolites in serum free media for 24h.....	60

## LIST OF FIGURES

Figure 1-1 A comparison of PCB congeners: Three major nomenclature types and <i>ortho</i> - substituent designations. ....	3
Figure 1-2 A crystal structure of HSA highlighting its fatty acid, heme, and major drug binding sites. Binding sites were elucidated by the analysis of HSA-ligand and/or fatty acid complexes. <sup>148</sup> The HSA crystal structure (PDB ID: IUOR) was modified using the PyMOL Molecular Graphics System, Version 1.7.4 Schrödinger, LLC. ....	14
Figure 3-1 HSA crystal structure indicating domains and subdomains, residues that form sites I and II, and site-selective fluorescent probes and ligands. Domains and subdomains (reds: Ia, Ib; blues: IIa, IIb; greys: IIIa, IIIb) are shown, including residues that surround sites I and II <sup>205</sup> which are highlighted in dotted spheres. Site selective fluorescent probes and positive control ligands for each site are also annotated. The HSA crystal structure (PDB ID: IUOR) was modified using the PyMOL Molecular Graphics System, Version 1.7.4 Schrödinger, LLC. ....	24
Figure 3-2 Binding curves for compounds that exhibited binding to Site I as determined by site-selective fluorescent probe displacement. Plots are of percent of control fluorescence vs. increasing ligand concentration. Each experiment consists of 10µM HSA and 20µM DNSA. Data were fit to a sigmoidal dose response ligand-binding algorithm (SigmaPlot v.11.0, Systat Software, Chicago, IL) and EC <sub>50</sub> values are reported in Figure 3-7. Mean ± SE, n=3. ....	30
Figure 3-3 Binding curves for compounds that exhibited binding to Site II as determined by site-selective fluorescent probe displacement. Plots are of percent of control fluorescence vs. increasing ligand concentration. Each experiment consists of 10µM HSA and 5µM DP. Data were fit to a sigmoidal dose response ligand-binding algorithm (SigmaPlot v.11.0, Systat Software, Chicago, IL) and EC <sub>50</sub> values are reported in Figure 3-7. Mean ± SE, n=3. ....	30
Figure 3-4 Binding curves for compounds that did not exhibited binding to Site I as determined by site-selective fluorescent probe displacement. Plots are of percent of control fluorescence vs. increasing ligand concentration. Each experiment consists of 10µM HSA and 20µM DNSA. Data were fit to a sigmoidal dose response ligand-binding algorithm (SigmaPlot v.11.0, Systat Software, Chicago, IL) and EC <sub>50</sub> values are reported in Figure 3-7. Mean ± SE, n=3. ....	31
Figure 3-5 Binding curves for compounds that did not exhibited binding to Site II as determined by site-selective fluorescent probe displacement. Plots are of percent of control fluorescence vs. increasing ligand concentration. Each experiment consists of 10µM HSA and 5µM DP. Data were fit to a sigmoidal dose response ligand-binding algorithm (SigmaPlot v.11.0, Systat Software, Chicago, IL) and EC <sub>50</sub> values are reported in Figure 3-7. Mean ± SE, n=3. ....	32
Figure 3-6 HPLC analysis of the recovery and reversibility of HSA-binding for representative PCB sulfates. HSA (50µM) and LC-PCB sulfate (50µM)	

incubated in potassium phosphate buffer (pH=7.4) and extracted into acetonitrile and analyzed by HPLC. Data points are presented as Mean $\pm$ SE, n=3. ....	33
Figure 3-7 HSA-binding of the monochlorinated PCB 3 and its hydroxylated and sulfated metabolites. Site I binding (DNSA displacement) is shown at the left of the graph and Site II binding (DP displacement) is shown at the right. Color coding is used to differentiate the PCBs (black), OH-PCBs (blue), and PCB sulfates (red). Compound names appear on the left of the graph and the corresponding structure is at the right. EC <sub>50</sub> values were obtained as described in Materials and Methods and reported as Mean $\pm$ SE, n=3. The vertical dashed lines indicate the EC <sub>50</sub> values for the positive control ligands at each site. ....	35
Figure 3-8 HSA-binding of dichlorinated PCB congeners and their hydroxylated and sulfated metabolites. Site I binding (DNSA displacement) is shown at the left of the graph and Site II binding (DP displacement) is shown at the right. Color coding is used to differentiate the PCBs (black), OH-PCBs (blue), and PCB sulfates (red). Compound names appear on the left of the graph and the corresponding structure is at the right. EC <sub>50</sub> values were obtained as described in Materials and Methods and reported as Mean $\pm$ SE, n=3. The vertical dashed lines indicate the EC <sub>50</sub> values for the positive control ligands at each site. ....	36
Figure 3-9 HSA-binding of tri-, tetra-, and penta- PCB congeners and their hydroxylated and sulfated metabolites. Site I binding (DNSA displacement) is shown at the left of the graph and Site II binding (DP displacement) is shown at the right. Color coding is used to differentiate the PCBs (black), OH-PCBs (blue), and PCB sulfates (red). Compound names appear on the left of the graph and the corresponding structure is at the right. EC <sub>50</sub> values were obtained as described in Materials and Methods and reported as Mean $\pm$ SE, n=3. The vertical dashed lines indicate EC <sub>50</sub> values for the positive control ligands at each site. ....	37
Figure 4-1 A representation of the compounds (PCBs, OH-PCBs, PCB sulfates) used in the neurotoxicity studies. The parent PCBs are among the 20 most frequently detected congeners in Chicago air samples. All authentic standards were prepared and characterized in the synthesis core of the Iowa Superfund Research Program. <sup>256-258</sup> .....	48
Figure 4-2 The cell viability of N27, SH-SY5Y, and HepG2 cells after exposure to LC-PCBs in serum free media for 24h assessed by MTT reduction. The data were represented as a percent of vehicle control vs. the log of the LC-PCB concentration, and fit to a four parameter logistic curve using SigmaPlot v.11.0, Systat Software, Chicago, IL. Data points are the mean $\pm$ SEM, n=3. ....	50
Figure 4-3 The cell viability of N27, SH-SY5Y, and HepG2 cells after exposure to OH-LC-PCBs in serum free media for 24h assessed by MTT reduction. The data were represented as a percent of vehicle control vs. the log of the OH-LC-PCB concentration, and fit to a four parameter logistic curve using SigmaPlot v.11.0, Systat Software, Chicago, IL. Data points are the mean $\pm$ SEM, n=3. ....	51

Figure 4-4 The cell viability of N27, SH-SY5Y, and HepG2 cells after exposure to LC-PCB sulfates in serum free media for 24h assessed by MTT reduction. The data were represented as a percent of vehicle control vs. the log of the LC-PCB sulfate concentration, and fit to a four parameter logistic curve using SigmaPlot v.11.0, Systat Software, Chicago, IL. Data points are the mean $\pm$ SEM, n=3.....	53
Figure 4-5 The cell viability of N27, SH-SY5Y, and HepG2 cells after exposure to LC-PCBs in serum free media for 24h as assessed by LDH release. The data were represented as a percent of vehicle control vs. the log of the LC-PCB concentration, and fit to a four parameter logistic curve using SigmaPlot v.11.0, Systat Software, Chicago, IL. Data points are the mean $\pm$ SEM, n=3.....	57
Figure 4-6 The cell viability of N27, SH-SY5Y, and HepG2 cells after exposure to OH-LC-PCBs in serum free media for 24h as assessed by LDH release. The data were represented as a percent of vehicle control vs. the log of the OH-LC-PCB concentration, and fit to a four parameter logistic curve using SigmaPlot v.11.0, Systat Software, Chicago, IL. Data points are the mean $\pm$ SEM, n=3.....	58
Figure 4-7 The cell viability of N27, SH-SY5Y, and HepG2 cells after exposure to LC-PCB sulfates in serum free media for 24h as assessed by LDH release. The data were represented as a percent of vehicle control vs. the log of the LC-PCB sulfate concentration, and fit to a four parameter logistic curve using SigmaPlot v.11.0, Systat Software, Chicago, IL. Data points are the mean $\pm$ SEM, n=3.....	59
Figure 4-8 The presence of human serum albumin (HSA) or horse serum (HS) supplementation in cell media mitigates the cytotoxic effects of both 4-OH-PCB 52, and 4-PCB 52 sulfate in N27 cells. N27 cells treated with 25 $\mu$ M PCB metabolite were co-incubated with increasing amounts of HSA or horse serum. Data are reported as the percent of control cell viability by MTT analysis. n=3, (* P<0.001 of control). .....	62
Figure 4-9 The distribution of OH-LC-PCBs and LC-PCB sulfates of non- <i>ortho</i> -substituted PCBs 3 and 11 in N27 cells as determined by HPLC analysis. Cells were treated with 25 $\mu$ M (2.5nmol) compound for 24h, and subjected to analysis of the extracellular media and intracellular contents. The treatment compound is annotated with an arrow. The values shown are the means $\pm$ SE, n=3. ....	64
Figure 4-10 The distribution of OH-LC-PCBs and LC-PCB sulfates of <i>ortho</i> -substituted PCBs 8 and 52 in N27 cells as determined by HPLC analysis. Cells were treated with 25 $\mu$ M (2.5nmol) compound for 24h, and subjected to analysis of the extracellular media and intracellular contents. The treatment compound is annotated with an arrow. The values shown are the means $\pm$ SE, n=3. ....	66
Figure 4-11 The distribution of OH-LC-PCBs and LC-PCB sulfates of non- <i>ortho</i> -substituted PCBs 3 and 11 in SH-SY5Y cells as determined by HPLC analysis. Cells were treated with 25 $\mu$ M (2.5nmol) compound for 24h, and subjected to analysis of the extracellular media and intracellular contents. The treatment compound is annotated with an arrow. The values shown are the means $\pm$ SE, n=3. ....	67



Figure 4-12 The distribution of OH-LC-PCBs and LC-PCB sulfates of <i>ortho</i> -substituted PCBs 8 and 52 in SH-SY5Y cells as determined by HPLC analysis. Cells were treated with 25 $\mu$ M (2.5nmol) compound for 24h, and subjected to analysis of the extracellular media and intracellular contents. The treatment compound is annotated with an arrow. The values shown are the means $\pm$ SE, n=3. ....	69
Figure 4-13 The distribution of OH-LC-PCBs and LC-PCB sulfates of non- <i>ortho</i> -substituted PCBs 3 and 11 in HepG2 cells as determined by HPLC analysis. Cells were treated with 25 $\mu$ M (2.5nmol) compound for 24h, and subjected to analysis of the extracellular media and intracellular contents. The treatment compound is annotated with an arrow. The values shown are the means $\pm$ SE, n=3. ....	70
Figure 4-14 The distribution of OH-LC-PCBs and LC-PCB sulfates of <i>ortho</i> -substituted PCBs 8 and 52 in HepG2 cells as determined by HPLC analysis. Cells were treated with 25 $\mu$ M (2.5nmol) compound for 24h, and subjected to analysis of the extracellular media and intracellular contents. The treatment compound is annotated with an arrow. The values shown are the means $\pm$ SE, n=3. ....	71
Figure A-1 Site I binding curves of monochlorinated LC-PCBs, OH-LC-PCBs, and LC-PCB sulfates plotted as percent of control fluorescence vs. increasing ligand concentration. A) ligands exhibiting dose dependent displacement of the fluorescent probe. B) ligands not exhibiting dose-dependent displacement of the fluorescent probe. Each experiment consists of 10 $\mu$ M HSA and 20 $\mu$ M DNSA. Data were fit to a sigmoidal dose response ligand-binding algorithm (SigmaPlot v.11.0, Systat Software, Chicago, IL) and EC <sub>50</sub> values are reported in Figure 3-7. Mean $\pm$ SE, n=3. ....	87
Figure A-2 Site II binding curves of LC-PCBs, OH-LC-PCBs, and LC-PCB sulfates plotted as percent of control fluorescence vs. increasing ligand concentration. A) monochlorinated compounds exhibiting dose dependent displacement of the fluorescent probe. B) all ligands not exhibiting dose-dependent displacement of the fluorescent probe from Site II. Each experiment consists of 10 $\mu$ M HSA and 5 $\mu$ M DP. Data were fit to a sigmoidal dose response ligand-binding algorithm (SigmaPlot v.11.0, Systat Software, Chicago, IL) and EC <sub>50</sub> values are reported in Figure 3-7. Mean $\pm$ SE, n=3. ....	88
Figure A-3 Site II binding curves of dichlorinated LC-PCBs, OH-LC-PCBs, and LC-PCB sulfates plotted as percent of control fluorescence vs. increasing ligand concentration. A and B) ligands exhibiting dose dependent displacement of the fluorescent probe. Each experiment consists of 10 $\mu$ M HSA and 5 $\mu$ M DP. Data were fit to a sigmoidal dose response ligand-binding algorithm (SigmaPlot v.11.0, Systat Software, Chicago, IL) and EC <sub>50</sub> values are reported in Figure 3-7. Mean $\pm$ SE, n=3. ....	89
Figure A-4 Site II binding curves of tri-, tetra-, and pentachlorinated LC-PCBs, OH-LC-PCBs, and LC-PCB sulfates plotted as percent of control fluorescence vs. increasing ligand concentration. A and B) ligands exhibiting dose dependent displacement of the fluorescent probe. Each experiment consists of 10 $\mu$ M HSA and 5 $\mu$ M DP. Data were fit to a sigmoidal dose response ligand-binding algorithm (SigmaPlot v.11.0, Systat Software, Chicago, IL) and EC <sub>50</sub> values are reported in Figure 3-7. Mean $\pm$ SE, n=3. ....	90

Figure A-5 Site I binding curves of dichlorinated LC-PCBs, OH-LC-PCBs, and LC-PCB sulfates plotted as percent of control fluorescence vs. increasing ligand concentration. A and B) ligands not exhibiting dose-dependent displacement of the fluorescent probe from Site I. Each experiment consists of 10 $\mu$ M HSA and 20 $\mu$ M DNSA. Data were fit to a sigmoidal dose response ligand-binding algorithm (SigmaPlot v.11.0, Systat Software, Chicago, IL) and EC <sub>50</sub> values are reported in Figure 3-7. Mean $\pm$ SE, n=3. ....	91
Figure A-6 Site I binding curves of tri-, tetra-, and pentachlorinated LC-PCBs, OH-LC-PCBs, and LC-PCB sulfates plotted as percent of control fluorescence vs. increasing ligand concentration. A and B) ligands not exhibiting dose-dependent displacement of the fluorescent probe from Site I. Each experiment consists of 10 $\mu$ M HSA and 20 $\mu$ M DNSA. Data were fit to a sigmoidal dose response ligand-binding algorithm (SigmaPlot v.11.0, Systat Software, Chicago, IL) and EC <sub>50</sub> values are reported in Figure 3-7. Mean $\pm$ SE, n=3. ....	92
Figure A-7 The presence of human serum albumin (HSA) or horse serum (HS) supplementation in cell media mitigates the cytotoxic effects of both 4'-OH-PCB 3, and 4-PCB 3 sulfate in N27 cells. N27 cells treated with 25 $\mu$ M PCB metabolite were co-incubated with increasing amounts of HSA or horse serum. Data are reported as the percent of control cell viability by MTT analysis. n=3, (* P<0.001 of control). ....	93
Figure A-8 The presence of human serum albumin (HSA) or horse serum (HS) supplementation in cell media mitigates the cytotoxic effects of both 4-OH-PCB 8, and 4-PCB 8 sulfate in N27 cells. N27 cells treated with 25 $\mu$ M PCB metabolite were co-incubated with increasing amounts of HSA or horse serum. Data are reported as the percent of control cell viability by MTT analysis. n=3, (* P<0.001 of control). ....	94
Figure A-9 The presence of human serum albumin (HSA) or horse serum (HS) supplementation in cell media mitigates the cytotoxic effects of both 4-OH-PCB 11, and 4-PCB 11 sulfate in N27 cells. N27 cells treated with 25 $\mu$ M PCB metabolite were co-incubated with increasing amounts of HSA or horse serum. Data are reported as the percent of control cell viability by MTT analysis. n=3, (* P<0.001 of control). ....	95
Figure A-10 Overlay of chromatograms from the HPLC analyses of extracellular media and cellular lysate extracts of N27 cells treated with 25 $\mu$ M 4'-OH-PCB 3 for 24 hours. Extracellular extract is represented in the blue dashed line. The lysate extract is represented in the dotted red line. Standards for the LC-PCB, the OH-LC-PCB, and the LC-PCB sulfate are represented in the solid black line. The extraction and HPLC conditions are described in detail in Chapter 6 Materials and Methods.....	96
Figure A-11 Overlay of chromatograms from the HPLC analyses of extracellular media and cellular lysate extracts of N27 cells treated with 25 $\mu$ M 4'-PCB 3 sulfate for 24 hours. Extracellular extract is represented in the blue dashed line. The lysate extract is represented in the dotted red line. Standards for the LC-PCB, the OH-LC-PCB, and the LC-PCB sulfate are represented in the solid black line. The extraction and HPLC conditions are described in detail in Chapter 6 Materials and Methods.....	97

Figure A-12 Overlay of chromatograms from the HPLC analyses of extracellular media and cellular lysate extracts of N27 cells treated with 25µM 4-OH-PCB 8 for 24 hours. Extracellular extract is represented in the blue dashed line. The lysate extract is represented in the dotted red line. Standards for the LC-PCB, the OH-LC-PCB, and the LC-PCB sulfate are represented in the solid black line. The extraction and HPLC conditions are described in detail in Chapter 6 Materials and Methods.....	98
Figure A-13 Overlay of chromatograms from the HPLC analyses of extracellular media and cellular lysate extracts of N27 cells treated with 25µM 4-PCB 8 sulfate for 24 hours. Extracellular extract is represented in the blue dashed line. The lysate extract is represented in the dotted red line. Standards for the LC-PCB, the OH-LC-PCB, and the LC-PCB sulfate are represented in the solid black line. The extraction and HPLC conditions are described in detail in Chapter 6 Materials and Methods.....	99
Figure A-14 Overlay of chromatograms from the HPLC analyses of extracellular media and cellular lysate extracts of N27 cells treated with 25µM 4-OH-PCB 11 for 24 hours. Extracellular extract is represented in the blue dashed line. The lysate extract is represented in the dotted red line. Standards for the LC-PCB, the OH-LC-PCB, and the LC-PCB sulfate are represented in the solid black line. The extraction and HPLC conditions are described in detail in Chapter 6 Materials and Methods.....	100
Figure A-15 Overlay of chromatograms from the HPLC analyses of extracellular media and cellular lysate extracts of N27 cells treated with 25µM 4-PCB 11 sulfate for 24 hours. Extracellular extract is represented in the blue dashed line. The lysate extract is represented in the dotted red line. Standards for the LC-PCB, the OH-LC-PCB, and the LC-PCB sulfate are represented in the solid black line. The extraction and HPLC conditions are described in detail in Chapter 6 Materials and Methods.....	101
Figure A-16 Overlay of chromatograms from the HPLC analyses of extracellular media and cellular lysate extracts of N27 cells treated with 25µM 4-OH-PCB 52 sulfate for 24 hours. Extracellular extract is represented in the blue dashed line. The lysate extract is represented in the dotted red line. Standards for the LC-PCB, the OH-LC-PCB, and the LC-PCB sulfate are represented in the solid black line. The extraction and HPLC conditions are described in detail in Chapter 6 Materials and Methods.....	102
Figure A-17 Overlay of chromatograms from the HPLC analyses of extracellular media and cellular lysate extracts of N27 cells treated with 25µM 4-PCB 52 sulfate for 24 hours. Extracellular extract is represented in the blue dashed line. The lysate extract is represented in the dotted red line. Standards for the LC-PCB, the OH-LC-PCB, and the LC-PCB sulfate are represented in the solid black line. The extraction and HPLC conditions are described in detail in Chapter 6 Materials and Methods.....	103
Figure A-18 Overlay of chromatograms from the HPLC analyses of extracellular media and cellular lysate extracts of SH-SY5Y cells treated with 25µM 4'-OH-PCB 3 for 24 hours. Extracellular extract is represented in the blue dashed line. The lysate extract is represented in the dotted red line. Standards for the LC-PCB, the OH-LC-PCB, and the LC-PCB sulfate are	

represented in the solid black line. The extraction and HPLC conditions are described in detail in Chapter 6 Materials and Methods. ....	104
Figure A-19 Overlay of chromatograms from the HPLC analyses of extracellular media and cellular lysate extracts of SH-SY5Y cells treated with 25µM 4'-PCB 3 sulfate for 24 hours. Extracellular extract is represented in the blue dashed line. The lysate extract is represented in the dotted red line. Standards for the LC-PCB, the OH-LC-PCB, and the LC-PCB sulfate are represented in the solid black line. The extraction and HPLC conditions are described in detail in Chapter 6 Materials and Methods. ....	105
Figure A-20 Overlay of chromatograms from the HPLC analyses of extracellular media and cellular lysate extracts of SH-SY5Y cells treated with 25µM 4-OH-PCB 8 for 24 hours. Extracellular extract is represented in the blue dashed line. The lysate extract is represented in the dotted red line. Standards for the LC-PCB, the OH-LC-PCB, and the LC-PCB sulfate are represented in the solid black line. The extraction and HPLC conditions are described in detail in Chapter 6 Materials and Methods. ....	106
Figure A-21 Overlay of chromatograms from the HPLC analyses of extracellular media and cellular lysate extracts of SH-SY5Y cells treated with 25µM 4-PCB 8 sulfate for 24 hours. Extracellular extract is represented in the blue dashed line. The lysate extract is represented in the dotted red line. Standards for the LC-PCB, the OH-LC-PCB, and the LC-PCB sulfate are represented in the solid black line. The extraction and HPLC conditions are described in detail in Chapter 6 Materials and Methods. ....	107
Figure A-22 Overlay of chromatograms from the HPLC analyses of extracellular media and cellular lysate extracts of SH-SY5Y cells treated with 25µM 4-OH-PCB 11 sulfate for 24 hours. Extracellular extract is represented in the blue dashed line. The lysate extract is represented in the dotted red line. Standards for the LC-PCB, the OH-LC-PCB, and the LC-PCB sulfate are represented in the solid black line. The extraction and HPLC conditions are described in detail in Chapter 6 Materials and Methods. ....	108
Figure A-23 Overlay of chromatograms from the HPLC analyses of extracellular media and cellular lysate extracts of SH-SY5Y cells treated with 25µM 4-PCB 11 sulfate for 24 hours. Extracellular extract is represented in the blue dashed line. The lysate extract is represented in the dotted red line. Standards for the LC-PCB, the OH-LC-PCB, and the LC-PCB sulfate are represented in the solid black line. The extraction and HPLC conditions are described in detail in Chapter 6 Materials and Methods. ....	109
Figure A-24 Overlay of chromatograms from the HPLC analyses of extracellular media and cellular lysate extracts of SH-SY5Y cells treated with 25µM 4-OH-PCB 52 for 24 hours. Extracellular extract is represented in the blue dashed line. The lysate extract is represented in the dotted red line. Standards for the LC-PCB, the OH-LC-PCB, and the LC-PCB sulfate are represented in the solid black line. The extraction and HPLC conditions are described in detail in Chapter 6 Materials and Methods. ....	110
Figure A-25 Overlay of chromatograms from the HPLC analyses of extracellular media and cellular lysate extracts of SH-SY5Y cells treated with 25µM 4-PCB 52 sulfate for 24 hours. Extracellular extract is represented in the blue	

dashed line. The lysate extract is represented in the dotted red line. Standards for the LC-PCB, the OH-LC-PCB, and the LC-PCB sulfate are represented in the solid black line. The extraction and HPLC conditions are described in detail in Chapter 6 Materials and Methods. ....	111
Figure A-26 Overlay of chromatograms from the HPLC analyses of extracellular media and cellular lysate extracts of HepG2 cells treated with 25µM 4'-OH-PCB 3 for 24 hours. Extracellular extract is represented in the blue dashed line. The lysate extract is represented in the dotted red line. Standards for the LC-PCB, the OH-LC-PCB, and the LC-PCB sulfate are represented in the solid black line. The extraction and HPLC conditions are described in detail in Chapter 6 Materials and Methods.....	112
Figure A-27 Overlay of chromatograms from the HPLC analyses of extracellular media and cellular lysate extracts of HepG2 cells treated with 25µM 4'-PCB 3 sulfate for 24 hours. Extracellular extract is represented in the blue dashed line. The lysate extract is represented in the dotted red line. Standards for the LC-PCB, the OH-LC-PCB, and the LC-PCB sulfate are represented in the solid black line. The extraction and HPLC conditions are described in detail in Chapter 6 Materials and Methods.....	113
Figure A-28 Overlay of chromatograms from the HPLC analyses of extracellular media and cellular lysate extracts of HepG2 cells treated with 25µM 4-OH-PCB 8 for 24 hours. Extracellular extract is represented in the blue dashed line. The lysate extract is represented in the dotted red line. Standards for the LC-PCB, the OH-LC-PCB, and the LC-PCB sulfate are represented in the solid black line. The extraction and HPLC conditions are described in detail in Chapter 6 Materials and Methods.....	114
Figure A-29 Overlay of chromatograms from the HPLC analyses of extracellular media and cellular lysate extracts of HepG2 cells treated with 25µM 4-PCB 8 sulfate for 24 hours. Extracellular extract is represented in the blue dashed line. The lysate extract is represented in the dotted red line. Standards for the LC-PCB, the OH-LC-PCB, and the LC-PCB sulfate are represented in the solid black line. The extraction and HPLC conditions are described in detail in Chapter 6 Materials and Methods.....	115
Figure A-30 Overlay of chromatograms from the HPLC analyses of extracellular media and cellular lysate extracts of HepG2 cells treated with 25µM 4-OH-PCB 11 for 24 hours. Extracellular extract is represented in the blue dashed line. The lysate extract is represented in the dotted red line. Standards for the LC-PCB, the OH-LC-PCB, and the LC-PCB sulfate are represented in the solid black line. The extraction and HPLC conditions are described in detail in Chapter 6 Materials and Methods.....	116
Figure A-31 Overlay of chromatograms from the HPLC analyses of extracellular media and cellular lysate extracts of HepG2 cells treated with 25µM 4-PCB 11 sulfate for 24 hours. Extracellular extract is represented in the blue dashed line. The lysate extract is represented in the dotted red line. Standards for the LC-PCB, the OH-LC-PCB, and the LC-PCB sulfate are represented in the solid black line. The extraction and HPLC conditions are described in detail in Chapter 6 Materials and Methods.....	117

Figure A-32 Overlay of chromatograms from the HPLC analyses of extracellular media and cellular lysate extracts of HepG2 cells treated with 25 $\mu$ M 4-OH-PCB 52 for 24 hours. Extracellular extract is represented in the blue dashed line. The lysate extract is represented in the dotted red line. Standards for the LC-PCB, the OH-LC-PCB, and the LC-PCB sulfate are represented in the solid black line. The extraction and HPLC conditions are described in detail in Chapter 6 Materials and Methods.....118

Figure A-33 Overlay of chromatograms from the HPLC analyses of extracellular media and cellular lysate extracts of HepG2 cells treated with 25 $\mu$ M 4-PCB 52 sulfate for 24 hours. Extracellular extract is represented in the blue dashed line. The lysate extract is represented in the dotted red line. Standards for the LC-PCB, the OH-LC-PCB, and the LC-PCB sulfate are represented in the solid black line. The extraction and HPLC conditions are described in detail in Chapter 6 Materials and Methods.....119

## LIST OF ABBREVIATIONS

AD	Alzheimer's disease
AhR	aryl hydrocarbon receptor
ALS	amyotrophic lateral sclerosis
BBB	blood brain barrier
CYP	cytochrome P450
DAT	dopamine active transporter
DDT	dichlorodiphenyltrichloroethane
DMEM	Dulbecco's Modified Eagle Medium
DNSA	dansylated amine
DP	dansylated proline
EC <sub>50</sub>	effective concentration providing 50% response
FA	fatty acid
HC-PCB	higher chlorinated biphenyls
HC-PCB	higher chlorinated biphenyls
HPLC	high pressure liquid chromatography
HS	horse serum
HSA	human serum albumin
LC-PCB	lower chlorinated biphenyl
LDH	lactate dehydrogenase
LOD	limit of detection
LOQ	limit of quantitation
MTT	3-(4,5-dimethylthiazol-2-yl)-2,5-diphenyltetrazolium bromide
NADH	nicotinamide adenine dinucleotide
OH-LC-PCB	hydroxylated lower chlorinated biphenyl

PCB	polychlorinated biphenyl
PD	Parkinson's disease
PDB	protein database
POP	persistent organic pollutant
ppb	parts per billion
ROS	reactive oxygen species
RPMI	Roswell Park Memorial Institute
SN	substantia nigra
SULT	sulfotransferase
TH	tyrosine hydroxylase
VMAT	vesicular monoamine



## CHAPTER 1: INTRODUCTION

### Polychlorinated Biphenyls (PCBs)

The class of environmental toxic compounds known as polychlorinated biphenyls (PCBs) has garnered much attention throughout much of the last century to the present for their tendency to persist in the environment and cause or contribute to deleterious health effects of exposed populations. Their persistence in the environment is due to their remarkable resistance to degradation by chemical or biological means which originally imparted on them a high degree of industrial utility.<sup>1-3</sup>

#### Background

The synthesis of chlorinated biphenyls was first published by German chemists in 1881,<sup>4</sup> after they were identified as a desirable byproduct of coal tar processing in 1865. PCB mixtures were industrially produced in Anniston, Alabama, USA by the Swann Chemical Company beginning in 1929. From this inception, until a national ban under the Toxic Substances Control Act (TSCA) in 1979, an estimated 1.5 million tons of PCB mixtures were produced worldwide under a variety of trademarks (Aroclor, Kanechlor, etc.) and by various industrial companies (e.g. Monsanto Chemical Company, Kaneka Corporation, etc.).<sup>5</sup> PCBs were used throughout most of the 20<sup>th</sup> century in various industrial applications and in the production of consumer goods.<sup>6</sup> The wide versatility of this class of compounds allowed for the production of mixtures with highly desirable qualities including thermal and chemical stability, high insulation and thermal conductivity, and high flash points, which led to their incorporation into various products (e.g. electrical transformers, condensers, paint, fluorescent light ballasts, flame retardants, lubricating oils, hydraulic fluids, sealants, plasticizers, etc.).

Industrially, PCB mixtures were synthesized using the iron catalyzed chlorination of biphenyl which resulted in concoctions that, depending on reaction conditions (e.g. time and temperature), varied by their degree of chlorination. The most commonly used

Aroclor mixtures included Aroclors 1242, 1254, and 1260 which are defined by their chlorine composition at the end of their synthetic chlorination reactions, i.e. 42%, 54%, and 60% chlorination, respectively. The 12 carbon biphenyl core can accommodate between one to ten chlorines. This configuration allows for up to 209 PCB congeners, 19 of them being axially chiral,<sup>7</sup> that follow the chemical formula  $C_{12}H_{10-n}Cl_n$ . Conventional naming of the 209 PCBs has followed a system proposed in 1980 by Ballschmiter and Zell (BZ numbering system)<sup>8</sup> that has since been revised to adhere to the International Union of Pure and Applied Chemistry (IUPAC) nomenclature rules,<sup>9</sup> and has become widely accepted. Figure 1-1 shows five distinct PCB congeners that differ by chlorination degree and pattern, accompanied by their commonly used BZ number and structural name, as well as their formal IUPAC names. The work discussed herein will use the BZ numbering system for simplicity and clarity. In Figure 1-1, information regarding the presence of chlorine, *ortho* to the biphenyl junction is also included. This becomes important as *ortho* chlorines alter the co-planarity of the molecule which influences its interactions with the aryl hydrocarbon receptor (AhR) and therefore, its potential mode of toxic effect.

#### Environmental distribution of PCBs

Although the deleterious effects associated with PCB exposure had become evident as early as 1937<sup>10</sup>, their presence in the environment and their potential effects on biological systems did not gain public interest until 1966 when Swedish scientist, Soren Jensen, discovered their presence in various environmental samples. The work of Rachel Carson in America regarding the dangerous environmental effects of the insecticide DDT,<sup>11</sup> (1,1'-(2,2,2-trichloroethane-1,1-diyl)bis(4-chlorobenzene)), prompted Jensen's pursuit of quantifying DDT in plant and wildlife throughout Sweden. A contaminating set of peaks by gas chromatography, later identified as PCBs, were confirmed in multiple biological milieu<sup>12</sup>. As these compounds would continue to be detected throughout the

world for many decades to come, it was further realized that these nonpolar compounds are environmentally persistent with a tendency to accumulate in tissues with high lipid content and magnify up the food chain where its bioaccumulation can lead to various toxic effects.<sup>13, 14</sup>

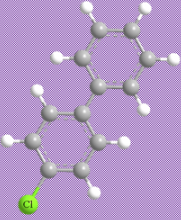
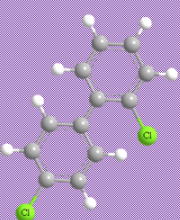
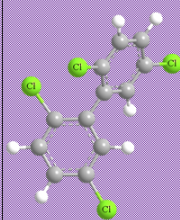
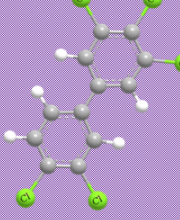
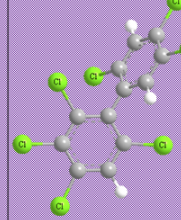
					
BZ numbering system	PCB3	PCB8	PCB52	PCB126	PCB183
Structural name	4-chlorobiphenyl	2,4'-dichlorobiphenyl	2,2',5,5'-tetrachlorobiphenyl	3,3',4,4',5-pentachlorobiphenyl	2,2',3,4,4',5,6-heptachlorobiphenyl
IUPAC name	4-monochloro-1,1'-biphenyl	2,4'-dichloro-1,1'-biphenyl	2,2',5,5'-Tetrachloro-1,1'-biphenyl	3,3',4,4',5-pentachloro-1,1'-biphenyl	2,2',3,4,4',5,6-heptachloro-1,1'-biphenyl
<i>ortho</i> -substituents	none	mono- <i>ortho</i>	di- <i>ortho</i>	none	tri- <i>ortho</i>

Figure 1-1 A comparison of PCB congeners: Three major nomenclature types and *ortho*- substituent designations.

Currently, the distribution of PCBs throughout the world is better understood due to decades of research. As PCB mixtures have become introduced into environmental systems through the degradation (both biological and physical) of PCB containing materials, accidental spills, recycling of electronic waste, irresponsible dumping of waste or the improper disposal and leaking of closed systems, they have polluted all levels of our troposphere.<sup>15-20</sup> The wide distribution of PCBs is due, like many persistent organic pollutants, to their movement throughout the environment by cycling between air, water,

and soil and biological systems.<sup>21, 22</sup> Throughout the world this includes large natural water systems (e.g. those in high mountain ranges, arctic glaciers, the Hudson Bay, the Hudson River, the Great Lakes, and the Baltic Sea),<sup>23-28</sup> sediment and soil from urban to rural areas,<sup>29, 30</sup> and in many species at virtually all trophic levels of life ranging from microbiota and fish to avian life and large mammals.<sup>31-34</sup>

The natural atmospheric transport system of prevailing winds and ocean currents has resulted in a large deposition of environmentally available PCBs, as well as other man-made modern chemicals, to the arctic regions.<sup>35</sup> There are a variety of additional meteorological routes by which persistent organic pollutants (POPs) such as PCBs can be mobilized to results in their worldwide distribution.<sup>36</sup> The combination of these natural global processes and the movement of temporal atmospheric routes between air, water, and soil, ensures that POPs, PCBs included, are distributed to all the corners of our planet. With virtually no industrial presence in the arctic to account for the presence of PCBs, this ecological drive can explain how humans and wildlife in this area have been amongst the highest exposed populations on Earth.<sup>37, 38</sup> Among the inhabitants of the Canadian arctic, the region's wildlife has served as a veritable reservoir for PCBs with high levels being detected in fish and marine life, gulls, eagles, and mammals such as the arctic fox and polar bear.<sup>39-41</sup> The high serum PCB levels in these animals has been implicated in toxic endpoints that include thyroid hormone and immune system dysfunction, as well as numerous effects on their reproduction.<sup>34, 41-43</sup>

The native Inuit people of the northern arctic regions of Quebec have also been shown to exhibit high serum concentrations of PCBs, when compared to low to mid latitude residing populations and even their southern arctic countrymen.<sup>44, 45</sup> Due to their reliance on PCB-rich fatty foods that include blubber from seal, walrus, whale and other fish such as char,<sup>46</sup> their otherwise healthy, fatty diet has resulted in PCB laden serum as well as breast milk.<sup>37</sup> The importance of PCB exposure levels lies in the many toxic effects that have been associated with them. In the general population, they have been

linked with toxicities that encompass many aspects of human diseases, *vide infra*, and perinatal exposure to PCBs has been implicated in adverse growth and neurodevelopmental effects. Because these compounds tend to bioaccumulate, the lipid-rich matrix of breast milk also allows for the buildup of PCBs which provides a concentrated route of exposure for the developing infant.<sup>47</sup>

### PCBs and human health

Throughout the world, organohalogen levels in blood have been measured in exposed populations. Determining the concentrations of PCBs in humans became essential after two well-documented accidental dietary exposure incidents in Japan in 1968 and again in Taiwan in 1979. In both cases, PCB mixtures being used as heat transfer agents in the production of rice cooking oil became inadvertent contaminants. In both cases, although the seemingly small amount of PCBs was consumed over an extended period of months (in Taiwan, an estimated 1 gram over the span of 9 months) the results were multifarious. They ranged from acne-and rashes (termed “chloracne”) as well as pigmentation of the skin and nails to disruptions in endocrine function (growth and menstruation), and high incidences of hepatic cancer and hepatomegaly.<sup>48-50</sup> Blood PCB levels were determined to be from 3 ppb to 1,156 ppb in the studied population. The detrimental effects observed in the adult population were eventually overshadowed by those who suffered as a result of perinatal exposure. Of the reported 13 women who were pregnant in the Japanese Yusho poisoning, two suffered stillborn children,<sup>51</sup> and in the Taiwanese Yu-Cheng incident, the 39 surviving prenatally exposed victims showed a high infant mortality rate and faced lifelong developmental challenges, both physical and mental.<sup>52, 53</sup> A longitudinal study of the Taiwanese group showed a prevalence of immune system dysfunction, motor and cognitive developmental defects, and reproductive and endocrine system disruption.<sup>48</sup>

Blood PCB levels have been determined in groups of people in various areas including the Slovak Republic, Spain, Africa, China and the Americas.<sup>54-57</sup> It is thought that nearly every person on Earth has been exposed to PCBs by some combination of route of exposure (air, water or sediment, food, etc.) and has a detectable concentration in their blood, fat, and, breast milk. The potential for adverse health effects is based on a combination of exposure time and quantity, and predisposed genetic or health conditions.<sup>2</sup>

In addition to the accidental ingestion by Yusho and Yu-Cheng victims, PCB exposures have been reported in worker-related incidents and in the general population. These events have been implicated in an array of human health effects including cardiovascular disease,<sup>58</sup> immunological disorders,<sup>59, 60</sup> hormonal dysfunction,<sup>61</sup> neurotoxicity,<sup>62-64</sup> and carcinogenesis.<sup>65, 66</sup>

The carcinogenicity of PCBs was first implicated in the effects associated with the contaminated rice oil consumption, and it was further established in the etiology and rise in non-Hodgkin's lymphoma and prostate cancer amongst highly exposed populations.<sup>67-69</sup> The prostate cancer study indicated that exposure effects were seen in male children born of once highly exposed mothers, which implicates a heritable genetic influence of these compounds.<sup>70</sup> Furthermore, a study on increased breast cancer and the connection to a genetic variation in the CYP1A1 gene was a further indicator of the genetic basis for the harmful effects of PCBs.<sup>71</sup> Because of the uncertainties associated with PCB exposure (i.e. 209 congeners, their mixtures, and co-exposure with other toxic substances), the concrete connection between this class of compounds and human health effects remains, for some, to be made. Despite the weight of evidence, detractors from the idea that PCB exposure has a causal relationship to initiating and promoting cancerous events, have published their converse analyses on epidemiological and toxicological studies.<sup>3, 72, 73</sup>

In 1979, under the Toxic Substances Control Act (TSCA), the United States Congress passed a ban on the deliberate production of PCBs and largely limited their use to closed systems.<sup>74</sup> In 2001, under the Stockholm Convention for Persistent Organic Pollutants, PCBs were included among the “dirty dozen”, the 12 most dangerous persistent organic pollutants to be banned worldwide, and in 2013, PCBs were recognized by the International Agency for Research on Cancer (IARC) as a class of “Group 1-carcinogenic to humans” compounds.<sup>66</sup> With most developed nations holding a ban on PCB production, the worldwide levels of PCBs have mostly decreased. There is, however, evidence for renewed sources of exposure. Older buildings, such as those used for housing, schools, and workplaces, have exhibited high levels of airborne PCBs.<sup>75</sup> In most cases, the congener profile matches the increases in those respective congeners measured in blood samples obtained from the exposed population.<sup>76-78</sup> PCBs are being detected in older buildings, as unintentional byproducts in production and use of paints and pigments, in the remediation and/or dredging of contaminated sites, and in the disposal or recycling of PCB containing materials.<sup>79-82</sup>

### Lower Chlorinated PCBs (LC-PCBs)

#### Airborne PCBs

In 1971, with growing interest in PCB-related public health issues, Monsanto voluntarily halted the production of all previous Aroclors and introduced a distillate of Aroclor 1242. Aroclor 1016 would be enriched in LC-PCBs and therefore reduce the amounts of toxic higher chlorinated congeners (HC-PCBs; >4 chlorine atoms per congener) from future use. While the HC-PCBs were known and acknowledged to bioaccumulate and be associated with detrimental health effects, it was assumed that the degree of chlorination of the compounds imparted on them their undesirable effects. While the worldwide levels of PCBs have shown to be decreasing since their production and use was limited to distinct closed systems,<sup>83</sup> studies show that indoor and outdoor air

samples in urban areas are high in lower chlorinated PCBs (LC-PCBs;  $\leq 4$  chlorine atoms per congener).<sup>78, 84</sup> This has been shown in areas in Denmark, Germany, and Canada, as well as in large US cities including New York, Cleveland, and Chicago.<sup>84-88</sup>

The Chicago study published by researchers from the University of Iowa brought to light the large amount of semi-volatile LC-PCBs that are present in air in an industrial city.<sup>89</sup> In this study, temperature dependent spatial variability and volatilization sources were identified as well as the presence of a particular dichlorinated PCB, PCB 11, that was not identified as a component of any Aroclor mixture ever in use.<sup>90</sup> The confirmation of this congener's presence led to an investigation regarding the ongoing, albeit inadvertent and therefore not illegal, production of PCBs.<sup>91</sup> It was found that that an additional current source of PCBs may be their synthesis in the manufacture of certain dyes and pigments.<sup>92</sup> A study of serum samples obtained from a highly exposed cohort in northern Indiana, alongside its control in eastern Iowa, (the Airborne Exposure to Semivolatile Organic Pollutants (AESOP) Study from the Iowa Superfund Research Program (ISRP)) detected the presence of 70 non-Aroclor PCBs in both cohorts where these compounds represented an average of 10% of total PCBs.<sup>93</sup> The presence of some LC-PCBs were attributed to known pigments that are used in household paints, packaging materials, cardboard boxes, plastic bags, etc.<sup>82</sup> The disposal or recycling attempts of these goods have resulted in LC-PCBs, including PCB 11, being confirmed in other areas of the world (i.e. China, the Delaware River, and the New York/New Jersey Harbor) in air, water, and sediment samples.<sup>94-97</sup> Exposure to volatile LC-PCBs via inhalation allows for their facile transfer into the blood via the lungs, thus exhibiting an important route of exposure to these airborne toxicants.<sup>98, 99</sup> In a study of air and serum samples taken from the Upper Hudson River communities in New York, a correlation was observed between the resulting congener profiles.<sup>100, 101</sup> A further study implicated this exposure in observed detrimental effects on memory, learning, and depression.<sup>102</sup>



Studies (epidemiological, *in vitro*, and *in vivo*) have established a range of LC-PCBs' toxic potentials in the initiation and promotion of carcinogenesis, cardiovascular disease, diabetes, and neuro-degenerative/developmental effects. Exposure to PCB 11 in male Sprague-Dawley rats showed its rapid distribution to all tested tissues, and the high quantity of metabolites created.<sup>98</sup> Furthermore, its toxicity in immortalized human prostate epithelial cells was measured and attributed to increased steady-state levels of intracellular hydroperoxide and superoxide that was ameliorated with the presence of superoxide dismutase and catalase.<sup>103</sup>

### Metabolism of LC-PCBs

When compared to HC-PCBs, the LC-PCBs are more highly susceptible to metabolic transformation. LC-PCBs are comprised of less chlorines, and therefore more chemical space is available for metabolic transformations when compared to HC-PCBs. Because of this, the volatile LC-PCBs are mostly considered transient species in the body, however, their metabolic vulnerability imparts on them the potential for the production of reactive and toxic species<sup>104, 105</sup> The metabolism and metabolites of PCBs have been widely studied in order to assess their toxic influence and to assess their potential use as biomarkers for exposure and determining body-burdens in human populations.<sup>106, 107</sup> PCB metabolism is often initiated with oxidative reactions catalyzed by the cytochrome P450 enzymes in the liver and other organs, which results in hydroxylated PCBs (OH-PCBs).<sup>108</sup> In fact, the analysis of these metabolites has been completed in biological samples from various species worldwide.<sup>34, 109, 110</sup> Surprisingly, however, in abiotic environmental surface water and precipitation samples obtained throughout Ontario, Canada, OH-PCBs have also been detected and quantified.<sup>111</sup> More recently, their presence was also verified in sediment from the Indiana Harbor and Ship Canal off of Lake Michigan, as well as in original Aroclor mixtures.<sup>112</sup>

The presence of OH-PCBs in human blood samples has been established for communities in eastern Slovakia, Japan, Romania, Belgium, and the U.S., among others. The limited array of hydroxylated congeners (approximately 40) reported (tetra- to nona-PCB) is a testament to the large analytical challenge in detecting and quantitating the 209 parent PCB congeners and, for the mono-hydroxylated PCBs, 837 metabolites.<sup>104</sup> The American AESOP study reported the persistence of, and variations in parent PCBs and OH-PCBs in children or adolescents and mother pairs in urban and rural areas with OH-PCB concentrations ranging from no-detection to 0.30ng/g for fresh weight samples.<sup>113</sup><sup>114</sup> The transplacental transfer of PCBs and OH-PCBs in pregnant women in Slovakia and the Netherlands are reported in the literature.<sup>115, 116</sup> The studies indicate that PCB and OH-PCB congener profiles in cord blood mimic those of the maternal blood composition, and that the rate of trans-placental transfer is congener-dependent. A follow-up on each cohort found a correlation between OH-PCB pre-natal exposure and reduced neurodevelopmental functioning, which was also congener dependent.<sup>117, 118</sup>

Although hydroxylated metabolites of LC-PCBs are less prevalent than those of HC-PCBs in previously studied human serum samples,<sup>113</sup> their contribution to toxic health effects have been studied *in vitro* and in live animals. OH-PCBs are thought to exhibit endocrine disruptive effects via their binding to the thyroid hormone transport protein transthyretin, and they have been widely implicated in neurotoxic effects. The further oxidation of OH-PCBs has been shown to result in catechol, *p*-hydroquinone, and quinone formation, and it is linked to the formation of cytotoxic reactive oxygen species.<sup>119, 120</sup> For the monochlorinated PCB 3, the resulting 3,4-quinone metabolite was the ultimate carcinogen in rat liver carcinogenesis, and it was proposed to have a similar pathway to a previous study of PCB 52 in rat liver and brain, *i.e.* the covalent adduction to proteins or DNA.<sup>121-124</sup> Additional PCB metabolites include glutathione conjugates and their mercapturic acid derivatives including methyl sulfones, glucuronides, and PCB sulfates.<sup>104, 125</sup>

## PCB sulfates

Of the aforementioned metabolites, PCB sulfates have recently garnered increased interest due to their potential activity as disruptors of endocrine signaling. While OH-PCBs have been shown to inhibit the sulfation of endogenous molecules including dehydroepiandrosterone (DHEA) and estradiol, many also serve as substrates for sulfate conjugation.<sup>126-128</sup> The resulting PCB sulfates have been shown to bind to the thyroid hormone carrying protein transthyretin, where, in some cases, they bind with similar affinity to that observed with thyroxine.<sup>129</sup> Moreover, a study on this binding found that PCB sulfates acted as modulators of an induced transthyretin fibrilogenesis model.<sup>130</sup> The potential of OH-PCBs to serve as substrates for sulfation catalyzed by several human and rat sulfotransferases has been published,<sup>128, 129</sup> and a study in Sprague-Dawley rats has indicated that hydroxylation followed by sulfation accounts for more than half of the metabolic fate after treatment with the monochlorinated PCB 3.<sup>131</sup> Furthermore, recent studies on 4-PCB 11 sulfate administered to rats indicate that PCB sulfates may be retained *in vivo* and undergo additional metabolism.<sup>132</sup> This suggests that, contrary to the general assumption that sulfation of an exogenous compound is simply a mode for its removal from the body, the sulfates derived from OH-PCBs may have distinct biological and toxicological activities.

## Human Serum Albumin (HSA)

The disposition of most xenobiotic and endogenous compounds in humans is often regulated by their binding to human serum albumin (HSA). Albumin is the most abundant protein in blood plasma, and it is a multifaceted player that is present in all vertebrates.<sup>133</sup>

### Synthesis, distribution, and function

HSA is a globular 66kDa non-glycosylated protein that is synthesized in the liver. There is also evidence for synthesis in other organs, and its production by activated

microglia has been observed.<sup>134</sup> Its high concentration in blood (approx. 700 $\mu$ M) allows for HSAs action in maintaining colloidal osmotic pressure in the perivascular space, and in transporting hormones, lipids, ions, metals, xenobiotics, and their metabolites throughout the body; an activity that has led to it being referred to as the “silent receptor”.<sup>135, 136</sup> It is widely accepted that binding affinity to HSA for steroids and lipophilic compounds is low when compared to other binding proteins in the blood, however its large concentration allows for their efficient and discrete transport and the retention of these compounds.<sup>137, 138</sup> In fact, even in individuals with analbuminemia, a genetic predisposition resulting in a 1000 fold reduction of albumin in the blood, no discernable health effects are evident, however low serum albumin concentrations are associated with a poor outcome in certain disease states.<sup>139, 140</sup> In addition to its vascular component, HSA is present in large amounts in extravascular compartments, being distributed to muscle and other tissue. HSA in the extravascular space accounts for more than half of its total body distribution.<sup>137</sup> Interestingly, HSA has also been shown to play an important role in the transplacental transfer of drugs and other compounds to the developing fetus.<sup>141-144</sup>

A further important aspect of HSAs versatile role is that of its enzymatic abilities. HSA exhibits phosphatase, glucuronidase, RNase, and esterase activity. These transformations take place at various sites throughout the protein, employing different nucleophilic residues (i.e. tyrosine, lysine, and cysteine) and with a broad range of substrate specificities.<sup>145</sup> These properties have been incorporated into the design of pro-drugs for their controlled release and transport, as well as in the detoxification of harmful agents (e.g. organophosphates and carbamates).<sup>146</sup> The role of albumin in the body is multifaceted and in many cases, compound specific.

## Binding to HSA

There are currently more than 80 HSA crystal structures available from the Research Collaboratory for Structural Bioinformatics Protein Data Bank (RCSB PDB).<sup>147</sup> The various ligand-bound and unbound crystal structures and protein fragments highlight the drug, hormone, fatty-acid (FA), ion, and heme-binding sites of HSA.<sup>148, 149</sup> Because of the importance that HSA plays in the distribution and half-lives of drugs in the body (e.g. warfarin, NSAIDs, etc.) the binding properties of this protein have been widely studied to assess their retention and free concentrations as well as any potential toxicity (i.e. drug-drug displacement interactions).<sup>150</sup> It is noted, however, that regardless of albumin being present in all vertebrates, its binding characteristics exhibit species-dependent differences.<sup>151</sup>

The work of Sudlow, et.al. has elucidated two major drug binding sites of HSA, Site I and Site II. This is in addition to the nine FA, heme and ion-binding, and additional biochemically uncharacterized sites that are present in some ligand-bound crystal structures; potentially due to the high ligand concentrations required for crystallization. Figure 1-2 highlights the locations of the HSA binding sites as established by a comparison of crystal structures for HSA-ligand and/or fatty acid complexes.<sup>152</sup> It has also been determined that the fatty-acid binding to HSA greatly influences binding to both Sites I and II.<sup>153</sup> In cases of poor health or disease states, this has clinical implications concerning the free-concentration of drugs or toxic substances in the body.<sup>154</sup> Capitalizing on this inevitable interaction, however, the coupling of medications to FA-HSA binding has resulted in improvements to their stability in the body.<sup>155, 156</sup>

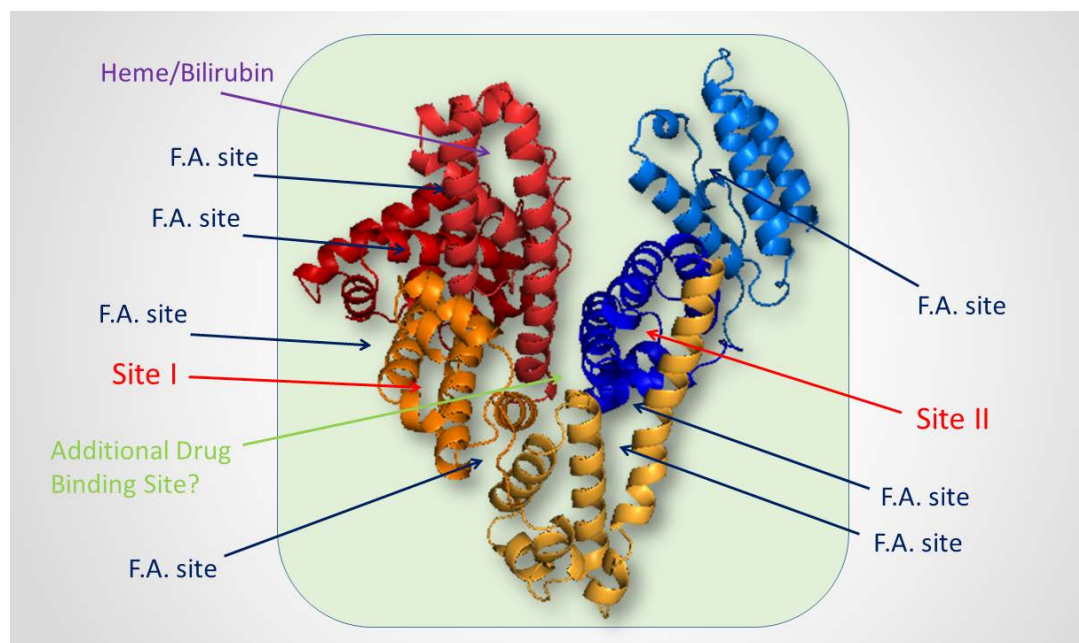


Figure 1-2 A crystal structure of HSA highlighting its fatty acid, heme, and major drug binding sites. Binding sites were elucidated by the analysis of HSA-ligand and/or fatty acid complexes.<sup>148</sup> The HSA crystal structure (PDB ID: IUOR) was modified using the PyMOL Molecular Graphics System, Version 1.7.4 Schrödinger, LLC.

Studies concerning the binding of PCBs to HSA are limited in the scientific literature. Their interaction has been implicated upon measuring the fractionation of Aroclor mixtures or individual congeners into plasma components. Work performed using PCB treated plasma from mice, pigeon, and humans shows that PCBs are largely associated with the albumin compartment of blood plasma, which is lipid content dependent.<sup>157-159</sup> Furthermore, in the guinea pig model, albumin concentration was shown to be correlated to the transplacental transfer of a hexachlorinated PCB.<sup>160</sup> This effect is thought to be related to the increase in HSA concentration induced by Aroclor 1254 reported in cultured primary rat hepatocytes.<sup>161, 162</sup> Spectroscopic and *in silico* studies of individual PCB congeners suggest that binding occurs at the aforementioned Sudlow sites as well as a distinct site not traditionally characterized by the work of

Sudlow, et. al. The results of these few studies, however, are sometimes contradictory.<sup>163-165</sup>

### Neurotoxic effects of PCB exposure

#### Epidemiological studies

The harmful and dangerous effects associated with perinatal PCB exposure was evident in the aftermath of the occurrences of Yusho and Yu-cheng. In the early 1980s, after confirming that “fish-eaters” from Lake Michigan presented three times the serum levels of PCBs than the general population, a longitudinal study on the developmental neurotoxic effects associated with high PCB consumption was initiated. In this work, a cohort from Michigan was employed and samples (blood: maternal, cord, and infant; breast milk) were obtained from pregnant women-infant pairs with high Lake Michigan fish consumption. This was done at childbirth and at ages 4 and 11, and the results from this work led to the conclusion that high PCB exposure during neurodevelopmental stages was associated with reduced cognitive and motor function, as well as altered intellectual function.<sup>166</sup> Similar results have been reported in cohorts in North Carolina, the Faroe Islands, and Germany.<sup>167-169</sup> Since this early work, the neurological effects of PCBs on exposed populations have been related to mood, depression, social and reproductive behaviors, cognition and motor function, and neurodegenerative diseases.<sup>170-173</sup> The well-established endocrine-disrupting abilities of PCBs have been implicated in many of these effects due to the central role of the neuroendocrine system in the maintenance and regulation of neuronal processes.<sup>61, 174</sup> These include mainly their androgenic and estrogenic properties, and their ability to bind to thyroid hormone binding proteins and receptors.<sup>62, 129</sup>

### In vitro and in vivo studies

Several *in vivo* and *in vitro* studies of PCB-induced neurotoxicity have been reported in the literature. Aside from the neuroendocrine disrupting abilities of these compounds, pathways involving reactive oxygen species (ROS) formation, calcium homeostasis, neurotransmitter activity, gene expression and signal transduction have been observed as a result of their exposure.<sup>175</sup> Aroclor mixtures induce neurotoxicity in human neuronal cells (astrocytoma, granule cells, cortical neurons, hippocampal, dopaminergic, etc.)<sup>176</sup> In cerebellar granule cells, *ortho*-substituted PCBs were shown to induce cell death by altering membrane structure and were associated with changes in intracellular calcium, ROS generation, and mitochondrial decoupling.<sup>177, 178</sup> Regarding the changes in calcium status of neuronal cells, the ryanodine receptor has received much attention, as it is proposed to be a convergent mechanism by which PCBs may impart their toxic effects.<sup>179</sup> In addition, studies have also implicated OH-PCBs in neuronal cell death mediated by ROS formation, signal transduction changes (protein kinase C translocation, c-Jun expression, impaired astrocytic differentiation), the dysregulation of calcium flux (cytosolic and from organelles), and aberrant neuronal growth.<sup>180-182</sup> These effects may stem from OH-PCBs' redox capability, interaction with ryanodine receptor (i.e. calcium homeostasis effects), or the covalent adduction of proteins or DNA.<sup>179, 183</sup>

### Dopaminergic system as a target for PCB induced toxicity

Numerous animal studies have confirmed the effects of PCB exposure on neurotransmitter regulation.<sup>184</sup> Effects on the dopaminergic system were first proposed after behavioral defects were observed in mice, and later confirmed in rhesus monkeys treated with Aroclor 1016.<sup>185, 186</sup> The reduced dopamine concentrations measured in monkey brain were attributed to *ortho*-chlorinated PCBs which have also been known to preferentially bioaccumulate in this tissue. Furthermore, an analysis of post-mortem Parkinson's Disease (PD) patient brain samples exhibited higher concentrations of di-



*ortho* chlorinated PCBs in the caudate nucleus, a component of the basal ganglia.<sup>187</sup> The vulnerable dopaminergic system is at the core of many neurodegenerative diseases that include Parkinson's (PD), Alzheimer's, amyotrophic lateral sclerosis (ALS), and dementia. Deterioration of dopaminergic neurons in the substantia nigra, a major part of the basal ganglia, is widely considered the hallmark of these disease states. Toxicology studies in dopaminergic neurons have determined the cytotoxicity of PCBs (Aroclor mixtures and individual congeners), and this was concurrent with a reduction in dopamine levels and dopamine transporter expression, calcium dysregulation, altered gene expression and protein function.<sup>176, 188, 189</sup> PCB exposure has been linked to the occurrence of Parkinson's disease and ALS in women in a set of epidemiological studies. A post-mortem follow-up study on an occupational exposure cohort found a correlation between high PCB serum concentrations and mortality, in women, due to ALS, PD, and dementia, however this was only observed when stratified by gender.<sup>190, 191</sup> These results are surprising considering that PD is more prevalent in men in the general population. A study of post-mortem brain samples obtained from the Emory Brain Bank from PD and non-PD patients also presented with higher PCB concentrations in PD patients versus controls, however, this was only observed in women.<sup>192</sup> Also as part of this study, post-mortem brain samples obtained from a separate population of women (Nun Study) who presented no clinical symptoms of neurodegeneration, showed a correlation between elevated brain-PCB concentrations and nigral depigmentation. Nigral depigmentation is an indication of dopaminergic neuronal loss in the substantia nigra.

The results highlighted here showcase the difficulty in assessing and determining the veritable risks and consequences associated with PCB exposure. Confounders that include different PCB mixtures, routes of exposure, metabolism, previous health conditions or genetic pre-disposition, co-exposure with other known toxicants, etc. all contribute to the challenges involved in risk assessment. With the large weight of

scientific evidence in its support, however, it is difficult to deny that PCBs are intimately involved in human health and disease.

## CHAPTER 2: STATEMENT OF THE PROBLEM

Although the worldwide levels of PCBs in the environment have been steadily decreasing, the detrimental health effects of these persistent organic pollutants (POPs) continue to be of interest.<sup>83</sup> The production of PCBs worldwide, estimated to be greater than 1.5 million tons, was beneficial and necessary in the technological expansion in the wake of World War I and in the midst of World War II and after. However, their widespread use and sometimes irresponsible disposal has led to many destructive effects on our planet's inhabitants. Currently, lower chlorinated PCBs (LC-PCBs) are being detected in urban and rural air samples, as well as in water and sediment. These congeners ( $\leq 4$  chlorine atoms per congener) are semi-volatile and, while many remain from legacy sources, others are being produced, although inadvertently, in the manufacturing and processing of paints and pigments.<sup>82, 91</sup> Although they are detected in water and sediment, a major route of exposure to these compounds is airborne via inhalation, an efficient route to the circulatory system.<sup>85, 89</sup> Furthermore, LC-PCBs are more highly susceptible to metabolic transformations than higher chlorinated congeners (HC-PCBs).<sup>104</sup>

The neurotoxic effects associated with PCB exposure have been elucidated in both epidemiological studies and in the laboratory setting, both *in vitro* and *in vivo*.<sup>108, 193</sup> Perinatal exposure to PCBs has been linked to cognitive and motor dysfunction, and altered intellectual function.<sup>117, 167, 170, 173</sup> Exposure to these POPs later in life has also been associated with neurological effects that encompass mood, depression, social and reproductive behaviors, cognition and motor function, and neurodegenerative diseases.<sup>61, 102, 175, 192</sup> Laboratory studies have shown that PCB exposure results in changes to the dopaminergic system (e.g., decreases in dopamine levels coincident with behavioral effects).<sup>186, 194-196</sup> These results correlate with the aforementioned epidemiological studies. Hydroxylated PCB metabolites have also been implicated in these toxic effects

both *in vivo* and *in vitro*. Amongst the neurodegenerative diseases, the association between the etiology of Parkinson's disease (PD) and POP exposure has garnered much interest.<sup>197, 198</sup> A hallmark of PD is the loss of dopaminergic neurons in the substantia nigra (SN), a component of the basal ganglia in the midbrain. Epidemiological studies have shown that high PCB exposure is correlated with the loss of dopaminergic neurons in the SN, and the occurrence of PD.<sup>192</sup> Furthermore, it is proposed that this may be due to the selective accumulation of *ortho*-substituted PCBs in the caudate nucleus, a component of the basal ganglia, which also shows increased sulfotransferase activity in PD brain samples.<sup>187, 199</sup>

Sulfation of both xenobiotics and endogenous substances is a fundamental metabolic pathway. For endogenous molecules, sulfation can regulate their activity such as in the endocrine system (e.g., dehydroepiandrosterone (DHEA), and estradiol) or in the central nervous system (e.g., catecholamines, and glycosaminoglycans). Although sulfation of xenobiotics is traditionally considered a mode of excretion from the body (i.e., sulfation increases water solubility and promotes detoxication), this metabolic route may lead to the formation of a more toxic species. Hydroxylated metabolites of LC-PCBs (OH-LC-PCBs) have been shown to inhibit and serve as substrates for rat and human sulfotransferases.<sup>126-128</sup> The resulting sulfates were shown to bind with high affinity to transthyretin, a thyroid hormone transport protein in serum and the major thyroid hormone-carrier in the central nervous system (CNS).<sup>129, 200</sup> These effects may play a role in the endocrine disruption and neurotoxic effects associated with PCB exposure. Furthermore, in a study of Sprague Dawley rats, treatment with a monochlorinated PCB, PCB 3, resulted in sulfation as the major metabolic pathway, accounting for more than half of all measured metabolites.<sup>131</sup> Although the presence of this sulfated metabolite was largely detected in urine and serum, treatment with the dichlorinated 4-PCB 11 sulfate resulted in high tissue distribution, further metabolism, and limited excretion in the urine, indicating a congener selective retention in the body.<sup>132</sup>

The distribution and half-lives of xenobiotics and their metabolites in vertebrates is largely mediated by binding to the most abundant protein in serum, serum albumin. In human serum, human serum albumin (HSA) is present at a concentration of 700 $\mu$ M, which accounts for less than half of the total amount in the body.<sup>137</sup> This versatile protein contains multiple binding sites (two major drug binding sites and at least 7 fatty acid binding sites) that allow for its transport of metals, ions, fatty acids, hormones, and xenobiotics and their metabolites (e.g., sulfates).<sup>201</sup> High affinity binding to the two major drug binding sites of HSA is usually selective for In fact, it has been shown that sulfation of naphthalene or *para*-nitrobenzoic acid increases their binding to HSA when compared to both the parent compounds and to their hydroxylated or glucuronidated counterparts.<sup>202</sup> The distribution of HSA into the extravascular space allows for facile movement of necessary (and sometimes unnecessary) compounds throughout the body. Although the CNS concentration of HSA is much smaller when compared to serum levels (less than 0.7% in a healthy adult), the integrity of the blood brain barrier (BBB) can be compromised by the presence of PCBs.<sup>203</sup>

In this work, we hypothesized that, similar to the studies on naphthol and *para*-nitrophenol described above, the LC-PCB sulfates would exhibit increased HSA-binding when compared to their LC-PCB or OH-LC-PCB counterparts. Furthermore, we hypothesized that this binding would display a selectivity amongst congeners and the two major drug-binding sites of HSA. A related hypothesis for the studies described in this thesis is that hydroxylated and sulfated metabolites of LC-PCBs are neurotoxic, exhibiting a selective toxicity to dopaminergic neuronal cells.

The serum protein-binding hypothesis was tested using commercially-available purified HSA. The displacement of fluorescent probes, selective for the two major drug binding sites of HSA, were used to assess the relative affinity of LC-PCBs and their hydroxylated and sulfated metabolites. The neurotoxic effects of a select set of LC-PCBs, and their hydroxylated and sulfated metabolites, were assessed using cell culture

techniques. For this study, immortalized cells derived from the rat midbrain (the N27 cell line) were used as a dopaminergic neuronal cell model, and the immortalized human neuroblastoma derived SH-SY5Y cell line was used as an additional neuronal cell model. For comparison, the immortalized human liver derived HepG2 cell line was used to assess cytotoxic selectivity. The studies presented in this thesis further establish the potential roles of LC-PCB metabolism, especially hydroxylation and sulfation, in the health effects associated with PCB exposure. Their high affinity binding to HSA would decrease the rate of corporeal removal, thereby increasing their half-lives and the potential for further metabolism and/or toxicity of these metabolites of LC-PCBs. Their selective dopaminergic neurotoxicity would indicate that this metabolism may be an important pathway in LC-PCB-related neurological dysfunction, such as in PD.

## CHAPTER 3: THE BINDING OF LC-PCB METABOLITES TO HSA

### HSA properties

Serum albumin is the most abundant soluble protein in human plasma, accounting for approximately 60% of protein content.<sup>140, 201</sup> It is a globular monomeric protein composed of three  $\alpha$ -helical domains (I, II, and III) which are each comprised of two subdomains (Ia, Ib; IIa, IIb, IIIa, IIIb). The crystal structure of HSA (PDB ID: 1UOR) is shown in Figure 3-1 and indicates the location of HSAs domains and subdomains (reds: Ia, Ib; blues: IIa, IIb; greys: IIIa, IIIb). Each sub-domain contributes to the shared common characteristic of the three major domains, which is that of a charged surface surrounding a hydrophobic core. Structurally, the tertiary structure of HSA resembles a heart-shaped configuration, which is thought to be more ellipsoidal in solution. There are 35 cysteines of which 34 form intramolecular disulfide bonds that provide HSA with a large versatility and flexibility evidenced by its high binding abilities and physiological roles. The lone free thiol of HSA imparts on it the ability to serve as a reductant within the redox environment of the extracellular milieu. This unconjugated cysteine (Cys34) has been used as a biomarker for assessing oxidative stress in the plasma of dialysis patients.<sup>204</sup> Nucleophilic residues, of which Cys34 is one, impart on HSA its hydrolytic activities, and they are distributed amongst the protein in different binding cavities. This enzymatic ability of HSA is seen in its esterase, glucuronidase, and phosphatase activity.<sup>145</sup>

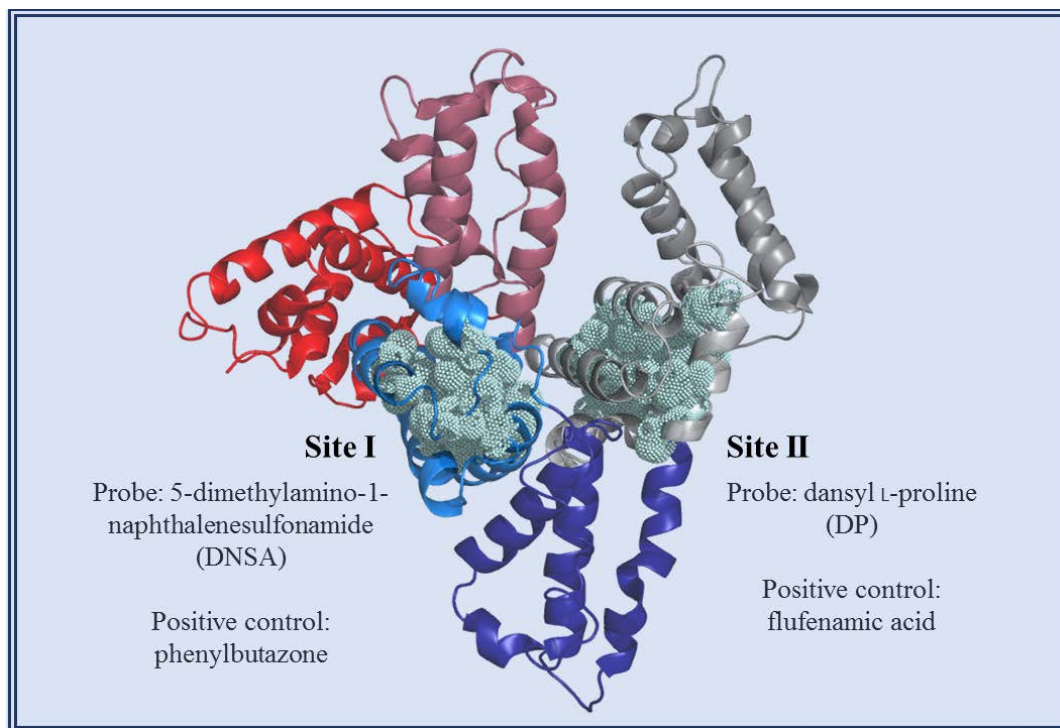


Figure 3-1 HSA crystal structure indicating domains and subdomains, residues that form sites I and II, and site-selective fluorescent probes and ligands. Domains and subdomains (reds: Ia, Ib; blues: IIa, IIb; greys: IIIa, IIIb) are shown, including residues that surround sites I and II<sup>205</sup> which are highlighted in dotted spheres. Site selective fluorescent probes and positive control ligands for each site are also annotated. The HSA crystal structure (PDB ID: IUOR) was modified using the PyMOL Molecular Graphics System, Version 1.7.4 Schrödinger, LLC.

### HSA binding sites

Ligand-bound crystal structures for the 66.5kDa protein show the various drug-, fatty acid-, ion-, and heme-binding sites of HSA,<sup>148</sup> The work of Sudlow, et. al., has elucidated the presence of two HSA major drug binding sites by use of a small library of drug molecules and fluorescent probes (mostly dansylated amino acids). Site I is situated within subdomain IIa and is characteristic of binding bulky hydrophobic molecules with negative charges on opposing ends. This includes dicarboxylic acids and xenobiotics including warfarin, phenylbutazone, and a dansylated amine (5-dimethylamino-1-naphthalenesulfonamide, DNSA). Site II is situated within subdomain IIIa and typically



binds compounds with a negative charge at one end of a molecule with a hydrophobic core. This includes diazepam, flufenamic acid, and dansylated proline. Whereas the larger area and flexibility of Site I imparts on it a more promiscuous binding, the smaller dimensions and less flexibility of Site II result in more stringent binding constraints. The “two drug-binding site” model of HSA has become dogmatic in describing the protein’s binding abilities, and has served as a good predictor of xenobiotic-HSA interactions. Figure 3-1 shows an illustration of the residues that form the hydrophobic core of both sites I and II, as well as representative ligands presented at their primary binding sites.<sup>205</sup>

### Binding assays

Because of the importance of HSA in influencing half-lives, solubility, and distribution of xenobiotics throughout the body, much research has been directed in establishing their binding characteristics. This includes binding modes, stoichiometry, binding affinity, and site selectivity. The approaches include ultrafiltration and equilibrium dialysis, isothermal calorimetry, high pressure liquid chromatography (HPLC), and electrochemical and spectroscopic means.<sup>206, 207</sup> Of the spectroscopic approaches, the intrinsic fluorescence of HSA (due to its lone tryptophan located in subdomain IIa, site I) has been used to determine site selectivity and binding constants. By measuring changes in fluorescence as a function of ligand concentration, the data can be fit to binding curves and affinity constants can be obtained.<sup>208</sup> A caveat for this approach, however, is that its basis on changes in the electronic environment surrounding Trp214 for determining either site selectivity or binding affinity undermines the high flexibility of the protein where any allosteric binding may alter HSAs tertiary structure. Additionally, it is known that the presence and concentration of fatty acids can greatly influence this configuration.<sup>153, 209</sup>

The use of fluorescent probe displacement has also been used to determine HSA binding.<sup>208</sup> Sudlow’s work introduced a number of fluorescent probes and small

molecules whose binding affinities to the two major sites were different, such that a site-selectivity could be imposed at the appropriate concentrations.<sup>210</sup> The fluorescent probes in these experiments are site-selective and exhibit an increase in fluorescence intensity upon binding to their hydrophobic site. If used at the proper concentrations, their displacement (i.e. decrease in the fluorescent signal) can be measured to determine binding characteristics such as site-selectivity and binding affinity.<sup>211</sup>

The binding of endogenous and xenobiotic metabolites has also garnered much interest in the role that HSA plays in their delivery and retention in the body. These include hydroxylated, myristylated, glucuronidated, and sulfated metabolites. The HSA-binding of bilirubin, a byproduct of heme catabolism, reduces its free concentration in blood and facilitates its transport to the liver for glucuronide conjugation and excretion. Similarly, the sulfation of xenobiotics involves the sulfotransferase-mediated transfer of a sulfuryl group from 3'-phosphoadenosine-5'-phosphosulfate (PAPS) to an acceptor molecule and often results in increased polarity, water solubility, and excretion of the sulfated product. It has been previously reported, however, that the formation of sulfated metabolites from either naphthalene or *para*-nitrobenzoic acid increases their binding to HSA when compared both to the parent compounds and to their hydroxylated and glucuronidated counterparts.<sup>202</sup> Similar to these sulfated aromatics, binding of other organic sulfates to HSA may be substantial and may serve as a mode for their retention and distribution *in vivo*.

#### PCB-HSA binding

Several experiments have measured the effects of PCB exposure on HSA activity. The effects of Aroclor 1254 on albumin gene expression and protein synthesis was reported in primary rat hepatocyte cultures. The increase in both of these factors was correlated to signaling through the aryl hydrocarbon receptor (AhR). This was done by relating the changes to the increase in expression of CYP1A1, which is mediated by the

AhR signaling pathway.<sup>161</sup> Furthermore, in rats, dietary exposure (0.03%) to Aroclor 1248 was shown to increase the synthesis of albumin,<sup>212</sup> and a study on the effects of PCB co-treatment (PCB 126 and PCB 153) on the lactational transfer of methyl mercury in mice reported an increase in albumin levels in maternal serum. This was correlated to an increase in PCBs detected in pup brain, kidney, and carcass.<sup>162</sup> Similarly, in a guinea pig *in situ* placental-model, the transfer of a hexa-chlorinated biphenyl was shown to be positively dependent on albumin concentration in the perfusion media.<sup>160</sup> In humans, however, an analysis of albumin concentration in a cohort of current and former transformer repair workers found a reduction in HSA concentration in blood samples.<sup>213</sup> This effect was also seen in an avian model where serum collected from pigeons after exposure to Aroclor 1254 exhibited a decrease in albumin concentration, concurrent with an increase in urea which indicated an increase in protein breakdown.<sup>214</sup> The inconsistencies in these reports stems from the difference in albumin proteins across species. This is evident in a comparison study of gull and human recombinant albumin and the relative affinities for organohalogens (i.e. heptachlorinated biphenyl, tetrabrominated diphenyl ether, and their metabolites) as it pertained to thyroid hormone binding and competition.<sup>215</sup> Regardless of the changes in albumin synthesis or degradation, studies of PCBs in blood consistently confirm that these compounds tend to be associated with the albumin-rich elements of fractionated blood samples across multiple species.<sup>157-159</sup>

The binding of individual PCB congeners to purified HSA has been studied to a lesser extent than mixtures binding to serum preparations. The binding of PCB 153 and the PCB 180 to HSA was determined using a combination of intrinsic fluorescence, probe displacement and molecular modelling. It was determined that both compounds bound to a single site of HSA, Sudlow Site II, and that binding was dominated by hydrophobic interactions.<sup>163, 165</sup> Interestingly, a separate study of PCB 118, 126, and 153 found that these compounds bound with high affinity to Sudlow Site I with no binding to Site II.

This work employed the intrinsic fluorescence of HSA and the use of a nonspecific fluorescent probe as well as molecular modelling.<sup>164</sup>

### Approach

The interest in LC-PCB sulfates and their high affinity for the thyroid hormone binding protein transthyretin suggests that other thyroid hormone binding proteins such as HSA may also bind these sulfates with high affinity. In the current work, we have measured the displacement of site-selective fluorescent probes from the two major drug-binding sites on HSA by LC-PCB sulfates. Two well-established selective probes (i.e., 5-dimethylamino-1-naphthalenesulfonamide (DNSA) for Site I and dansyl L-proline (DP) for Site II)<sup>210</sup> were used, and LC-PCBs, and their hydroxylated metabolites were included in the study, where available. This approach is useful in determining site-selectivity when concerning the binding to HSA, and it allows for a quantitation of binding affinity to the respective site. However, although it has been used to determine binding affinity constants using the method of Cheng and Prusoff, the fluorescent probes' affinity overlap for the two concurrently existing binding sites precludes the assumptions required for such an approach. Because of this, the results of the current work were reported alongside those for positive controls whose binding affinity constants have been published elsewhere using isothermal titration calorimetry.<sup>216</sup> Furthermore, the potential sulfatase activity of HSA with the LC-PCB sulfates was also evaluated by HPLC. Full methods and procedures are included in Chapter V: Materials and Methods.

### Results and discussion

#### Displacement of probes from HSA by PCBs, OH-PCBs, and PCB Sulfates

After incubation of the HSA with a site-selective probe, changes in fluorescence intensity of the probe were determined upon addition of the compound. Representative

graphs of the change in fluorescence intensity (% change) vs. log of ligand concentration are shown in Figures 3-2, and 3-3. Figures A-1 through A-6 of the appendix, include the binding curves for all reported compounds. The criterion that at least 50% of the probe was displaced within the range of ligand-concentrations tested was used to confidently ascribe an EC<sub>50</sub> value to a ligand. Those ligands that did not significantly interact with the HSA at concentrations less than 50μM were simply reported as having an EC<sub>50</sub> greater than 50μM. It was noted, however, that in a few cases (e.g., 4'-PCB 33 sulfate and 4'-PCB 35 sulfate in Figures 3-4, 3-5), the fluorescence signal increased at higher concentrations of ligand. These effects, however, were only seen at the higher concentrations of ligand that were beyond any physiological relevance and, therefore, were not further explored.

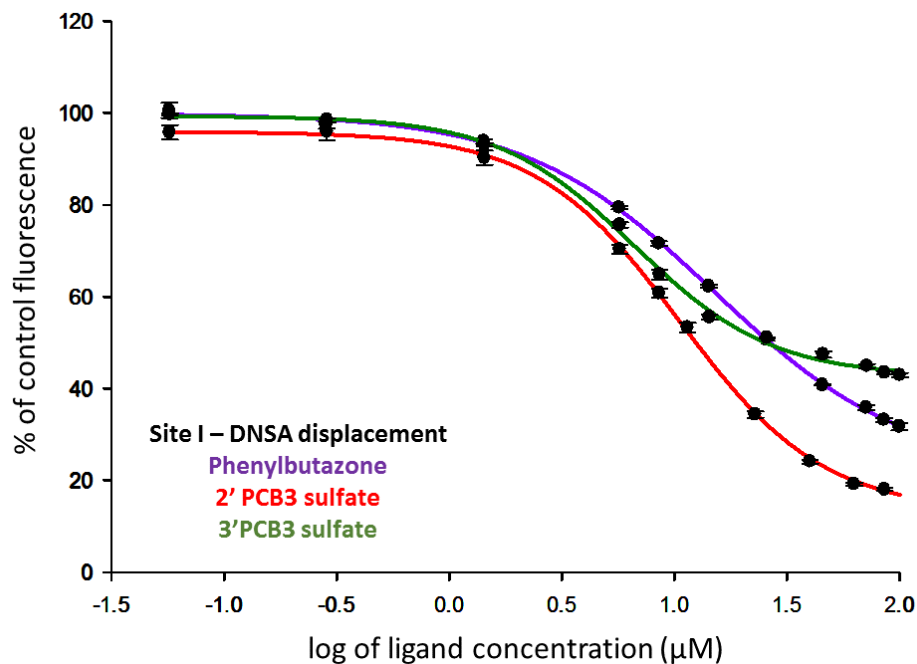


Figure 3-2 Binding curves for compounds that exhibited binding to Site I as determined by site-selective fluorescent probe displacement. Plots are of percent of control fluorescence vs. increasing ligand concentration. Each experiment consists of 10 $\mu$ M HSA and 20 $\mu$ M DNSA. Data were fit to a sigmoidal dose response ligand-binding algorithm (SigmaPlot v.11.0, Systat Software, Chicago, IL) and EC<sub>50</sub> values are reported in Figure 3-7. Mean  $\pm$  SE, n=3.

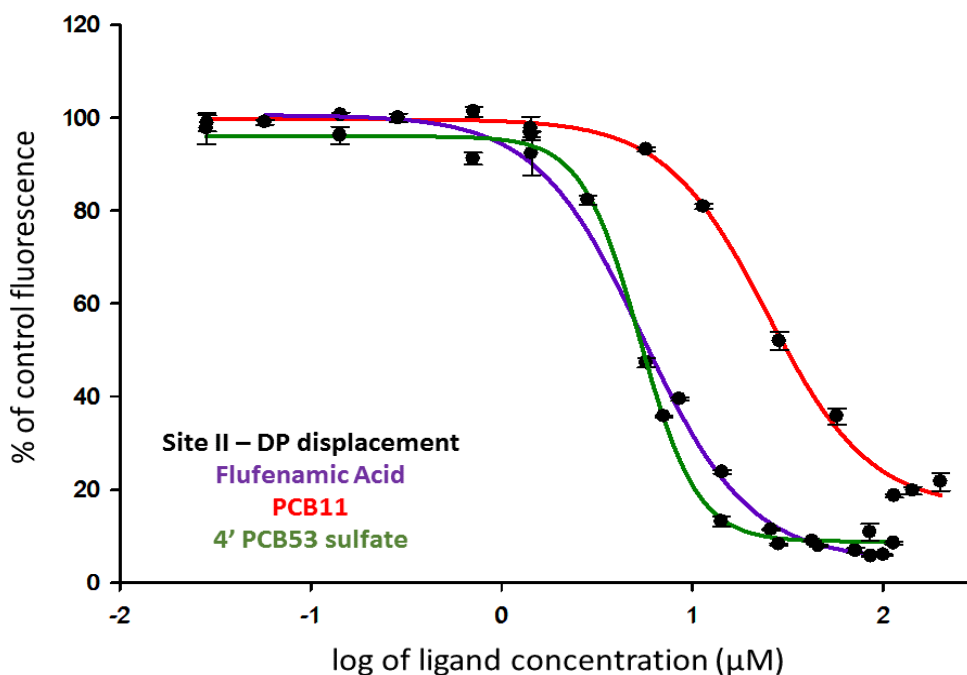


Figure 3-3 Binding curves for compounds that exhibited binding to Site II as determined by site-selective fluorescent probe displacement. Plots are of percent of control fluorescence vs. increasing ligand concentration. Each experiment consists of 10 $\mu$ M HSA and 5 $\mu$ M DP. Data were fit to a sigmoidal dose response ligand-binding algorithm (SigmaPlot v.11.0, Systat Software, Chicago, IL) and EC<sub>50</sub> values are reported in Figure 3-7. Mean  $\pm$  SE, n=3.

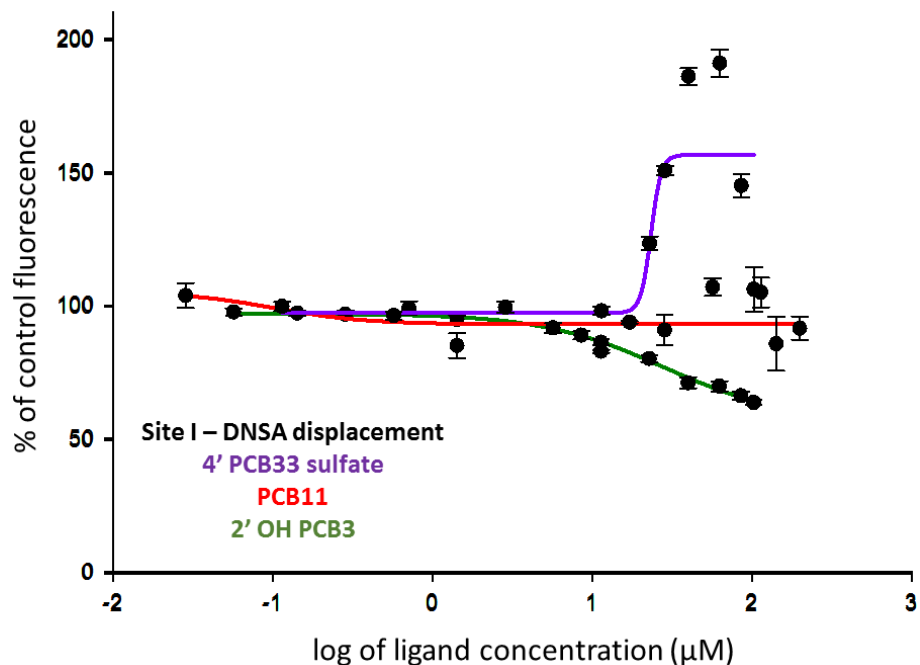


Figure 3-4 Binding curves for compounds that did not exhibit binding to Site I as determined by site-selective fluorescent probe displacement. Plots are of percent of control fluorescence vs. increasing ligand concentration. Each experiment consists of 10 $\mu$ M HSA and 20 $\mu$ M DNSA. Data were fit to a sigmoidal dose response ligand-binding algorithm (SigmaPlot v.11.0, Systat Software, Chicago, IL) and EC<sub>50</sub> values are reported in Figure 3-7. Mean  $\pm$  SE, n=3.

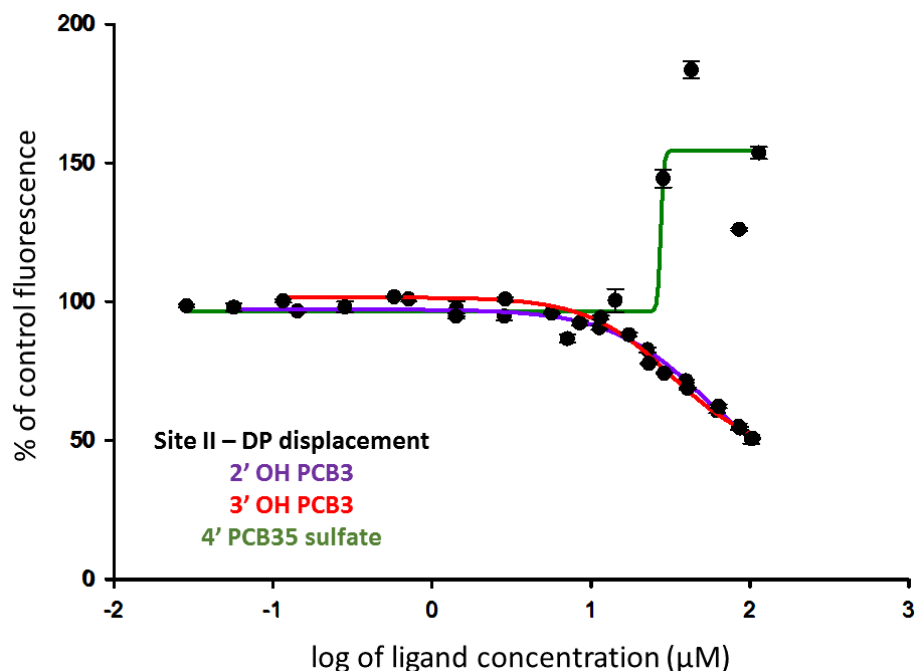


Figure 3-5 Binding curves for compounds that did not exhibit binding to Site II as determined by site-selective fluorescent probe displacement. Plots are of percent of control fluorescence vs. increasing ligand concentration. Each experiment consists of 10 $\mu$ M HSA and 5 $\mu$ M DP. Data were fit to a sigmoidal dose response ligand-binding algorithm (SigmaPlot v.11.0, Systat Software, Chicago, IL) and EC<sub>50</sub> values are reported in Figure 3-7. Mean  $\pm$  SE, n=3.

#### Recovery of PCB sulfates following incubation with HSA

Since HSA has been reported to catalyze hydrolysis of phosphates, glucuronides, and carboxylic acid esters, we sought to determine if a PCB sulfate could serve as a substrate for hydrolysis (i.e. sulfatase activity).<sup>217,218</sup> Moreover, it was also important to establish that the PCB sulfate concentration was not changing throughout the course of the experiment, with full recovery of the ligand. Analyses that were conducted by acetonitrile extraction and HPLC showed that during incubations up to 270 min, the PCB sulfates were stable. These results, shown in Figure 3-6, indicated that no hydrolysis of the PCB sulfate to the corresponding phenol was occurring during the experiment, and the quantitative extraction at each time point further indicated that no chemical changes



were occurring to the ligand in question. The PCB sulfates chosen for this study were a representative group of the chlorination number and patterns that were used for the HSA binding experiments (i.e., mono-, di-, tetra-chlorinated and *zero-ortho-* to *di-ortho* substitution).

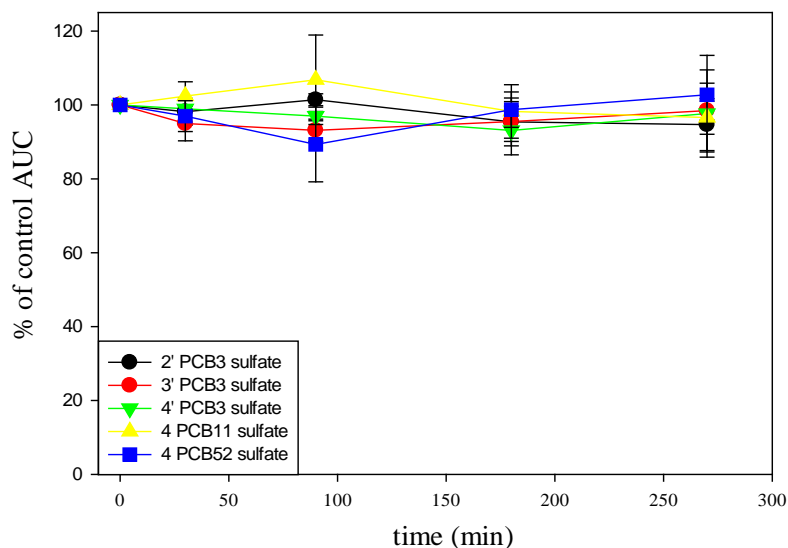


Figure 3-6 HPLC analysis of the recovery and reversibility of HSA-binding for representative PCB sulfates. HSA (50 $\mu$ M) and LC-PCB sulfate (50 $\mu$ M) incubated in potassium phosphate buffer (pH=7.4) and extracted into acetonitrile and analyzed by HPLC. Data points are presented as Mean  $\pm$  SE, n=3.

### Binding of the monochlorinated PCB 3 and its hydroxylated and sulfated metabolites to HSA

The data shown in Figure 3-7 illustrate the binding characteristics of the monochlorinated PCB 3 and its hydroxylated and sulfated metabolites to HSA. In vivo studies with Sprague-Dawley rats have shown that treatment with PCB 3 (via intraperitoneal injection or inhalation) is largely metabolized to hydroxylated (3'-OH-PCB 3, and 4'-OH-PCB 3) and sulfated (3-PCB 3 sulfate, 2'-PCB 3 sulfate, 3'-PCB 3

sulfate, and 4'-PCB 3 sulfate) derivatives, where the 4'-PCB 3 sulfate was the primary component.<sup>131, 219, 220</sup> In this work, neither PCB 3 nor its 2'-OH and 3'-OH metabolites bound with significant affinity to either of the two drug-binding sites on HSA. In comparison, their sulfated counterparts showed moderate to high affinity for both sites. Regarding the 4' metabolites, where both the chlorine and sulfate functional groups are *para* to the biphenyl linkage, there was significant binding to site II of both the OH-PCB and PCB sulfate, while the latter retained its high affinity for site I. A sulfate group at the 2-position of the same aromatic ring as the 4-chloro, however, resulted in some selectivity in binding at HSA Site I in preference to Site II, although this was not statistically different by a Student's t-test analysis. The results obtained for PCB 3 highlight a general trend in the binding of the LC PCBs studied, namely that HSA binding affinity follows the trend: PCB sulfate  $\geq$  OH-PCB > PCB.

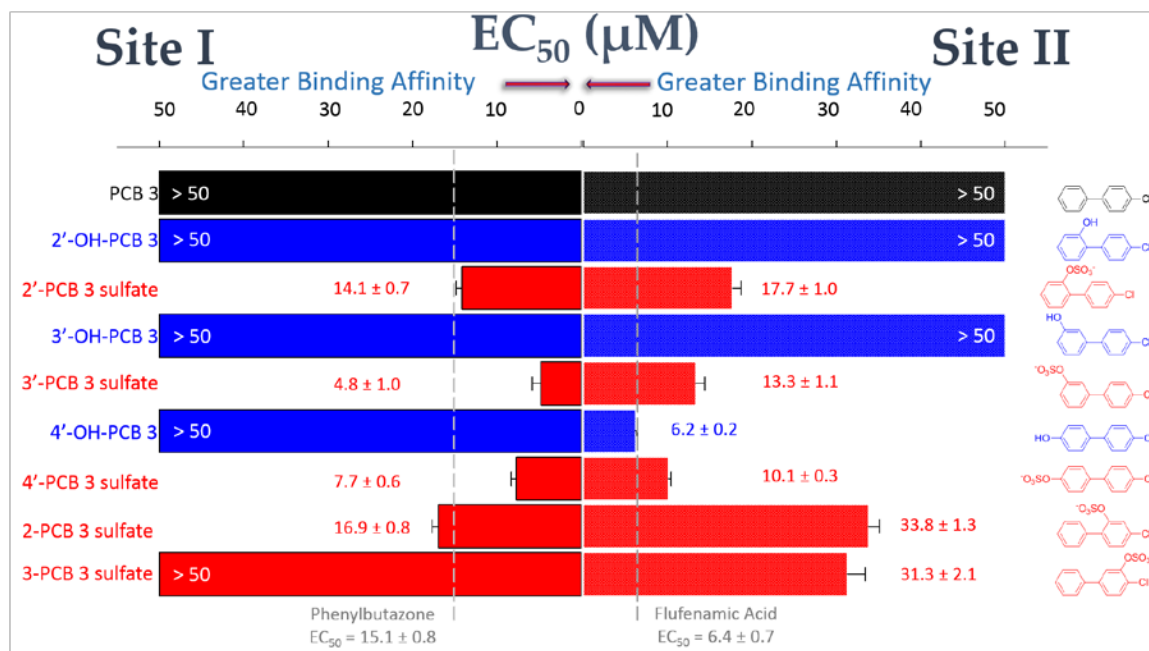


Figure 3-7 HSA-binding of the monochlorinated PCB 3 and its hydroxylated and sulfated metabolites. Site I binding (DNSA displacement) is shown at the left of the graph and Site II binding (DP displacement) is shown at the right. Color coding is used to differentiate the PCBs (black), OH-PCBs (blue), and PCB sulfates (red). Compound names appear on the left of the graph and the corresponding structure is at the right. EC<sub>50</sub> values were obtained as described in Materials and Methods and reported as Mean ± SE, n=3. The vertical dashed lines indicate the EC<sub>50</sub> values for the positive control ligands at each site.

#### Binding of dichlorinated PCB congeners and their metabolites to HSA

As seen in Figure 3-8, the binding of dichlorinated PCB congeners and their metabolites displayed significant selectivity for HSA site II. Unlike the results seen for the monochlorinated PCB sulfates, there was no significant binding to Site I observed for any of the dichlorinated PCB metabolites. Binding affinity to site II, however, was increased for the dichlorinated PCBs and OH-PCBs in comparison to their monochlorinated counterparts. It is interesting to note that in this set of compounds, one of the PCB sulfates (4'-PCB 12 sulfate) and one of the OH-PCBs (4'-OH PCB 9) showed no significant binding to either site. We have also noted a similar lack of interaction with either binding site on HSA for the trichlorinated 4'-PCB 35 sulfate. A common feature of these two PCB sulfates is the presence of a 3,4-dichloro substitution pattern in the aromatic ring that does not bear the 4'-sulfate. Further studies will be needed to ascertain the basis for this structural specificity for Site II binding.

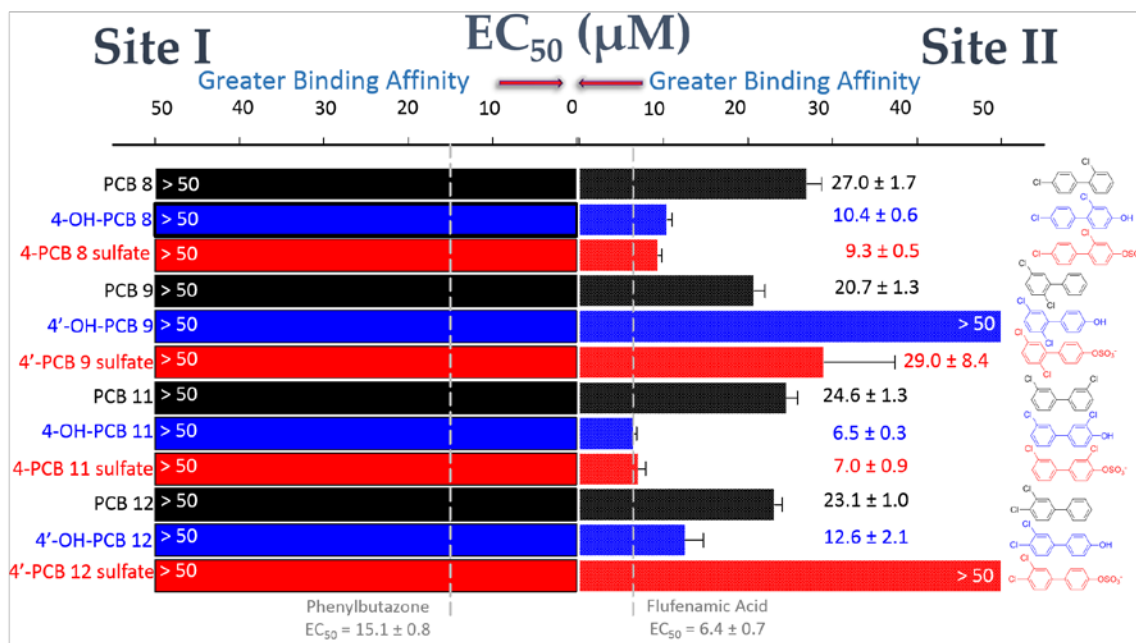


Figure 3-8 HSA-binding of dichlorinated PCB congeners and their hydroxylated and sulfated metabolites. Site I binding (DNSA displacement) is shown at the left of the graph and Site II binding (DP displacement) is shown at the right. Color coding is used to differentiate the PCBs (black), OH-PCBs (blue), and PCB sulfates (red). Compound names appear on the left of the graph and the corresponding structure is at the right.  $EC_{50}$  values were obtained as described in Materials and Methods and reported as Mean  $\pm$  SE, n=3. The vertical dashed lines indicate the  $EC_{50}$  values for the positive control ligands at each site.

### Binding of tri-, tetra-, and penta- PCB congeners and their metabolites to HSA

The interactions of selected tri- and tetra-chlorinated PCBs and their metabolites are shown in Figure 3-9. These results are consistent with the interpretation that HSA site II was the major binding site for most of the di-chlorinated PCB derivatives studied. With the exception of the tri-chlorinated 4'-PCB 35 sulfate, there was an association between the degree of chlorination and binding affinity for the hydroxylated and sulfated PCBs. While most of the tri-, tetra-, and penta-chlorinated PCB derivatives generally

appeared to have greater affinity for site II than those of the dichlorinated congeners, it was consistently observed that there was no binding of these compounds to Site I.

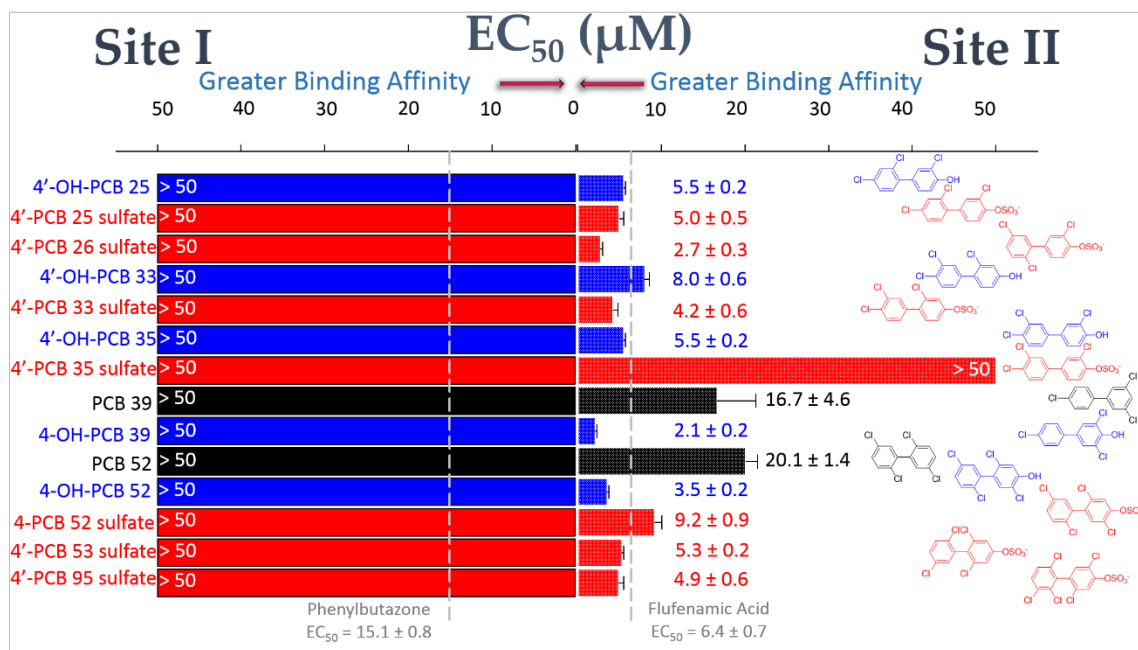


Figure 3-9 HSA-binding of tri-, tetra-, and penta- PCB congeners and their hydroxylated and sulfated metabolites. Site I binding (DNSA displacement) is shown at the left of the graph and Site II binding (DP displacement) is shown at the right. Color coding is used to differentiate the PCBs (black), OH-PCBs (blue), and PCB sulfates (red). Compound names appear on the left of the graph and the corresponding structure is at the right.  $EC_{50}$  values were obtained as described in Materials and Methods and reported as Mean  $\pm$  SE,  $n=3$ . The vertical dashed lines indicate  $EC_{50}$  values for the positive control ligands at each site.

### Discussion and conclusions

The method employed for this study involved the displacement of site-selective fluorescent probes from these two major drug binding sites. Although this approach does not allow for the direct determination of an affinity constant ( $K_a$ ), it gives information on selectivity for these two drug-binding sites, and, when reported alongside positive control

compounds, gives a relative determination of binding affinity. Because of the important role that albumins play in the distribution of endogenous and exogenous molecules in vertebrates,<sup>221</sup> the extent of association of PCBs and their metabolites with this protein is critical in understanding how they are distributed in living systems.

The data presented here suggests that LC-PCB sulfates bind with higher affinity than their corresponding PCB or OH-PCB counterparts. Furthermore, LC-PCBs and their hydroxylated and sulfated metabolites preferentially bind to Site II of the major drug binding sites in HSA. Interestingly, however, the monochlorinated metabolites bound with high affinity to both Sites I and II. Previous studies on the binding of individual PCB congeners to HSA found that binding occurred at Site II.<sup>163, 165</sup> One study, however, determined that binding occurred at Site I.<sup>164</sup> These seemingly contradictory conclusions stem from the differences in the studies. The latter study was based on a non-selective probe and the analysis of the intrinsic fluorescence of HSA, which can be misleading based on the protein's high flexibility. Furthermore, different crystal structures were used for the molecular dynamics simulations of which the latter study used a structure with no bound ligand.

The work presented here highlights the critical role that albumin may play in the binding, transport, and/or disposition of environmental toxic species such as PCBs and their metabolites. The presence and shared physiological roles of serum albumin in all vertebrates<sup>221</sup> makes the understanding of this interaction helpful in determining the fates of these toxic species and their distribution to sensitive tissues. This work also underscores the importance that metabolic hydroxylation and sulfation may have on binding to serum albumin and on subsequent distribution and half-lives of the PCB metabolites in humans as well as other animals. This potential for retention and redistribution of PCB sulfates supports the idea that this has been a largely overlooked component of the overall picture of PCB exposure and toxicity. An additional concern relates to the importance that albumin plays in the transplacental transfer of drugs and

other compounds to the developing fetus.<sup>141-143, 222</sup> Thus, it is of interest for future investigation whether such an albumin-mediated transfer of LC-OH-PCBs and LC-PCB sulfates may have a role in developmental effects that have been associated with PCB exposure. Finally, the selectivity of specific PCB metabolites for the major drug/toxicant binding sites on HSA may also be a factor that needs to be considered in the overall assessment of the contribution to toxic responses made by individual PCB congeners derived from exposure to PCB mixtures. This may be particularly important for airborne exposures to LC-PCBs where the PCB itself may be metabolized and not be detected in standard assays, yet OH-PCBs and PCB sulfates may be retained and either have toxic effects of their own or be further converted to other metabolites with adverse effects.

## CHAPTER 4: THE NEUROTOXICITY OF LC-PCB METABOLITES

### Persistent organic pollutants and neurotoxicity

The neurotoxic effects related to man-made organohalogenes have been the subject of many studies since the early 20<sup>th</sup> century. These persistent organic pollutants (POPs), of which PCBs are one class, have been implicated in adverse neurological effects in populations worldwide.<sup>170, 223</sup> As their moniker implies, they are resistant to degradation and are persistent in the environment and in living systems. Their presence at different periods of neuronal development (perinatally and throughout one's life) have been implicated in developmental dysfunction as well as neurodegenerative diseases that present later in life. Among these ailments are Parkinson's disease (PD), Alzheimer's disease (AD), amyotrophic lateral sclerosis (ALS) and dementia. Although the occurrence of these illnesses can sometimes overlap, they are each signified by distinct pathological origins and symptoms. Few occurrences of these diseases are seemingly due to purely genetic factors, and thus the interplay of environmental contaminants with genetic predispositions has been implicated in their etiology.<sup>224</sup> One example is the tentative connection between PD and rural living, thought to be due to high pesticide exposure.<sup>197</sup>

Parkinson's disease is the second most prevalent neurodegenerative disorder, second to AD, with an estimated 6.3 million affected worldwide. It is a progressive disease that causes motor ability dysfunction characterized by resting tremors, bradykinesia, and rigidity. Pathologically, it is associated with the presence of protein aggregates, Lewy bodies, within neuronal cells, and accompanied by a significant loss of dopaminergic neurons mostly found in the substantia nigra of the basal ganglia. Neurochemically, PD is marked by a decrease in the neurotransmitter dopamine and is susceptible to early symptomatic treatment with L-DOPA, a dopamine precursor, although the progressive nature of the disease precludes this treatment as serving as a cure.<sup>225</sup> These assessments have been confirmed in animal models treated with



neurotoxic agents as well as in human post-mortem brain samples of PD diagnosed patients after measuring the loss of pigmentation of the substantia nigra, due to dopaminergic neuronal cell loss.<sup>192, 226</sup> Interestingly, it is thought that the loss of these dopaminergic neurons begins far in advance of any evident symptoms.

### PCBs and neurotoxicity

After the accidental contamination of rice-cooking oil in Japan and Taiwan, it was evident that perinatal PCB exposure resulted in defects in cognition and motor development.<sup>227</sup> The follow-up studies in the United States on communities in Michigan and North Carolina verified these effects and further established the correlation between perinatal exposure to PCBs and neurodevelopmental effects involving motor skills, and cognitive function.<sup>167</sup> More recent studies have implicated PCB exposure in the increased instances of attention deficit and hyperactivity disorders and autism.<sup>228</sup> In adulthood, acute PCB exposure has been linked with neurological effects such as reduced memory and learning, and altered mood, depression, and social behaviors.<sup>61, 102</sup> Furthermore, it has been shown that PCBs (both coplanar and non-coplanar) can increase the permeability of the blood brain barrier (BBB).<sup>203</sup> These observations have influenced the current theory that early environmental exposures can lead to neurological anomalies later in life.<sup>198</sup>

### The dopaminergic system as a target for PCB induced neurotoxicity

The neurodevelopmental issues that arose after the events of Yusho and Yu Cheng influenced the hypothesis that the effects were as a result of alterations on the dopaminergic system. Furthermore, when considering PCB mixtures and congener-specific toxicities, it was often assumed that only co-planar PCBs exhibited toxic effects by their interactions with the AhR and downstream cytotoxic effectors, while non coplanar PCBs (*ortho*- substituted congeners) were inert in exhibiting toxic effects.<sup>108, 229</sup>

Early experimental evidence of PCBs' effects on the dopaminergic system was obtained in studies involving mice and rhesus monkeys.<sup>185, 195</sup> In rhesus monkeys, low level exposure to Aroclors 1016 and 1260 resulted in the regioselective (i.e., caudate nucleus, putamen, substantia nigra, and hypothalamus) decrease of dopamine content in the brain which persisted following removal of the PCB mixture exposure.<sup>230</sup> The changes in dopamine levels coincided with a co-accumulation of non-coplanar *ortho*-substituted LC-PCBs in these sensitive regions.<sup>186</sup> These results have since been confirmed in murine models (perinatal as well as adult exposure), and primary and immortalized dopaminergic neuronal cell models.<sup>189, 231</sup> In rat primary midbrain cell culture, Aroclor mixtures have been associated with a decrease in the concentration of free dopamine, decreases in the expression of the dopamine active transporter (DAT) and the vesicular monoamine transporter (VMAT), and, in some cases, a decrease in tyrosine hydroxylase (TH) activity.<sup>232-235</sup> Although many explanations concerning the origins of these results have been postulated (e.g. tyrosine hydroxylase inhibition, androgen or neurotransmitter dysfunction, mitochondrial toxicity, etc.), a concrete pathway leading to PCB-induced selective toxicity to the dopaminergic system has yet to be determined.

#### PCBs and Parkinson's disease

Epidemiological studies on the effects of PCBs on PD etiology have been conducted in cohorts ranging from those with high occupational exposure, and victims of terminal PD, to a cohort consisting of nuns in America. A series of studies on post-mortem brain samples from PD patients confirmed the selective accumulation of di-*ortho*-substituted PCBs in the midbrain (i.e., in the basal ganglia, and especially the caudate nucleus).<sup>187</sup> Furthermore, a retrospective mortality study of a previously established PCB occupational cohort, reported a correlation between previously recorded high levels of serum PCBs (approximately ten times that of community controls) and ALS, dementia, and PD for women.<sup>236</sup> Surprisingly, these same results were not seen in

the total study population or in men, despite the higher prevalence of PD in men in the general population.<sup>237</sup> A study of post-mortem brain tissue obtained from PD and non-PD patients via the Emory University Brain Bank, showed an increase in PCB concentration in brain tissue accompanied by increased nigral depigmentation in terminal PD patients.<sup>192</sup> The same study employed a population of women and found that nigral depigmentation was also correlated with brain PCB concentrations, even in the absence of PD symptoms. The women in this latter cohort were part of the Nun Study which was established as a control for the general population in the midwestern, eastern, and southern United States. As in most epidemiological cases, there is an intrinsic difficulty in assessing the correlation between the exposure to and the onset of the disease by a distinct toxic species. Although these previously mentioned studies appear to make this positive correlation (i.e., increased PCB exposure leads to PD etiology), there are epidemiological studies that conclude the contrary.<sup>238, 239</sup> In fact, a Finish study found that increasing serum PCB concentrations was inversely correlated with the occurrence of PD.<sup>240</sup> These discrepancies may be attributed to differences in diet, lifestyle, co-exposure to other toxicants, genetic variations, etc.

#### PCB metabolites and neurotoxicity

Of the PCB metabolites, OH-PCBs have been the more widely studied class concerning neurotoxic effects. Epidemiological studies have shown a correlation between the concentrations of OH-PCBs and reduced infant thyroid stimulating hormone.<sup>241</sup> In Eastern Slovakia, a positive correlation was seen between 4-OH-PCB107 and decreased cognitive development, memory, and habituation.<sup>118</sup> Similarly, a Dutch study correlated prenatal exposure to this congener metabolite with neurological dysfunction when assessed at 3 months.<sup>173</sup> This study, however, also reported a positive effect of PCBs on neurological function at the same age.<sup>117</sup> *In vitro* studies with OH-PCBs have shown neurotoxic effects with implications in dendritic development, ROS

production, protein kinase C translocation, and altered calcium homeostasis.<sup>180, 182, 183, 242</sup> In fact, the effects of PCBs on calcium signaling via the ryanodine receptor has gained much interest as a convergent mechanism towards both toxicity and aberrant neuronal cell development.<sup>179, 243, 244</sup>

### Neuronal cellular models

The use of animal models to study neuronal effectors is a valuable resource for determining various aspects of toxicity (e.g., brain distribution and accumulation, regio-selective toxicity, behavioral and developmental effects, etc.). For initial studies, however, animal models may be more difficult due to the necessary requirements for animal acquisition, housing, and disposal. The use of cultured cells (primary and immortalized) provides a controlled environment in which to evaluate cytotoxicity, biochemical pathways, cell signaling and cascades, the formation of reactive oxygen species (ROS), and calcium homeostasis. Cellular models can be derived from distinct portions of the brain that dictate their biochemical activities and characteristics. In neurochemistry, cell culture has been used to further the understanding of neurotoxicity, neuronal signaling, and its dysfunction. In essence, cellular models serve as minute examples of how their tissue of origin may react *in vivo*.

### N27 cells

The N27 cells are a T-antigen immortalized rat mesencephalic dopaminergic neuronal cell line. They were established to study the effects of neuronal transplantation in animal models of Parkinsonism, and as a tool for neurobiological studies.<sup>245</sup> They have since been extensively used in the study of PD, its etiology, potential pathways, and treatment options, as well as in determining the selective toxicological pathways by xenobiotics on the dopaminergic system.<sup>246</sup>

### SH-SY5Y cells

The SH-SY5Y cells are an immortalized human cell line derived from a metastatic neuroblastoma isolated from the bone marrow. Similar to the N27 cells, this cell line has also been used in the study of PD as a dopaminergic cell model. Unlike the N27 cells, however, the dopaminergic characteristics of these cells are debatable. Studies have shown that the SH-SY5Y cells can be further differentiated to exhibit more dopaminergic characteristics by treatment with chemical agents.<sup>247</sup> Various studies, however, use the native SH-SY5Y cells without differentiation. In an undifferentiated state, these cells are commonly accepted as having a cholinergic activity, although this assumption is also debatable.<sup>247-249</sup>

### HepG2 cells

The HepG2 cells are immortalized human derived liver cells. The biochemical characteristics of these cells are substantially different from those of the neuronal models, due to their different tissues of origin. When compared to primary hepatic cells, the HepG2 cell line has been shown to exhibit comparable levels of phase II conjugation enzyme activities, as well as the sensitivities of nuclear receptors to xenobiotic-induced signaling.<sup>250</sup> A study in HepG2 cells of the role that PCBs play in the induction of gene expression using microarray analysis found an enrichment in apoptosis and oxidative stress pathways. This study further determined that the effects were congener specific and acted by divergent mechanisms (e.g., co-planar PCBs via the AhR vs. non co-planar PCBs via the tumor necrosis factor (TNF) receptor).<sup>251</sup> Furthermore, in a related study, the cellular uptake of individual PCB congeners alongside their toxic response was conducted, and it was reported that cytotoxicity was related to rate of uptake as well as maximal internal concentrations.<sup>252</sup>

## Determining cell viability

There are various endpoints that can be determined to assess the viability of a cell. The most commonly used endpoints are mitochondrial health, membrane permeability, nuclear fragmentation, and ATP synthesis. Mitochondrial health can be assessed by their reductive capability. One method to assess this is by measuring the mitochondrial reduction of a tetrazolium dye to the water insoluble formazan product. Solubilization of the product results in a color change (absorbance detected at 570nm), and the extent of spectroscopic change can be used to determine cellular viability.<sup>253</sup> Cell membrane permeability can be assessed by measuring the release of lactate dehydrogenase (LDH) from the cell into the extracellular matrix.<sup>254</sup> A hallmark of cell death, is the loss of cell membrane integrity which allows for cytosolic contents to move from that cellular compartment into the extracellular medium. Lactate dehydrogenase is found in virtually all living cells and catalyzes the reduction of pyruvate to lactate via the oxidation of NADH to NAD<sup>+</sup>. This conversion can be monitored spectroscopically as the consumption of NADH at 340nm.<sup>254</sup>

## Approach

The approach taken in this study is to assess the role that hydroxylated and sulfated metabolites may play in the neurotoxicity associated with exposure to LC-PCBs. It has been shown that LC-PCBs are readily metabolized to PCB sulfates *in vivo*,<sup>131, 219, 220</sup> and bind with high affinity to the serum proteins transthyretin and albumin.<sup>129</sup> Furthermore, PCB exposure is linked with an increase in BBB-permeability.<sup>203</sup> It is therefore necessary to assess the role that PCB sulfates may play in neurological dysfunction, and this work will help to determine whether PCB sulfates may be largely overlooked as toxic species. Because the dopaminergic system has been proposed to lie at the core of PCB-related neurotoxic effects, the N27 cell line was used in the current study to represent this brain system. As a neuronal model, toxicity to the

SH-SY5Y cell line was assessed alongside the dopaminergic cell line to serve as a comparison. Furthermore, the HepG2 cell line was used to represent a non-neuronal cell model. Figure 4-1 illustrates the LC-PCBs and metabolites included in this study. They were chosen to represent some of the most frequently detected PCB congeners in Chicago air samples, and encompass varying chlorination degrees and substitution patterns. These subtle differences dictate, among other properties, their tendency to adopt a co-planar configuration (i.e., non-, mono-, di-*ortho*-substituted LC-PCBs).<sup>104</sup> The toxicity of these compounds was assessed by evaluating mitochondrial integrity (MTT reduction), and cell membrane permeability (LDH release) after exposure to target compounds for 24 hours at varying concentrations. Considering the results presented in Chapter 3 (i.e., PCB sulfates bind with high affinity to HSA), the experimental exposure media contained no serum supplementation, which is representative of the low protein content in the central nervous system. Generally it is accepted that HSA concentration in cerebrospinal fluid (CSF) in a healthy adult is less than 0.7% that of serum.<sup>255</sup> PCB induced cytotoxicity studies commonly use serum supplemented media during exposure. Thus, the current study also included an assessment of the presence of albumin or serum supplementation in the media on the toxic response after exposure to LC-PCBs and metabolites. Furthermore, the distribution of the treatment compounds was assessed using high pressure liquid chromatography (HPLC). By measuring their concentrations in the extracellular and intracellular experimental components, it was possible to determine their permeability into cells, as well as detect changes in their chemical identities (i.e., oxidation of parent, hydrolysis of sulfates, or sulfation of OH LC-PCBs).

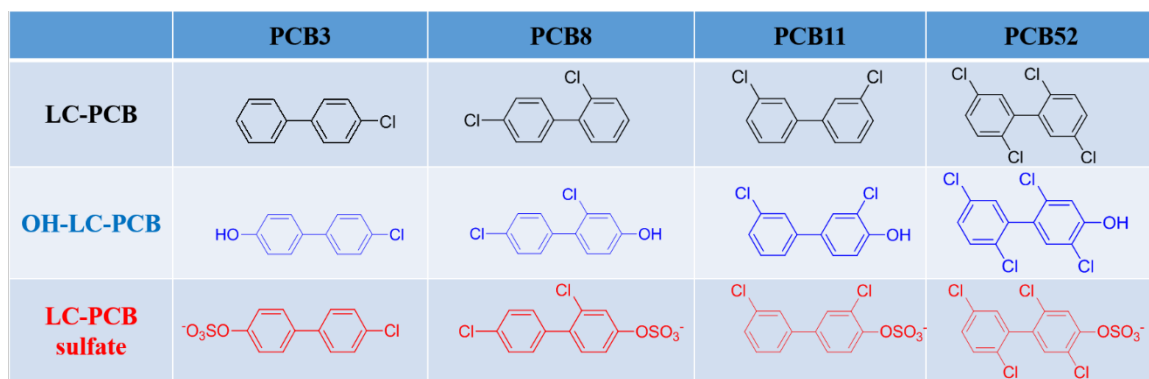


Figure 4-1 A representation of the compounds (PCBs, OH-PCBs, PCB sulfates) used in the neurotoxicity studies. The parent PCBs are among the 20 most frequently detected congeners in Chicago air samples. All authentic standards were prepared and characterized in the synthesis core of the Iowa Superfund Research Program.<sup>256-258</sup>

## Results and discussion

Detailed procedures for the work presented here are included in Chapter 5:

Materials and methods.

### Cell viability by MTT reduction - results

#### Parent LC-PCBs

Figure 4-2 shows the results from MTT reduction across the three cell lines for the four parent PCBs. The graphs are plots of MTT reduction capability (expressed as a percent of vehicle treated control values) as a function of PCB concentration. Plotting the data in a logarithmic form allowed for analysis by fitting to a sigmoidal dose response curve from which an effective concentration (EC<sub>50</sub>) that afforded half of the total mitochondrial effect was calculated. In the cases where a sigmoidal dose response was evident and able to be modeled, the fitted curve is indicated by a dashed line. This is contrary to those that did not display a sigmoidal curve, which are represented by line/scatter plots. The resulting EC<sub>50</sub> values are included in Table 4-1.



Generally, the LC-PCBs in this study showed little toxicity to all cell lines. The di-*ortho*-substituted congener PCB 52, however, showed moderate toxicity to the dopaminergic N27 cell line with an EC<sub>50</sub> value of 28.5 ± 2.4 μM. In fact, in the N27 cells, all PCBs showed some toxicity within the experimental range (i.e., up to 100μM), however to a lesser degree than PCB 52.

#### OH-LC-PCBs

Figure 4-3 shows the results of MTT analysis for the neuronal and hepatic cell lines treated with OH-LC-PCBs. These data indicate that the OH-LC-PCBs were more toxic to all tested cell lines than the corresponding parent PCBs, however with higher potency to the neuronal cells. The mono-chlorinated 4'-OH-PCB 3 showed the least potent toxicity throughout, and the *ortho*-chlorinated congeners (4-OH-PCB 8 and 4-OH-PCB 52) showed the highest. The dichlorinated non-*ortho*-substituted 4-OH-PCB 11 exhibited selective toxicity to the neuronal cells with significantly higher potency in the dopaminergic neuronal cells. This result was similar to that seen for treatment with the dichlorinated mono-*ortho*-congener OH-PCB 8. Interestingly, the tetra-chlorinated di-*ortho*-substituted 4-OH-PCB 52 showed the highest toxicity with all three cell lines, however it displayed significantly higher potency with the neuronal SH-SY5Y cells when compared to both the N27 and HepG2, although the effect was still selective for the neuronal cells (i.e., SH-SY5Y > N27 > HepG2). The dopaminergic N27 cells generally exhibited the highest susceptibility to the OH-LC-PCBs tested, with the exception of treatment with 4-OH-PCB 52 which had a more potent toxic response in the SH-SY5Y cells. These results are summarized in Table 4-1.

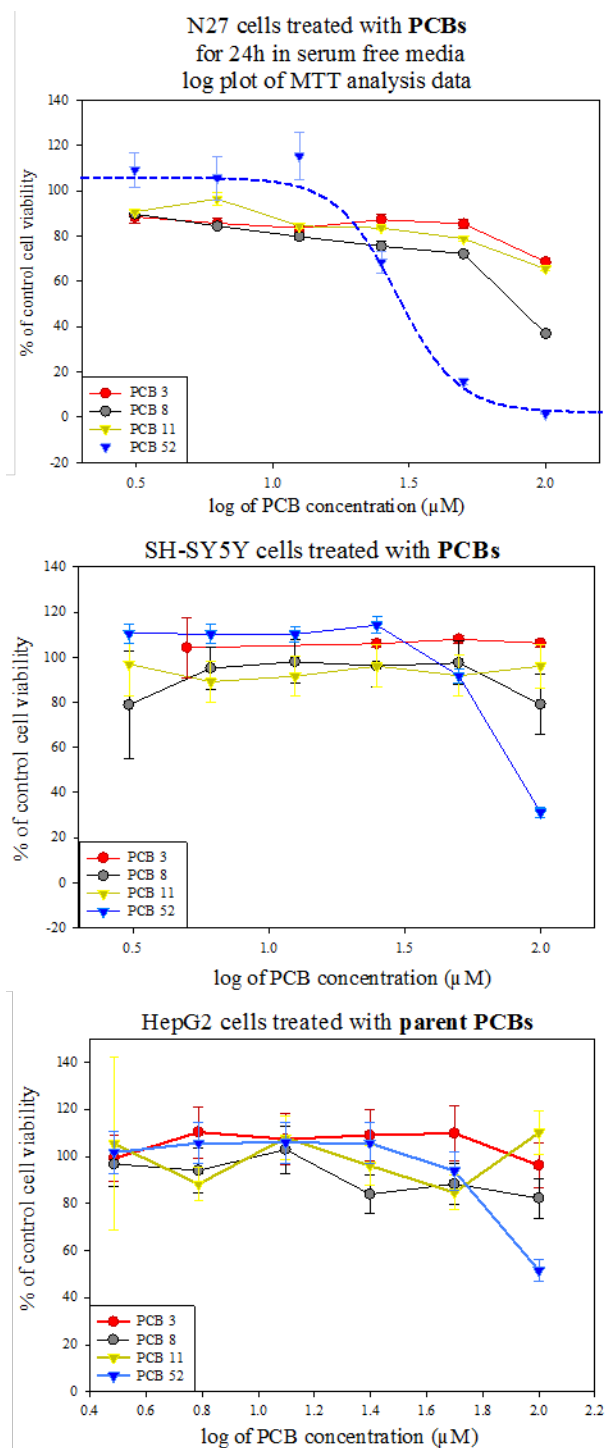


Figure 4-2 The cell viability of N27, SH-SY5Y, and HepG2 cells after exposure to LC-PCBs in serum free media for 24h assessed by MTT reduction. The data were represented as a percent of vehicle control vs. the log of the LC-PCB concentration, and fit to a four parameter logistic curve using SigmaPlot v.11.0, Systat Software, Chicago, IL. Data points are the mean  $\pm$  SEM, n=3.

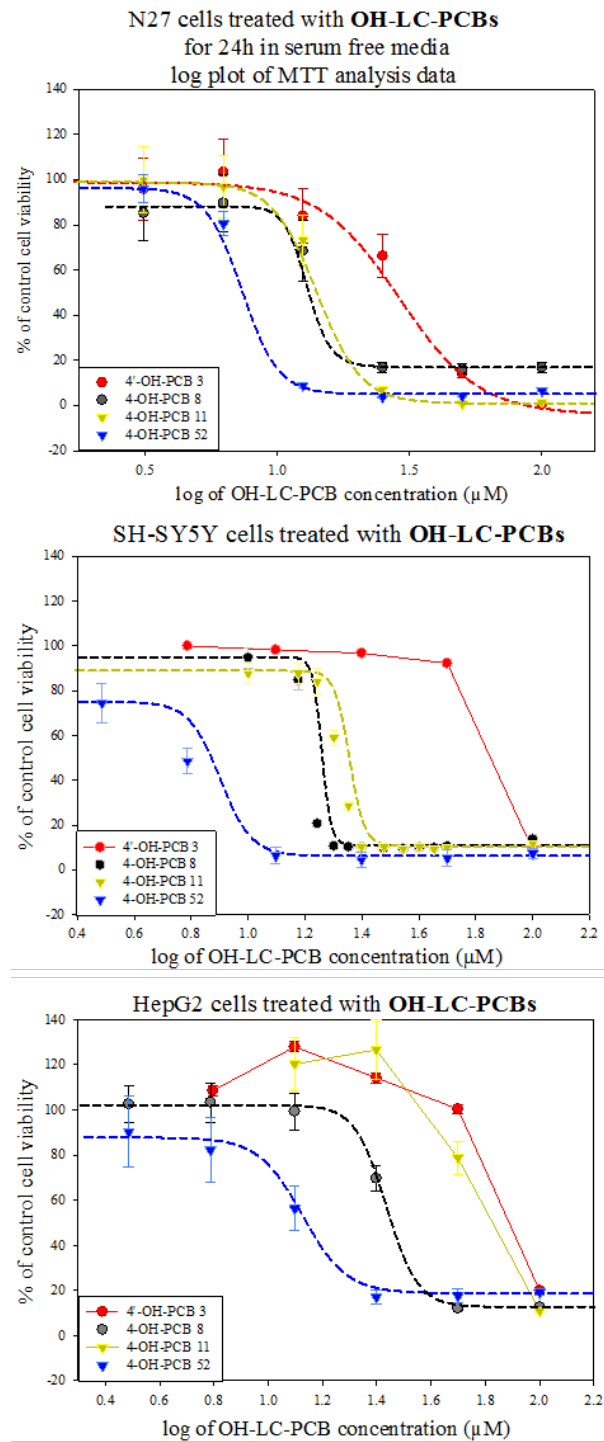


Figure 4-3 The cell viability of N27, SH-SY5Y, and HepG2 cells after exposure to OH-LC-PCBs in serum free media for 24h assessed by MTT reduction. The data were represented as a percent of vehicle control vs. the log of the OH-LC-PCB concentration, and fit to a four parameter logistic curve using SigmaPlot v.11.0, Systat Software, Chicago, IL. Data points are the mean  $\pm$  SEM, n=3.

### LC-PCB sulfates

Figure 4-4 shows the results of MTT analyses after treatment of each cell line with LC-PCB sulfates. The results indicate that, similar to the effects with LC-PCBs, LC-PCB sulfates also showed limited toxicity to the cell lines tested, at least with regards to mitochondrial function. Interestingly, the 4-PCB 52 sulfate showed toxicity in all cell lines within the concentration range tested. Furthermore, the dopaminergic N27 cell line exhibited a significantly lower EC<sub>50</sub> value (i.e., higher potency) than either the SH-SY5Y or HepG2 cells, by a factor of approximately 2. Of further importance is that the 4-PCB 52 sulfate exhibited a toxic response similar to that of many of the OH-LC-PCBs with the exception of its hydroxylated counterpart, 4-OH-PCB 52. The results are summarized in Table 4-1.

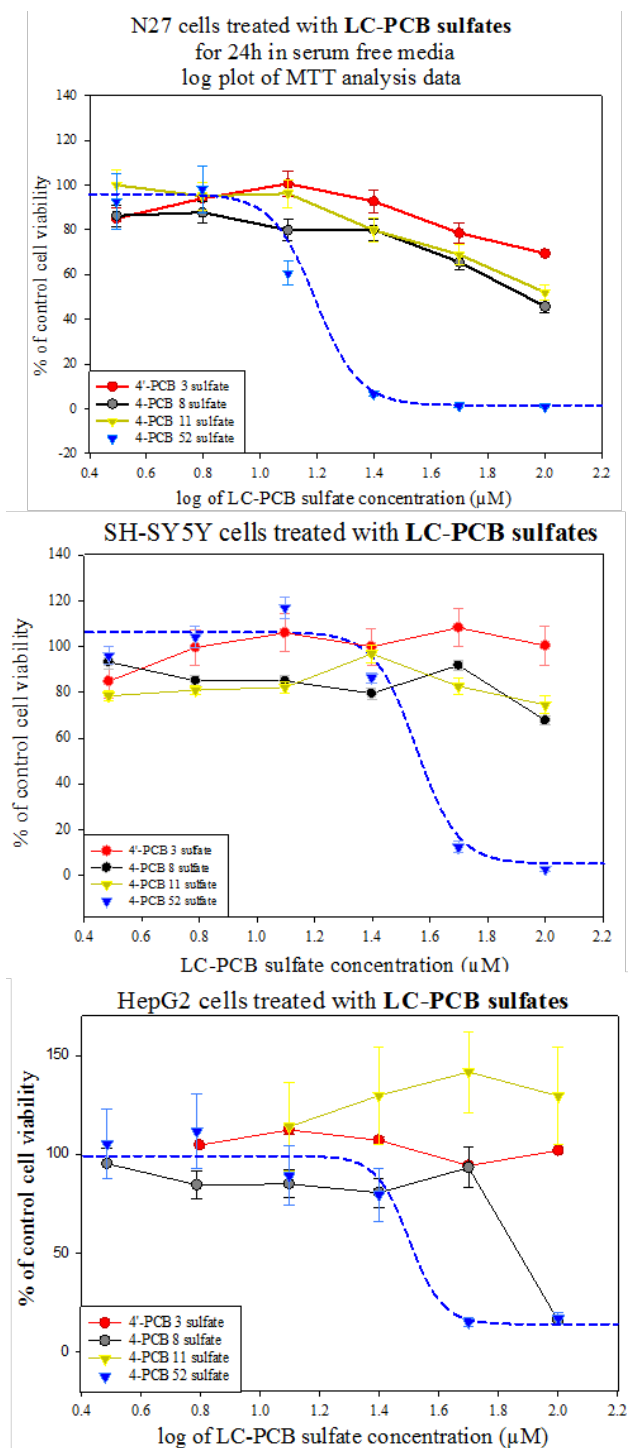


Figure 4-4 The cell viability of N27, SH-SY5Y, and HepG2 cells after exposure to LC-PCB sulfates in serum free media for 24h assessed by MTT reduction. The data were represented as a percent of vehicle control vs. the log of the LC-PCB sulfate concentration, and fit to a four parameter logistic curve using SigmaPlot v.11.0, Systat Software, Chicago, IL. Data points are the mean  $\pm$  SEM, n=3.

Table 4-1 A comparison of MTT-reduction EC<sub>50</sub> values across three cell lines (N27, SH-SY5Y, HepG2) after exposure to LC-PCBs or their hydroxylated or sulfated metabolites in serum free media for 24h.

<b>Compound</b>	<b>N27 cells</b>	<b>SH-SY5Y cells</b>	<b>HepG2 cells</b>
<b>PCB 3</b>	<b>&gt; 50</b>	<b>&gt; 50</b>	<b>&gt; 50</b>
<b>PCB 8</b>	<b>&gt; 50</b>	<b>&gt; 50</b>	<b>&gt; 50</b>
<b>PCB 11</b>	<b>&gt; 50</b>	<b>&gt; 50</b>	<b>&gt; 50</b>
<b>PCB 52</b>	<b>28.5 ± 2.4</b>	<b>&gt; 50</b>	<b>&gt; 50</b>
<b>4'-OH-PCB 3</b>	<b>31.4 ± 4.2</b>	<b>&gt; 50</b>	<b>&gt; 50</b>
<b>4-OH-PCB 8</b>	<b>13.8 ± 2.1<sup>b</sup></b>	<b>16.2 ± 0.05</b>	<b>27.0 ± 0.7<sup>b,c</sup></b>
<b>4-OH-PCB 11</b>	<b>15.2 ± 0.2<sup>a</sup></b>	<b>20.7 ± 0.1<sup>a</sup></b>	<b>&gt; 50</b>
<b>4-OH-PCB 52</b>	<b>7.9 ± 0.1<sup>a,b</sup></b>	<b>6.7 ± 0.2<sup>a,c</sup></b>	<b>13.0 ± 0.3<sup>b,c</sup></b>
<b>4'-PCB 3 sulfate</b>	<b>&gt; 50</b>	<b>&gt; 50</b>	<b>&gt; 50</b>
<b>4-PCB 8 sulfate</b>	<b>&gt; 50</b>	<b>&gt; 50</b>	<b>&gt; 50</b>
<b>4-PCB 11 sulfate</b>	<b>&gt; 50</b>	<b>&gt; 50</b>	<b>&gt; 50</b>
<b>4-PCB 52 sulfate</b>	<b>14.3 ± 0.6<sup>a,b</sup></b>	<b>32.7 ± 2.2<sup>a</sup></b>	<b>28.8 ± 3.9<sup>b</sup></b>

<sup>a</sup>significant difference between N27 and SH-SY5Y (P<0.05)

<sup>b</sup>significant difference between N27 and HepG2 (P<0.05)

<sup>c</sup>significant difference between SH-SY5Y and HepG2 (P<0.05)

Statistical significance determined using one way ANOVA with Bonferoni post hoc analysis on SigmaPlot v. 11.0, Systat Software, Chicago, IL.

#### Cell viability by LDH release - results

##### LC-PCBs

The results of LDH release of each cell line after treatment with LC-PCBs is shown in Figure 4-5. Overall, the results from LDH-release assays mimic those that were obtained using the reduction of MTT. There was minimal toxic response (i.e., LDH release) to treatment with these compounds. Also similar to the MTT reduction results, PCB 52 was the only congener that elicited a toxic response, however not in the HepG2 cells as was seen previously. Interestingly, the release of LDH, even at the highest

concentrations, was not quantitative in comparison to the high control (i.e., treatment with the cell lysing detergent Triton-X 100), which was seen in the mitochondrial assays. Also, the effect was greater in the SH-SY5Y cells when compared to the dopaminergic N27 cells which was contrary to what was seen in the MTT reduction assay. Due to the minimal change in LDH release, the data obtained for the N27 cells were not amenable to analysis by fitting to a sigmoidal dose-response curve, and a quantitative assessment of toxicity was not possible.

#### OH-LC-PCBs

The results for LDH release upon treatment with OH-LC-PCBs are shown in Figure 4-6 and the summarized  $EC_{50}$  values are presented in Table 4-2. Again, these results were generally consistent with those obtained in the MTT-reduction experiments. The hydroxylated PCB 3 congener exhibited the lowest toxicity to all cells tested. While some response was present in the N27 cells, the signal was low enough that a sigmoidal dose curve fit was unable to be fit to the data. In fact, this was true of most of the LDH release results. The lack of complete cellular LDH release (when compared to absolute release in the high controls) indicated that some membrane integrity remained even when the cells were not metabolically active by MTT-reduction analysis. Despite this trend, it was possible to obtain  $EC_{50}$  values for many of the cell treatment experiments by non-linear curve fitting of the data on LDH release. The di- and tetra-chlorinated OH-LC-PCBs displayed a selective toxicity to the neuronal cells versus the hepatic cells, with the *ortho*-substituted congeners doing so at a lower concentration (higher potency). The di-*ortho*-substituted 4-OH-PCB 52 showed the highest toxicity in all cells, and it showed a significantly lower  $EC_{50}$  value in the dopaminergic cells. The activity of this congener metabolite in the neuronal cells is contrary to what was determined in the MTT reduction assay (i.e., N27 vs. SH-SY5Y selective toxicity), however in both cases selective toxicity was observed for the neuronal cells in relation to the hepatic cells.

### LC-PCB sulfates

Figure 4-7 shows the LDH release results for PCB sulfate-treatment of the neuronal and non-neuronal cell lines. Again, no toxic response was evident by LDH-release in most cases except for the 4-PCB 52 sulfate. For the experiments in which  $EC_{50}$  values could be calculated (i.e., treatment of the SH-SY5Y and HepG2 cells), the data correspond well with the MTT reduction experimental values. In the case of the N27 cells, however, the signal was too low to obtain a proper fit to the sigmoidal dose response. The  $EC_{50}$  data for these experiments are summarized in Table 4-2.



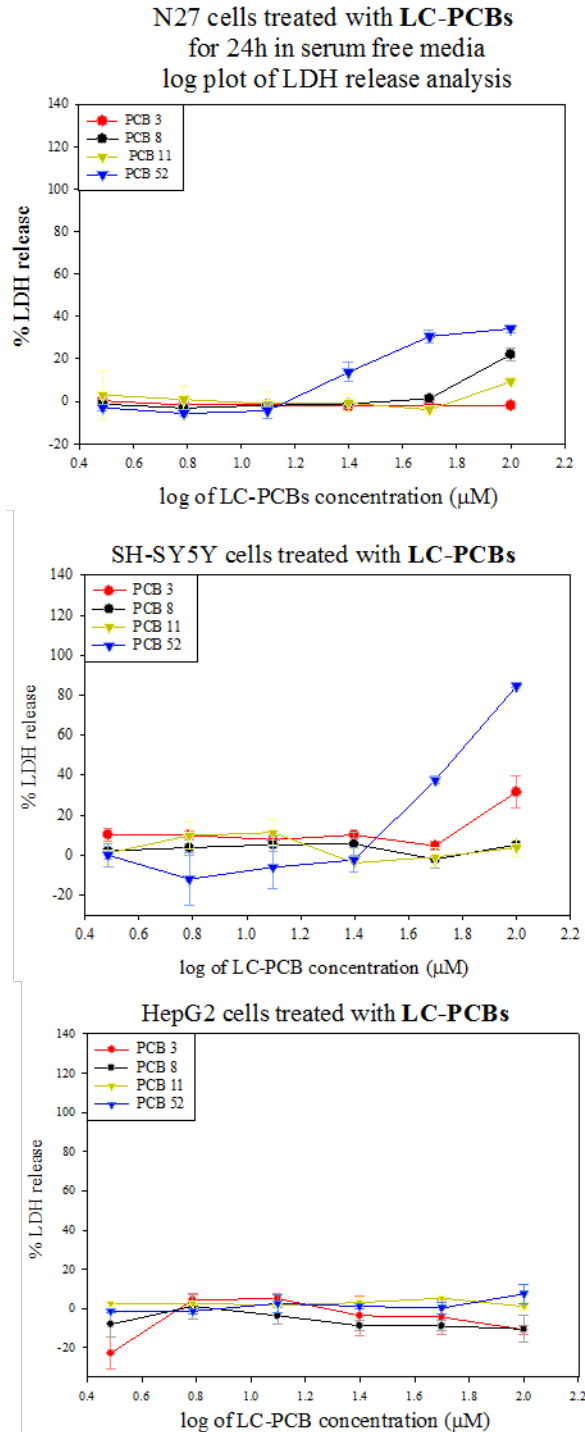


Figure 4-5 The cell viability of N27, SH-SY5Y, and HepG2 cells after exposure to LC-PCBs in serum free media for 24h as assessed by LDH release. The data were represented as a percent of vehicle control vs. the log of the LC-PCB concentration, and fit to a four parameter logistic curve using SigmaPlot v.11.0, Systat Software, Chicago, IL. Data points are the mean  $\pm$  SEM, n=3.

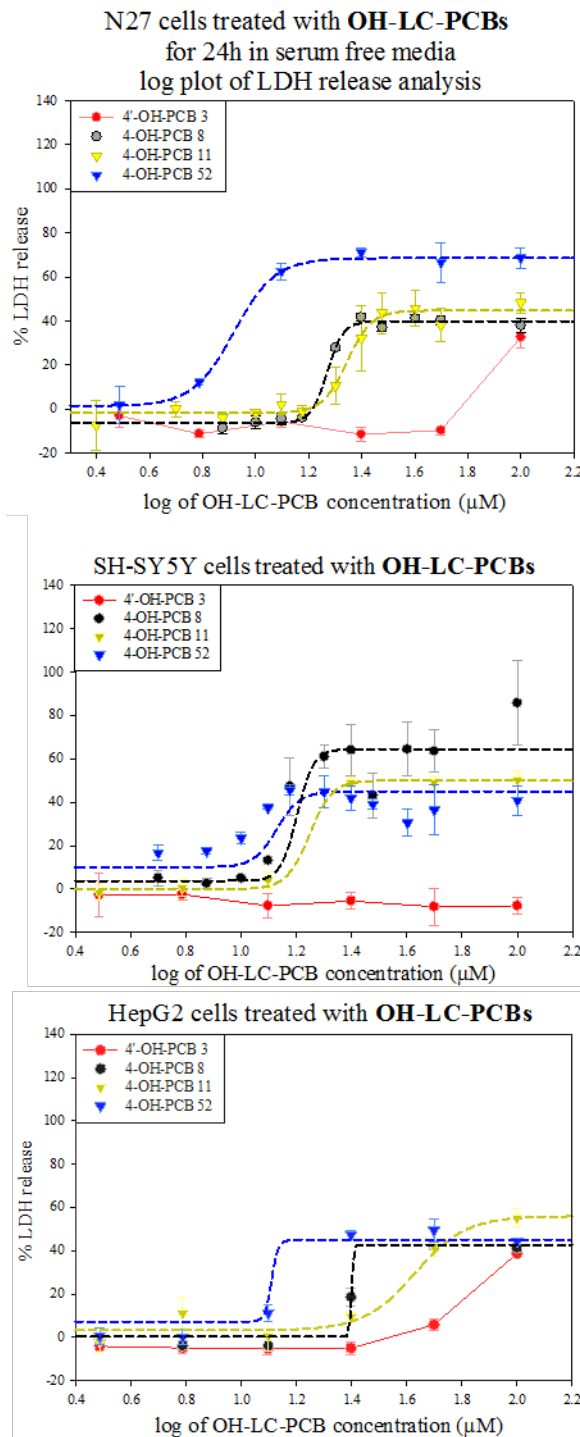


Figure 4-6 The cell viability of N27, SH-SY5Y, and HepG2 cells after exposure to OH-LC-PCBs in serum free media for 24h as assessed by LDH release. The data were represented as a percent of vehicle control vs. the log of the OH-LC-PCB concentration, and fit to a four parameter logistic curve using SigmaPlot v.11.0, Systat Software, Chicago, IL. Data points are the mean  $\pm$  SEM, n=3.

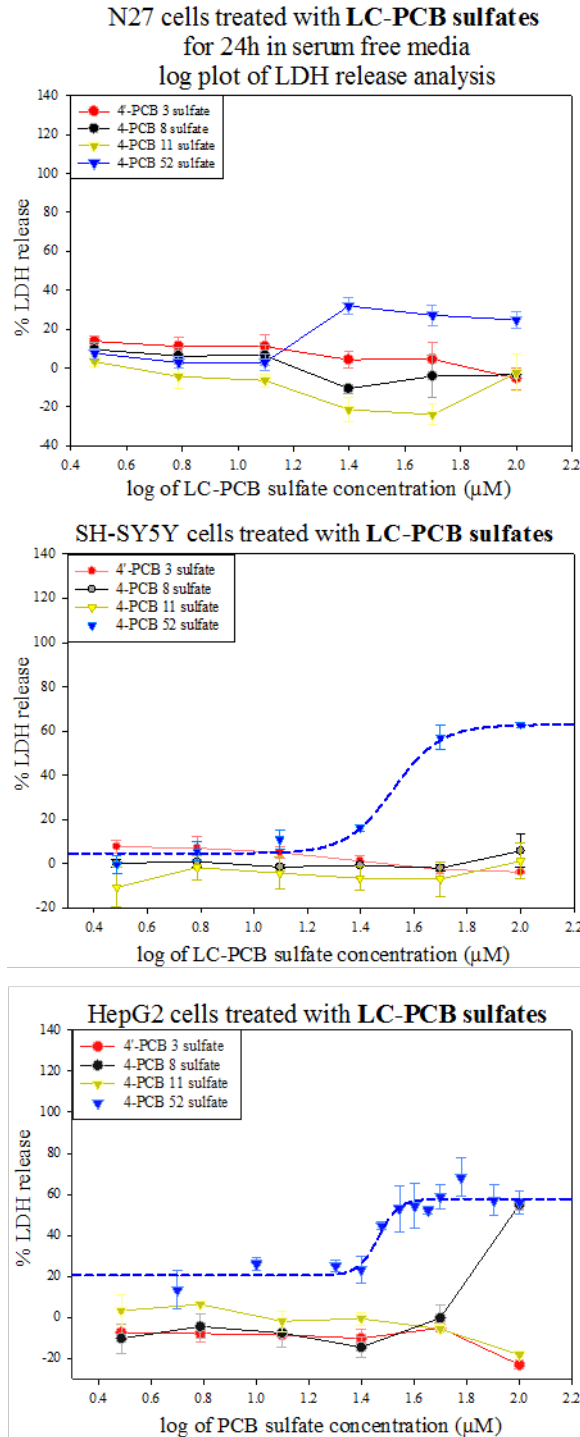


Figure 4-7 The cell viability of N27, SH-SY5Y, and HepG2 cells after exposure to LC-PCB sulfates in serum free media for 24h as assessed by LDH release. The data were represented as a percent of vehicle control vs. the log of the LC-PCB sulfate concentration, and fit to a four parameter logistic curve using SigmaPlot v.11.0, Systat Software, Chicago, IL. Data points are the mean  $\pm$  SEM, n=3.

Table 4-2 A comparison of LDH-release EC<sub>50</sub> values across three cell lines (N27, SH-SY5Y, HepG2) after exposure to LC-PCBs or their hydroxylated or sulfated metabolites in serum free media for 24h.

Compound	N27 cells	SH-SY5Y cells	HepG2 cells
PCB 3	> 50	> 50	> 50
PCB 8	> 50	> 50	> 50
PCB 11	> 50	> 50	> 50
PCB 52	> 50	> 50	> 50
4'-OH-PCB 3	> 50	> 50	> 50
4-OH-PCB 8	18.5 ± 0.4 <sup>a,b</sup>	14.0 ± 0.5 <sup>a,c</sup>	25.1 ± 2.6 <sup>b,c</sup>
4-OH-PCB 11	22.2 ± 0.9 <sup>b</sup>	16.8 ± 1.1 <sup>c</sup>	39.8 ± 4.1 <sup>b,c</sup>
4-OH-PCB 52	8.3 ± 0.6 <sup>a,b</sup>	10.2 ± 0.5 <sup>a,c</sup>	15.3 ± 0.5 <sup>b,c</sup>
4'-PCB 3 sulfate	> 50	> 50	> 50
4-PCB 8 sulfate	> 50	> 50	> 50
4-PCB 11 sulfate	> 50	> 50	> 50
4-PCB 52 sulfate	> 50	33.3 ± 2.5	29.2 ± 1.3

<sup>a</sup>significant difference between N27 and SH-SY5Y (P<0.05)

<sup>b</sup>significant difference between N27 and HepG2 (P<0.05)

<sup>c</sup>significant difference between SH-SY5Y and HepG2 (P<0.05)

Statistical significance determined using one way ANOVA with Bonferoni post hoc analysis on SigmaPlot v. 11.0, Systat Software, Chicago, IL.

#### The effects of serum on neurotoxicity - results

Many published studies, describe PCB-related assessments of cellular viability, calcium homeostasis, ROS formation, and other endpoints using serum supplemented media (ranging from 2-10% horse or fetal calf serum, or some mix thereof) throughout the duration of PCB exposure. This is assumed to be due to the requirement for serum-supplemented media during cell seeding and the growth period before PCB treatment. The experiments reported in this chapter concerning the cytotoxicity of select LC-PCBs and their hydroxylated and sulfated metabolites were all performed in serum-free media throughout PCB exposure. This was designed so that the cell incubation medium would

more closely resemble the protein-deficient composition of the CSF (i.e., 0.7% of that in serum).<sup>255</sup> In the following experiments, serum or HSA-media supplementation was used to address this difference and compare the toxic effects seen in the presence or absence of proteins that can bind the LC-PCBs and their metabolites.

Figure 4-8 shows the effects of human serum albumin (HSA)- or horse serum (HS)-supplementation in the media of N27 cells as they were treated with 25 $\mu$ M concentrations of 4-OH-PCB 52 or 4-PCB 52 sulfate. In these experiments, the untreated (both by PCB metabolite or supplementation) controls were set at 100%, and differing conditions were reported in comparison. Treatment of the cells with 25 $\mu$ M PCB 52 metabolites resulted in a significant decrease in cell viability that correlated with the results seen in Figures 4-3 and 4-4. This concentration of LC-PCB metabolite was chosen to facilitate comparison across all compounds in the N27 cells (i.e., it includes both toxic and non-toxic responses). The concentrations of HSA were chosen to represent a 1:2, 1:1, 2:1 molar ratio of metabolite:HSA, and the HS supplementation was chosen to be in a range to mimic the media composition (i.e., 2%-10% HS or FBS) in previously published PCB-exposure studies.<sup>176, 180, 189, 251, 259</sup> The results indicate that even at a 1:2-metabolite:HSA ratio, the protective effects of albumin-binding were sufficient to decrease toxicity substantially to a level that was statistically indistinguishable from untreated controls. The experiments shown here for PCB 52 metabolites are representative of the results seen for each of the metabolites tested in this manner. The complete collection of results are included in figures A-7 through A-9.

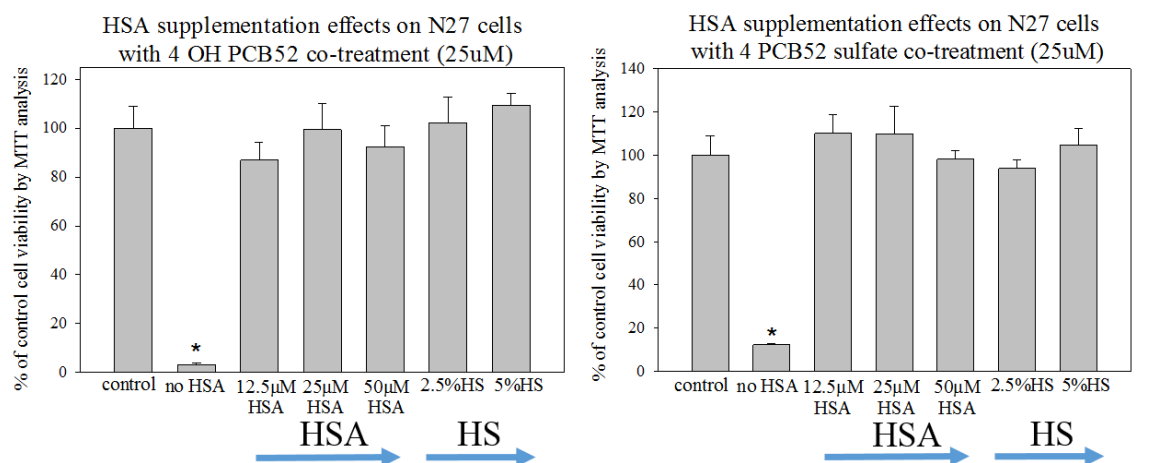


Figure 4-8 The presence of human serum albumin (HSA) or horse serum (HS) supplementation in cell media mitigates the cytotoxic effects of both 4-OH-PCB 52, and 4-PCB 52 sulfate in N27 cells. N27 cells treated with 25µM PCB metabolite were co-incubated with increasing amounts of HSA or horse serum. Data are reported as the percent of control cell viability by MTT analysis. n=3, (\* P<0.001 of control).

#### Intracellular and extracellular distribution of OH-LC-PCBs and LC-PCB sulfates

The results of the cellular distribution studies are presented in the following section. These experiment were designed to determine the distribution of the LC-PCB metabolites within the extracellular and intracellular milieu of the cultured cells. Furthermore, they were intended to investigate any degradation or other chemical changes that may be occurring throughout the exposure period of 24 hours. Because the standards used in this study were limited to those presented in figure 4-1, only their presence and interconversion was verified and quantitated. Using a mass balance approach, this experiment gave some insight into the movement of the LC-PCB metabolites into the cells, as well as their potential for further metabolism, degradation, or protein binding. The experimental design included a great effort to reduce the amount of cross contamination between the two systems (e.g., non-adherent cells that would be wrongfully counted as part of the extracellular medium or compounds associated with

cell surfaces that would be misrepresented as intracellular) so that the compounds' distributions may help to interpret the variable degrees of toxic responses.

The results are presented in Figures 4-9 through 4-14. The treatment compounds are denoted with an arrow in each case for orientation, and the entries represent the two isolated experimental compartments (i.e., the extracellular medium and the cellular component), as well as the metabolite standards used in this study. The ordinate axes (left and right) are included to represent both the amount of compound extracted in the experiment, and its percentage of the initial treatment (i.e., 2.5nmol in 100 $\mu$ L; 25 $\mu$ M), respectively. It is noted here that, in none of the treatments was there any detected parent LC-PCB. Furthermore, analyses of LC-PCB treatment experiments showed no detectable parent, hydroxylated, or sulfated LC-PCB. Thus, the data included in this study is focused on treatment with OH-LC-PCBs and LC-PCB sulfates.

#### N27 cells

The results for the dopaminergic N27 cell line treated with the two non-*ortho*-substituted OH-LC-PCBs (3 and 11) are presented in Figure 4-9. A comparison of the hydroxylated compounds shows that, after 24 hours, there is substantial distribution for both of these congeners from the treatment medium to the intracellular space, and seemingly more so for the dichlorinated 4-OH-PCB 11. From a comparison of these LC-PCB sulfates, it is evident that there are virtually no sulfated compounds present in the N27 dopaminergic cells, however, this experiment cannot discern between a lack of entry into or an efficient efflux out of the cells. These results compare well with the cytotoxic responses seen in MTT reduction and LDH release. Thus, the lack of toxicity of LC-PCB sulfates 3 and 11 may be due to poor cellular transport. Similarly, the difference in potency of their hydroxylated counterparts may be due to a metabolite and congener-selective transport (i.e., 4-OH-PCB 11 > 4'-OH-PCB 3 in both cases). Importantly, in each experiment, a near quantitative mass balance was achieved (2.3nmol  $\pm$  0.1; 91%  $\pm$

6) which indicates no substantial further metabolism, sequestration in cellular organelles or components, nor loss due to interactions with the experimental setup (i.e., mainly the collagen coated-, polystyrene- 96-well plates.

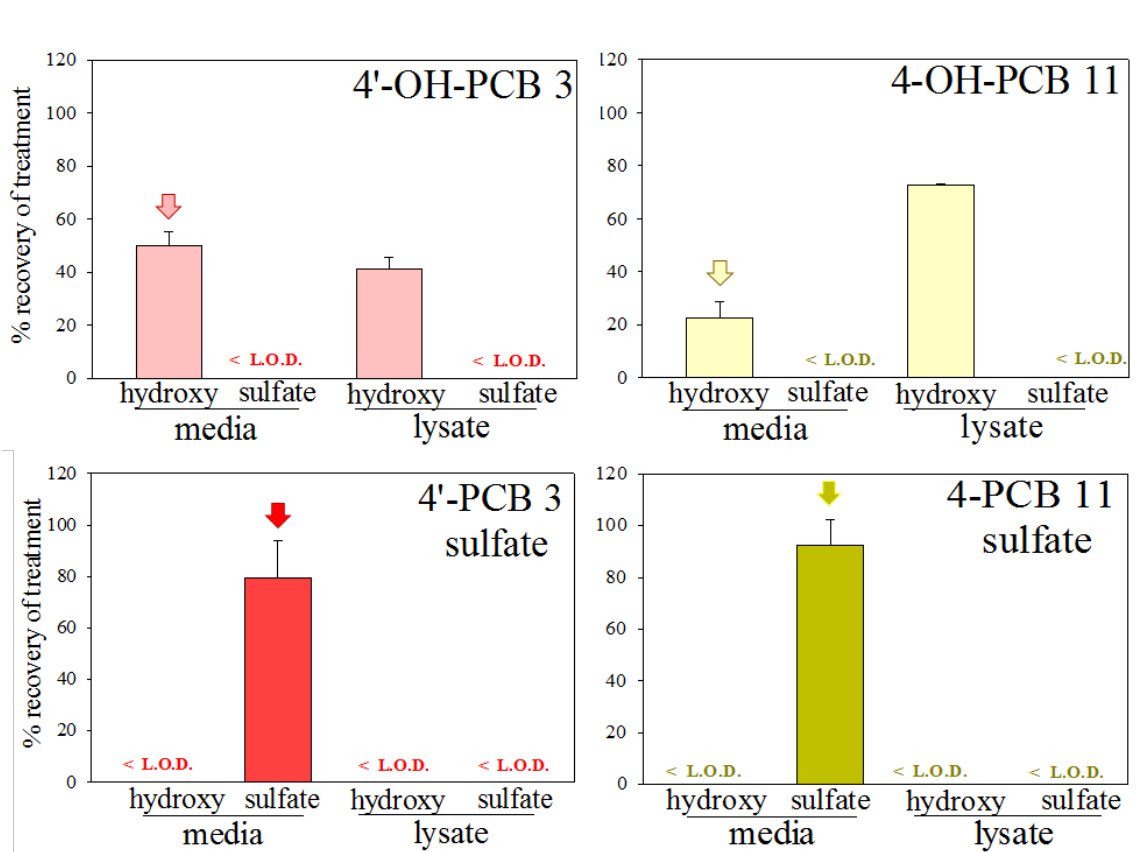


Figure 4-9 The distribution of OH-LC-PCBs and LC-PCB sulfates of non-*ortho*-substituted PCBs 3 and 11 in N27 cells as determined by HPLC analysis. Cells were treated with 25 $\mu$ M (2.5nmol) compound for 24h, and subjected to analysis of the extracellular media and intracellular contents. The treatment compound is annotated with an arrow. The values shown are the means  $\pm$  SE, n=3.

The results for treatment of the N27 cells with the two *ortho*-substituted LC-PCB congener metabolites are presented in Figure 4-10. Similar to the results with the non-*ortho*-substituted OH-LC-PCBs, the hydroxylated metabolites of LC-PCBs 8 and 52



showed a substantial distribution into the cells, and more so for 4-OH-PCB 52. These results also correlated well with the N27 toxicity studies. Interestingly, treatment with both corresponding sulfates indicated the presence of hydrolyzed sulfates (OH-LC-PCBs) after 24h incubation, albeit to a much lesser degree with the 4-PCB 8 sulfate. Cell-free control experiments of LC-PCB sulfates incubated in serum free media for 24 hours under cell exposure conditions showed no spontaneous hydrolysis. This was in agreement with the HSA-PCB sulfate stability studies described in Chapter 3. Their hydrolysis is due, presumably, to cellular sulfatases. Incubation of the N27 cells 4-PCB 52 sulfate led to substantial hydrolysis and redistribution of the resulting hydroxyl to the extracellular medium. This distribution resembled that of the treatment with OH-PCB 52. In fact, the toxicity of 4-PCB 52 sulfate may be due, in part, to the presence of the toxic 4-OH-PCB 52, since, of the sulfates tested, only it showed a toxic response in the N27 cells. The presence of hydrolysis in both of these experiments indicates that these sulfates enter the cell, and either become hydrolyzed and redistributed or removed by efflux, and that this phenomenon is related to the toxic response. It is important to note that although cell-mediated hydrolysis of the sulfates was seen, there was no sulfation of the OH-LC-PCBs. Similar to the previous results, however, the data shown here appear to be near quantitative throughout. This suggests that there are no other substantial metabolic reactions occurring during the 24 hour treatment of the cells.

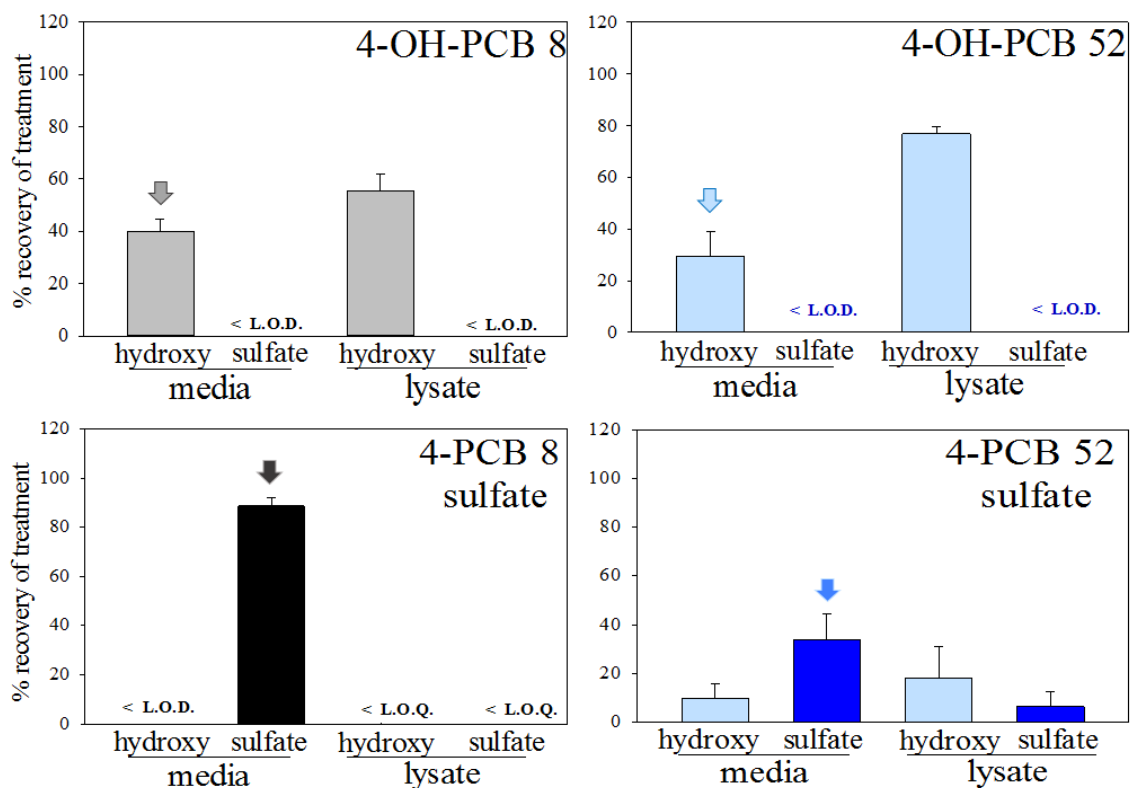


Figure 4-10 The distribution of OH-LC-PCBs and LC-PCB sulfates of *ortho*-substituted PCBs 8 and 52 in N27 cells as determined by HPLC analysis. Cells were treated with 25 $\mu$ M (2.5nmol) compound for 24h, and subjected to analysis of the extracellular media and intracellular contents. The treatment compound is annotated with an arrow. The values shown are the means  $\pm$  SE, n=3.

### SH-SY5Y cells

The neuronal SH-SY5Y cell line treatment results are shown in Figures 4-11 and 4-12. Treatment with the two non-*ortho*-substituted LC-PCB congener metabolites, presented in Figure 4-11, shows similarities to the observations in the N27 cell line. While the sulfated metabolites remain largely in the media, the OH-LC-PCBs appear to distribute within the cells, however with a seemingly lower ratio than in the dopaminergic N27 cells. This may explain the low toxic response as determined by MTT reduction and LDH release. Furthermore, although most of the treatments retain a semi-quantitative characteristic with respect to mass balance, the recovery of 4-OH-PCB 11 resulted in far

less than the expected amounts. This indicated the potential for further metabolism which can lead to the covalent binding of cellular components (e.g., glutathione, proteins, DNA, etc.). Interestingly, hydrolysis products of the 4-PCB 11 sulfate were indicated by HPLC, however they were below the limit of quantitation.

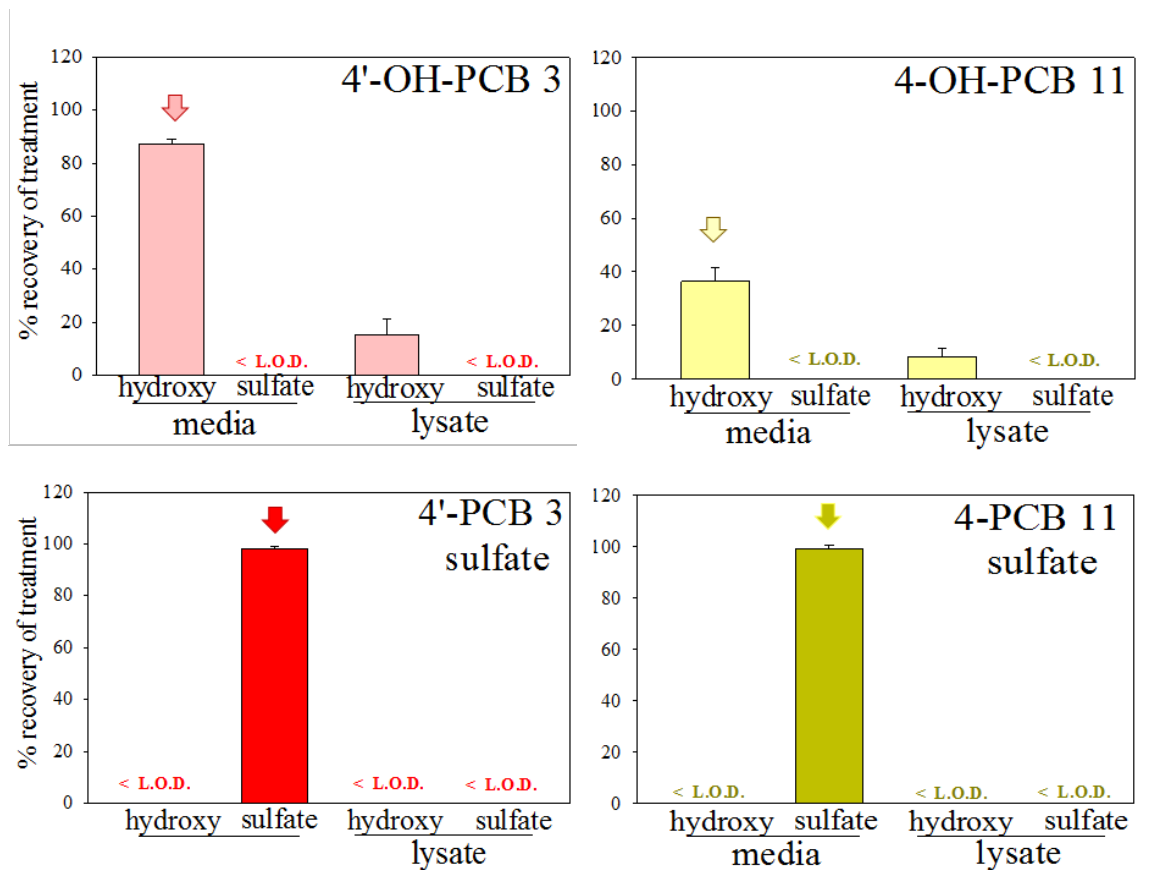


Figure 4-11 The distribution of OH-LC-PCBs and LC-PCB sulfates of non-*ortho*-substituted PCBs 3 and 11 in SH-SY5Y cells as determined by HPLC analysis. Cells were treated with 25 $\mu$ M (2.5nmol) compound for 24h, and subjected to analysis of the extracellular media and intracellular contents. The treatment compound is annotated with an arrow. The values shown are the means  $\pm$  SE, n=3.

Results from SH-SY5Y cell treatments with the *ortho*-substituted LC-PCB metabolites are shown in Figure 4-12. There was a large deficit in the sums of

metabolites recorded when these cells were treated with 4-OH-PCBs 8 and 52, similar to that seen with 4-OH-PCB 11. Again, no sulfation was observed with either compound. Treatment with the LC-PCB sulfates mimicked the dopaminergic N27 cell line treatment results in their preference for the extracellular media, however, 4-PCB 52 sulfate was not quantitatively assessed in the SH-SY5Y-based experiment. Considering the results of the N27 cells, 4-PCB 52 sulfate may be hydrolyzed in SH-SY5Y cells and quickly metabolized beyond the corresponding 4-substituted hydroxyl. Interestingly, although 4-OH-PCB 52 exposure to SH-SY5Y cells displayed the most toxicity when compared across congeners, metabolites, and cell lines, 4-PCB 52 sulfate exerted a less potent toxicity in these same cells. This implies either a rapid metabolic conversion of the hydrolyzed PCB 52 sulfate or an alternative metabolic route that is not initiated by hydrolysis.

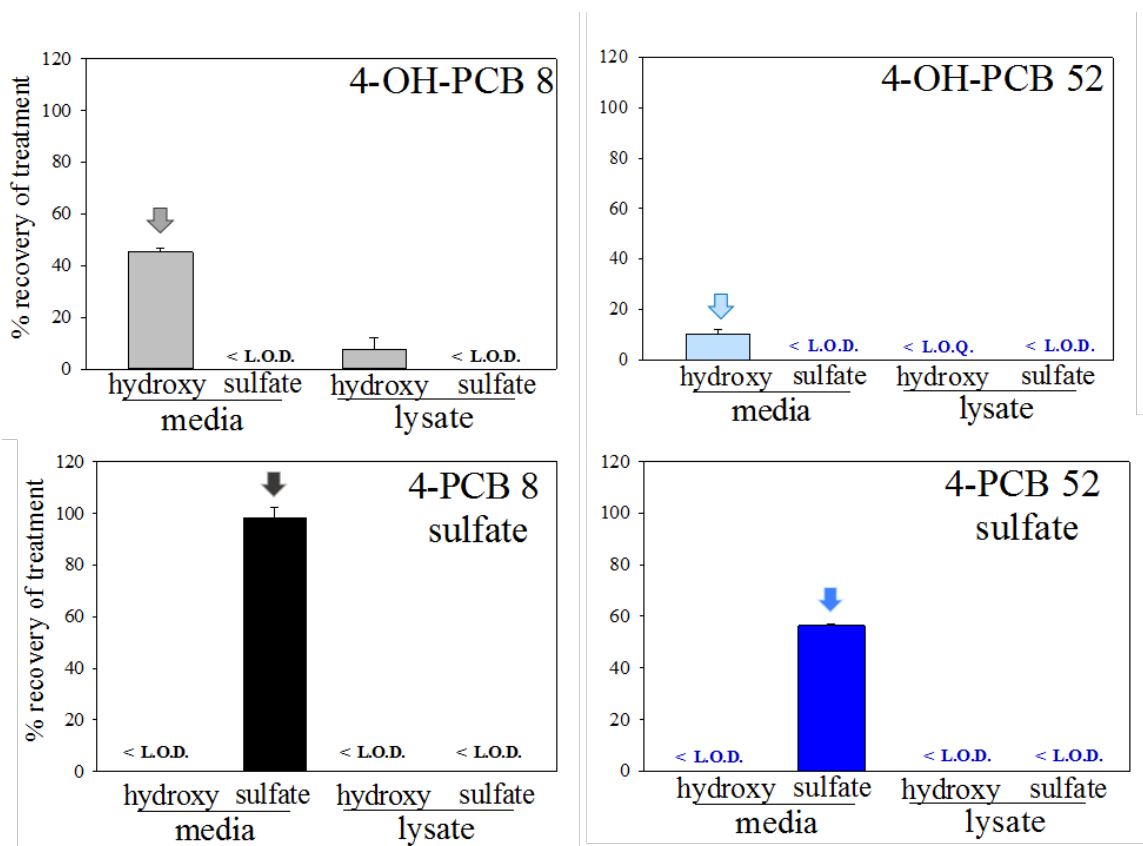


Figure 4-12 The distribution of OH-LC-PCBs and LC-PCB sulfates of *ortho*-substituted PCBs 8 and 52 in SH-SY5Y cells as determined by HPLC analysis. Cells were treated with 25 $\mu$ M (2.5nmol) compound for 24h, and subjected to analysis of the extracellular media and intracellular contents. The treatment compound is annotated with an arrow. The values shown are the means  $\pm$  SE, n=3.

### HepG2 cells

Figure 4-13 shows the distribution of the non-*ortho*-substituted LC-PCB metabolites following their incubation with HepG2 cells. Because HepG2 is a metabolically competent hepatic cell line, the extent of metabolism seen in these compounds is not surprising. The hydroxylated congeners exhibited sulfation to the corresponding LC-PCB sulfates. This chemical transformation was not seen with any congener in any of the neuronal cells included in this study. The distribution of the resulting sulfates varies by congener, however, because the spontaneous sulfation of any OH-PCB in media without cells does not occur, the distribution of the hydroxylated LC-PCBs into the cell must precede sulfation. Furthermore, recovery was much lower for these congeners when compared to either neuronal cell line. This indicates further metabolic transformations. Interestingly, the sulfation of the 4-OH-PCB 11 may account for the lack of toxicity of this hydroxylated LC-PCB when compared to the neuronal cells, since sulfation was not seen in the latter. Although this may be the case with the monochlorinated 4'-OH-PCB 3, this hydroxylated metabolite showed minimal toxicity to all cell lines.

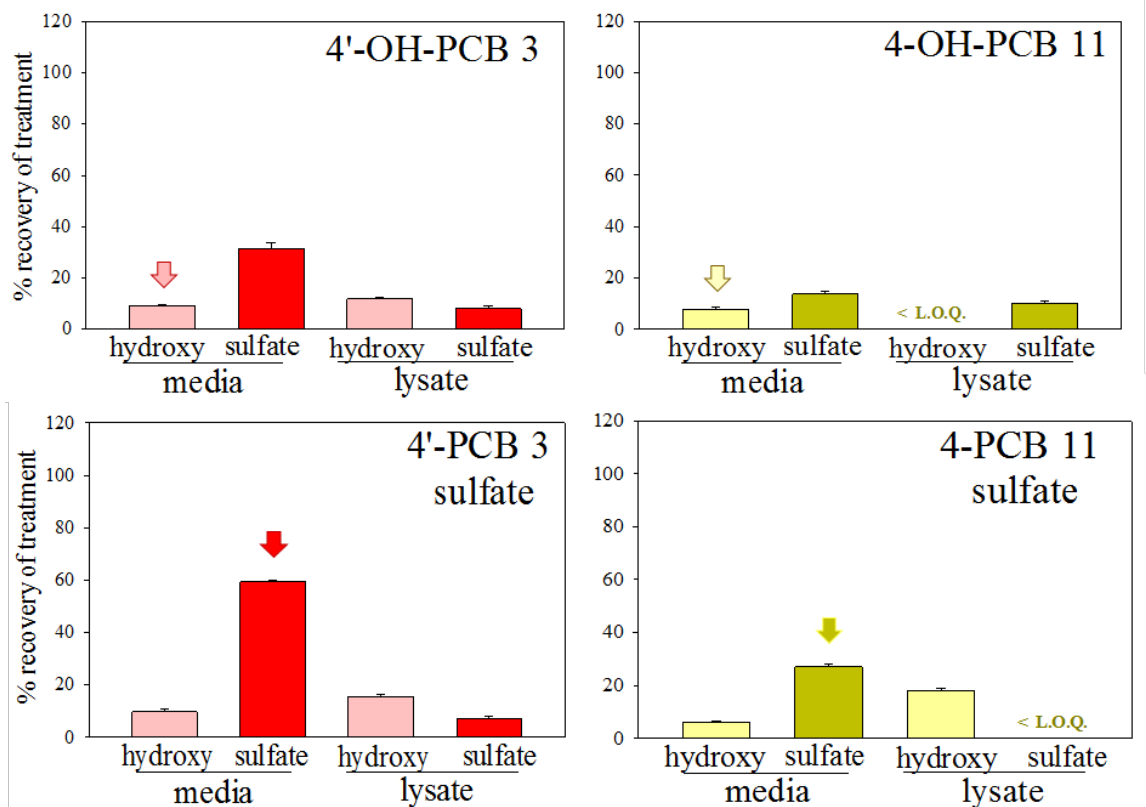


Figure 4-13 The distribution of OH-LC-PCBs and LC-PCB sulfates of non-*ortho*-substituted PCBs 3 and 11 in HepG2 cells as determined by HPLC analysis. Cells were treated with 25 $\mu$ M (2.5nmol) compound for 24h, and subjected to analysis of the extracellular media and intracellular contents. The treatment compound is annotated with an arrow. The values shown are the means  $\pm$  SE, n=3.

Similar to the non-*ortho*-substituted LC-PCB metabolites, those with *ortho*-substitutions displayed metabolic transformations and a reduction in the total amount of metabolites accounted for. The mono-*ortho*-substituted 4-OH-PCB 8 exhibited a high distribution into the cells followed by sulfation and subsequent redistribution. In the case of 4-OH-PCB 52, no sulfated product was observed, although the hydroxylated compound was still present in both media and the cellular mixture, albeit in low concentrations. This result is similar, yet less pronounced, to that seen for the SH-SY5Y cells in the efficient metabolism or other degradation of the di-*ortho*-substituted OH-LC-

PCB. As with 4-PCB 52 sulfate, however, where there was no hydrolyzed product present after 24 hours in the SH-SY5Y cells, analysis of HepG2 cell treatment exhibited hydrolysis of the sulfate and retention of the resulting hydroxyl both inside and outside of the cells. Concerning the hydrolysis of 4-PCB 8 sulfate, although 4-OH-PCB 8 was present in the lysate, there appeared minimal toxicity to the cells at this concentration. Hydrolysis of the sulfate may, however, explain the toxicity associated with 4-PCB 8 sulfate observed at higher concentrations.

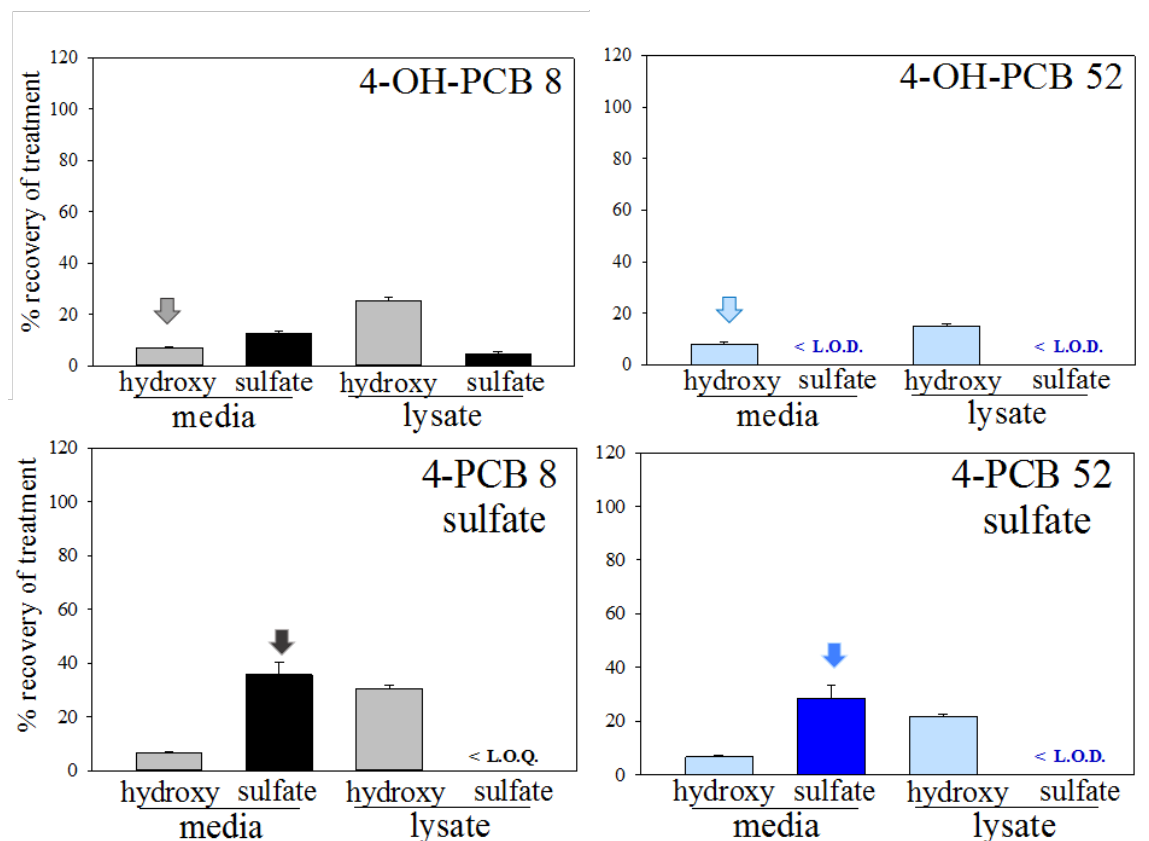


Figure 4-14 The distribution of OH-LC-PCBs and LC-PCB sulfates of *ortho*-substituted PCBs 8 and 52 in HepG2 cells as determined by HPLC analysis. Cells were treated with 25 $\mu$ M (2.5nmol) compound for 24h, and subjected to analysis of the extracellular media and intracellular contents. The treatment compound is annotated with an arrow. The values shown are the means  $\pm$  SE, n=3.

## Conclusions

The work presented here highlights the importance that metabolism of LC-PCBs may play in the neurotoxic potential of PCB exposure. PCBs have been linked to neurodevelopmental dysfunction and neurodegenerative disorders, with the dopaminergic system implicated as being at the core of these effects. This includes the etiology of Parkinson's disease (PD). Although PCB synthesis has been banned in most modern countries, and their use has been greatly limited to closed systems, LC-PCBs have been detected in indoor and outdoor air samples, in water and sediment, and as byproducts of paints and pigments. Unlike the more highly chlorinated congeners, LC-PCBs are semi-volatile and exposure occurs through inhalation, a facile transport system to the circulatory system. They are also more susceptible to metabolic transformations and their sulfated metabolites have been shown to bind to human serum proteins and, in rats, account for more than half of the metabolic fate of the monochlorinated PCB 3. PCBs have been shown to weaken the blood brain barrier,<sup>203</sup> and *ortho*-substituted PCBs have been detected in post-mortem PD brain samples where they selectively distribute to the caudate nucleus.<sup>187</sup> The caudate nucleus is associated with increased sulfotransferase activity in post-mortem PD brain samples.<sup>199</sup> The current study was designed to investigate the effects that metabolism may play in LC-PCB-induced neurotoxicity. The twelve compounds were chosen to represent congeners from among the top 20 most commonly detected PCBs in air samples and select hydroxyl and sulfated metabolites. Their effects were measured in immortalized neuronal and non-neuronal cells.

Of the compounds tested, the OH-LC-PCBs exhibited cytotoxicity with the highest potency, and were selective for the neuronal cell lines. With the exception of the di-*ortho*-substituted 4-OH-PCB 52, the dopaminergic N27 cells showed the highest susceptibility to these metabolites. Of the LC-PCBs and their sulfated metabolites, only the PCB 52 derivatives showed any toxicity at the concentrations examined, and were, again, selective to the N27 cells. In the case of 4-PCB 52 sulfate, the potency was equal



to or less than that for most of the OH-LC-PCBs. Furthermore, tracking of the hydroxylated compounds from the treatment media into the neuronal cells showed their efficient distribution, and the extent of this delivery correlated well with results from cell viability assays. With the exception of 4-PCB 52 sulfate, LC-PCB sulfates did not distribute into the cells, and this may explain the observed lack of toxicity. In neuronal cells, 4-PCB 52 sulfate exhibited a high extent of metabolism, from the measured hydrolysis products in N27 cells to the lack of further metabolites and a lack of mass balance of extracted metabolites in SH-SY5Y cells. Taken along with the relative toxicity (N27 > SH-SY5Y cells), this variability cannot be fully explained by its distribution and metabolism. In the HepG2 cells, however, OH-LC-PCBs and their corresponding sulfates all underwent metabolism to a greater degree than with the neuronal cells. The reduced toxicity of the OH-LC-PCBs in HepG2 cells, compared to the neuronal cells, may be explained by the high degree of sulfation in the hepatic cell line. Furthermore, the LC-PCB sulfate toxicity exhibited in these cells at higher concentrations may be explained by hydrolysis and subsequent exposure to the more toxic hydroxylated metabolites.

The results of these experiments support the hypothesis that the metabolism of LC-PCBs may play a role in the toxicity and degeneration of neurons, especially in the dopaminergic system. This is especially true of the *ortho*-substituted congeners, particularly of 4-OH-PCB 52 and its corresponding sulfate. PCB 52 has been implicated in *in vivo* and *in vitro* studies as a neurotoxic congener and has been shown to covalently modify DNA bases and proteins, presumably through a reactive quinone intermediate.<sup>123, 124, 189, 231, 260</sup> With the proximal location of the caudate nucleus to the sensitive dopaminergic substantia nigra region, and the associated accumulation of *ortho*-substituted PCBs and increased sulfotransferase activity in PD patients, sulfation (and desulfation) may be largely overlooked as a pathway toward LC-PCB induced neurodegeneration. Further studies on the location and activities of sulfotransferases and

sulfatases in these areas will be necessary to elucidate this interplay, as well as the selectivity of cellular transport proteins.

## CHAPTER 5: CONCLUSIONS

The research presented in this thesis has further elucidated the role that metabolism of LC-PCBs may play in their corporeal retention and distribution, as well as their toxic effects. In particular, these studies have focused on hydroxylated and sulfated metabolites of these compounds. The major goals of this study were to determine their binding affinities to human serum albumin (HSA), and their neurotoxic potential.

The HSA-binding studies indicated that, generally, sulfation of LC-PCBs increases their binding affinities when compared to LC-PCBs and OH-LC-PCBs. This was assessed using the dose-dependent displacement of site-selective fluorescent probes from the major drug binding sites of HSA. For the monochlorinated sulfates, binding to both Site I and Site II was observed, with the exception of the 3-PCB 3 sulfate which did not exhibit binding to Site I. Interestingly, with the exception of 4'-OH-PCB 3, which exhibited a high affinity for Site II, neither the LC-PCBs nor the OH-LC-PCBs exhibited binding to either Site I or Site II in this assessment. Furthermore, the binding affinities of the LC-PCB sulfates were generally comparable to that of the positive control ligand for Site I, phenylbutazone, while binding affinities for Site II varied more widely when compared to its positive control ligand, flufenamic acid. The di, tri, tetra, and penta chlorinated compounds exhibited no binding to Site I in these assays. The results for Site II, however, indicated that in most cases, LC-PCB sulfates bound with higher affinity than OH-LC PCBs and LC-PCBs. Generally, HSA-binding affinity followed the trend: LC-PCB sulfates  $\geq$  OH-LC-PCBs  $>$  LC-PCBs. Interestingly, both hydroxylated and sulfated metabolites often showed comparable, and sometimes higher, affinity for HSA Site II than the positive control ligand. Because the concentration of HSA was fairly low compared to that in serum (10 $\mu$ M versus 700 $\mu$ M), a lack of binding under these conditions should not indicate a lack of binding *in vivo*. In fact, in serum samples across species, PCBs tend to associate mostly with albumin-rich fractions.<sup>157-159</sup> This assay,

however, provides insight as to the high affinity, site-selective binding of LC-PCBs to albumin.

The neurotoxicity studies indicated that the OH-LC-PCBs were generally more potent than LC-PCBs and LC-PCB sulfates, with the exception of the di-*ortho*-substituted PCB 52 and PCB 52 sulfate. This toxicity was selective for dopaminergic cells and, in the case of the toxic 4-PCB 52 sulfate, may be due to intracellular hydrolysis of the sulfate to form the hydroxylated metabolite. The neurotoxic potential of these compounds was assessed using immortalized cell cultures. The cell lines chosen for this study included the rat midbrain-derived dopaminergic N27 cells, the human neuroblastoma-derived SH-SY5Y cells, and the human liver-derived HepG2 cells. Viability of these cells was assessed using two orthogonal assays (i.e., the reduction of MTT and the release of LDH) in a dose-dependent manner. These studies showed that the OH-LC-PCBs exhibited the most potent toxicity with the cells tested, with a selectivity to the neuronal models. Moreover, the toxic effects were greater in the dopaminergic neuronal cells, with the exception of 4-OH-PCB52 which showed a higher potency in the SH-SY5Y cells. Of the LC-PCBs and the LC-PCB sulfates, only the di-*ortho*-substituted congener and its sulfated metabolite showed appreciable toxicity, with a selectivity for the dopaminergic N27 cells. In fact, 4-PCB 52 sulfate showed comparative toxicity to that of most of the hydroxylated compounds in the same cells. HPLC analysis of the distribution of the compounds into the cells indicated that the lack of toxicity for many of the LC-PCB sulfates may be due to the low permeability of these metabolites into the cells. 4-PCB52 sulfate, however, was an exception. In the dopaminergic neuronal cells, this sulfated congener was hydrolyzed to the more toxic hydroxylated congener and redistributed amongst the extracellular and intracellular compartments. The highest amount of metabolism was seen in the hepatic HepG2 cells where both OH-LC-PCBs and LC-PCB sulfates were interconverted by metabolism. In contrast to the HepG2 cells, treatment of the neuronal cells with OH-LC-PCBs indicated

no metabolic sulfation, which may explain the marked differences in OH-LC-PCB-induced toxicity. In all cases, however, 4-PCB 52 sulfate showed the highest metabolic conversion across all cell lines.

The work presented here highlights the critical role that albumin may play in the binding, transport, and/or disposition of LC-PCBs and their metabolites, and provides insight into the resulting neurotoxic effects. The presence and shared physiological roles of serum albumin in all vertebrates<sup>221</sup> makes the understanding of this interaction helpful in determining the fates of these toxic species *in vivo*. Additionally, the metabolic transformation of LC-PCBs into their hydroxylated and sulfated derivatives may affect cellular distribution and toxicities such as neurological effects through retention and transport via serum protein binding. Thus, the selectivity of specific PCB metabolites for the major drug/toxicant binding sites on HSA and their activity in distinct neurological areas may be a factor that needs to be considered in the overall assessment of the contribution to toxic responses made by individual PCB congeners derived from exposure to PCB mixtures. This may be particularly important for airborne exposures to LC-PCBs where the PCB itself may be metabolized and not be detected in standard assays, yet OH-PCBs and PCB sulfates may be retained and either have toxic effects of their own or be further converted to other chemical species with adverse effects. This potential for retention, redistribution, and associated toxicity of PCB sulfates supports the idea that this has been a largely overlooked component of the overall picture of PCB exposure and its burden on human health.

Future directions of this work include the analysis of OH-LC-PCBs and LC-PCB sulfates in PD and non-PD post-mortem brain tissue and preferably by brain region. The inherent difficulty in this is the analytical techniques necessary to assess large number of potential PCBs, and their hydroxylated and sulfated metabolites. Furthermore, the mechanistic pathways by which hydroxylated or sulfated LC-PCBs impart their neurotoxic effects are of great interest. Some potential mechanisms include ROS

formation, calcium flux and homeostatic dysfunction, and receptor activation (e.g., ryanodine or nuclear receptors). It has been shown that OH-LC-PCBs are, similar to their corresponding LC-PCBs, potent inducers of ROS and exhibit cytotoxic effects in cerebellar granule cells.<sup>103</sup> Toxic effects of LC-PCBs have also been shown to be dependent on substitution patterns, with *ortho*-substituted congeners showing greater effects than those with no *ortho*-substitutions. Ortho-substituted congeners have been reported to preferential accumulate in brain tissue,<sup>186</sup> disrupt neuronal cell membranes,<sup>177,</sup><sup>178</sup> decrease dopamine levels *in vivo* and *in vitro*,<sup>189, 230</sup> and form protein and DNA adducts.<sup>123, 124</sup> Further studies include an analysis of the role that sulfation of LC-PCBs may play in these pathways, and this includes sulfate hydrolysis. Presumably, PCB sulfate hydrolysis in neuronal cells would occur via one or more sulfatases, of which relatively little is known. Furthermore, the selective diffusion of OH-LC-PCBs versus LC-PCB sulfates into neuronal cells may be mediated by cell membrane transporters (e.g., neurotransmitter transporters, organic anion transporters), which appears to be congener-selective in these studies. This would influence the effective cellular exposure to the toxic compounds. Thus, the results presented here point to a need to better understand the interconversion of PCBs and their corresponding OH-PCBs and PCB sulfates in the context of retention via serum protein binding and their neurotoxic responses.

## CHAPTER 6: MATERIALS AND METHODS

### HSA binding experiments

#### Materials

Human serum albumin (fatty acid and globulin free,  $\geq 99\%$  pure), phenylbutazone, and 5-dimethylamino-1-naphthalenesulfonamide (dansylamide; DNSA) were purchased from Sigma-Aldrich (St. Louis, MO). Flufenamic acid was purchased from Fluka Analytical (Buchs, Switzerland), and dansyl-L-proline (DP) was purchased from TCI (Cambridge, MA). Acetonitrile (Optima, HPLC grade), DMSO (reagent grade), and triethylamine (HPLC grade) was obtained from Fisher Chemicals (Pittsburgh, PA). All PCBs and metabolites were prepared and characterized in the synthesis core of the Iowa Superfund Research Program as previously described.<sup>256-258</sup>

#### Human Serum Albumin (HSA) binding assay

The displacement of site-selective fluorescent probes from HSA has been used to identify the relative binding affinity and selectivity of a large number of compounds. We used this approach for LC-PCBs and their metabolites by employing a modification of a method that was first described by Sudlow, et. al.<sup>210, 261</sup> Briefly, a 96-well plate format was used for analysis of solutions containing 10  $\mu\text{M}$  HSA (based on a 66.5kDa molecular weight) in 0.1 M potassium phosphate buffer, pH 7.4, a fluorescent probe (20 $\mu\text{M}$  for Site I-selective DNSA and 5  $\mu\text{M}$  for Site II-selective DP), and increasing concentrations of ligand (i.e., PCB, OH-PCB, PCB sulfate, or positive control ligand). The experiments were performed using a quartz 96-well microplate purchased from Molecular Devices (Sunnyvale, CA). Stock solutions of ligands were made in DMSO, and the final assay concentration of DMSO was less than 0.8% v/v. This concentration of DMSO was shown to have no significant effect on the fluorescence of either HSA-DP or HSA-DNSA. After mixing using a multipipettor, the fluorescence intensity was obtained after

3 minutes at 25°C (DNSA Excitation: 350nm; Emission: 460nm) (DP Excitation: 375nm; Emission: 460nm) in a Spectramax M5 fluorimeter (Molecular Devices, Sunnyvale, CA). Each ligand was assayed in triplicate and each data point was an average of six fluorescence readings taken once per minute and reported as a percent of control signal. Controls contained the same amount of DMSO, but without any ligand. Values for 50% decrease in the fluorescence intensity of the probe (EC50) were determined by plotting the percentage of control fluorescence intensity versus the log of the concentration of the test ligand and then utilizing a sigmoidal dose response ligand-binding algorithm (SigmaPlot v.11.0, Systat Software, Chicago, IL). The EC50 binding parameters for all ligands were calculated by a best fit to the equation:  $y = \frac{\text{min} + (\text{max} - \text{min})}{(1 + 10^{(EC_{50} - x)^{Hillslope}})}$ ; where min and max are the minima and maxima of the sigmoidal curve, y and x are the percent of control fluorescence and ligand concentration, respectively; Hillslope characterizes the slope of the curve at its midpoint, and the EC50 parameter is the ligand concentration where half of the total fluorescent probe displacement occurs. A further requirement for these studies was that at least 50% of the total probe must have been displaced within the range of concentrations examined. It is important to note that, in the case of high affinity binding to both sites, the overall binding to HSA will be somewhat underestimated by this method due to the fact that only one site is observed at any given time, regardless of whether or not the other site is occupied by the ligand.

#### HPLC analysis of recovery and reversibility in the binding of PCB sulfates to HSA

A solution of HSA (50 μM) and PCB sulfate (50 μM) was prepared in 0.1 M potassium phosphate buffer, pH 7.4, and 100 μL aliquots were sampled and extracted after incubation at 25°C for 0, 30, 90, 180, and 270 minutes. Each aliquot was extracted with 100μL acetonitrile after the addition of 15 mg NaCl, and the samples were subjected to vortex-mixing followed by centrifugation at 5000 rpm (1500 x g) for 5 minutes. The



acetonitrile layer was analyzed by HPLC using a Shimadzu Model LC-20-AT liquid chromatograph equipped with an SPD-20-AT UV/VIS detector and a C18 AQ 5 $\mu$ m (4.6 x 250 mm) column (Grace, Deerfield, IL). The HPLC separation was afforded by using linear gradients formed between 0.04% (v/v in deionized and distilled water) triethylammonium acetate (pH 7.4) and the indicated concentration of acetonitrile (MeCN): 0-1 min at 15% MeCN, 1-10 min at 15-100% MeCN, 10-14 min at 100% MeCN, and 14-15 min at 15% MeCN. Analysis of the eluate was carried out by absorbance at 254 nm. Concentrations of PCB sulfates were determined by relating the peak area to a standard curve obtained using synthetic standards.

### Neurotoxicity experiments

#### Materials

Cell culture materials were obtained from Gibco by Life Technologies (Madison, WI, USA) These include: Roswell Park Memorial Institute (RPMI) medium, Dulbecco's Modified Eagle's Medium (DMEM), Opti-MEM, Dulbecco's phosphate buffered saline (DPBS), Trypsin –EDTA (0.25%), penicillin/streptomycin, sodium pyruvate (100mM), fetal bovine serum (FBS), horse serum (HS), and MEM non-essential amino acids (MEM NEAA). Corning Falcon tissue culture 100mm<sup>2</sup> petri dishes, and Corning Costar 96-well plates were purchased from Fisher Scientific (Radnor, PA, USA). Human serum albumin (HSA, fatty acid and globulin free,  $\geq$ 99% pure), 3-(4,5-dimethylthiazol-2-yl)-2,5-diphenyltetrazolium bromide (MTT, 98% pure), and NADH ( $\geq$ 99% pure by HPLC) were purchased from Sigma Aldrich (St. Louis, MO, USA). Spectroscopic analyses were performed using a Spectramax M5 fluorimeter (Molecular Devices, Sunnyvale, CA, USA), and statistical analysis and sigmoidal dose response ligand-binding analyses were obtained using SigmaPlot v.11.0, Systat Software (Chicago, IL, USA).

## Cell lines and culture conditions

### N27 cells

The rat midbrain-derived dopaminergic N27 cells were obtained through a collaborative work with Professor Jonathan Doorn and graduate student Brigitte Vanle at the University of Iowa, College of Pharmacy. N27 cells were seeded at a density of 1M cells in collagen-coated 100 mm<sup>2</sup> tissue culture dishes and maintained in RPMI 1640 media supplemented with 10% heat-inactivated HS, penicillin (100 I.U./mL) and streptomycin (100 µg/mL) at 37°C in a 5% CO<sub>2</sub> atmosphere. Media was changed every other day until near confluence (approximately four days). The N27 cells used in this study were between passages 17 through 30.

### SH-SY5Y cells

The rat midbrain-derived dopaminergic N27 cells were obtained through collaborative work with Professor Jonathan Doorn and graduate student Brigitte Vanle at the University of Iowa, College of Pharmacy. SH-SY5Y cells were grown in collagen-coated 100 mm<sup>2</sup> tissue culture dishes and maintained in Opti-Mem media supplemented with 10% heat-inactivated FBS, non-essential amino acids, sodium pyruvate (500µM), penicillin (100 I.U./mL), and streptomycin (100 µg/mL) at 37°C in a 5% CO<sub>2</sub> atmosphere. Media was changed every other day until near confluence (approximately seven days). The SH-SY5Y cells used in this study were between passages 15 through 30.

### HepG2 cells

The immortalized human liver-derived HepG2 cells were a generous gift from Dr. Susanne Flor in the Department of Occupational and Environmental Health. HepG2 cells were grown in 100mm<sup>2</sup> tissue culture dishes and maintained in DMEM supplemented with 10% heat-inactivated FBS, penicillin (100 I.U./mL), and streptomycin (100 µg/mL)

at 37°C in a 5% CO<sub>2</sub> atmosphere. Media was changed every other day until near confluence (approximately 4 days). The HepG2 cells used in this study were between passages 21 through 32.

## Neurotoxicity studies

### Cell treatment

Following culture in 100mm<sup>2</sup> tissue culture dishes, cells were seeded at 25k cells/well in 96-well plates (collagen coated for the N27 and SH-SY5Y cell) and allowed to grow at 37°C in a 5% CO<sub>2</sub> environment for 48 hours with a media change after 24 hours. The cells were then washed twice with 100µL DPBS, and treated with phenol red-free, serum-free media (prepared respective to cell line-specific medium composition), containing 100µL of the desired LC-PCB, OH-LC-PCB, or LC-PCB sulfate concentration. The concentration gradients were obtained using serial dilutions of a stock solution (i.e., 100µM in s.f. media). The concentrated stock solutions of LC-PCBs and metabolites were made in DMSO at a concentration of 200mM, and the resulting concentration of DMSO in the media stocks was 0.1%. The untreated controls in these experiments contained the respective DMSO amounts (i.e., ≤ 0.1%), although no change in cell viability was seen at these DMSO concentrations. Each plate contained four sets of three control wells. The cells were incubated for 24 hours at 37°C in a 5% CO<sub>2</sub> environment. Cellular toxicity was assessed by measuring the cellular reduction of MTT and the release of LDH. Because these assessments are orthogonal to measuring cellular viability and their conditions are not mutually exclusive, both assays were completed in tandem.

For the HSA supplementation and toxicity studies, these same conditions were met, however stock solutions of 50µM compound were made in serum free media and the HSA stock solutions were made in the same medium at 100µM based on a molecular

weight of 66.5kDa. Untreated serum free medium was used to dilute the final exposure medium to the desired concentration.

#### LDH release analysis

LDH activity was measured according to the procedure described by Vassault, et. al.<sup>254</sup> After 24 hours of exposure to each concentration of LC-PCB, OH-LC-PCB, or LC-PCB sulfate, 10uL of a triton-X 100 solution (20% v/v in serum free media) was added to the high control wells (2% final triton-X 100 well concentration) in the plate and the plate was incubated for 15min. Lysis of untreated cells and subsequent complete release of cellular LDH provides the high control for this assay. 50uL of each well was then transferred to a new 96-well plate. This step was performed carefully so as to not disrupt the cells that will be assessed using the MTT-reduction assay. To the new 96-well plate was added 50uL of a DPBS solution containing 200µM NADH (100µM) and 3.2mM sodium pyruvate (1.6mM); concentrations in parenthesis are final concentrations in each well. The consumption of NADH was determined by monitoring the absorbance at 340nm every 31 seconds over a period of 15 minutes at 25°C. The catalytic activity of the reaction was calculated using the equation:

$$z = \frac{\Delta A * V}{1000 * \epsilon * d * \Delta t}$$

where z is the catalytic activity (mol/s or kat),  $\Delta A$  is the change in absorbance at 340nm, V is the assay volume (L),  $\epsilon$  is the absorption coefficient for NADH ( $0.63 \text{ mmol}^{-1} * \text{mm}^{-1}$ ), d is the pathlength (10mm, corrected for 96-well plates by Spectramax M5 fluorimeter, Sunnyvale, CA), and  $\Delta t$  is the change in time (s). The results were reported as a percent of control catalytic activity of NADH consumption (i.e., pyruvate reduction catalyzed by LDH) and further analyzed using the four-parameter curve-fitting algorithm described above.

### MTT reduction analysis

The cellular reduction of MTT was measured according to the procedure described by van Meerloo, et al.<sup>262</sup> After the 24 hour exposure time, 50 $\mu$ L of the exposure media was carefully removed and placed in a separate 96-well plate. 50 $\mu$ L of a 1mg/mL MTT solution in DPBS was added to the initial cell-containing wells and was allowed to incubate for 1 hour at 37°C in a 5% CO<sub>2</sub> environment. The plate was removed and 100 $\mu$ L of acetonitrile was added to each well and the water-insoluble formazan crystals were dissolved using a multi-pipetor. The plate was then read at 570nm and 650nm. The signal at 650nm was subtracted from the 570nm signal, and the resulting signals were then plotted as a percent of control versus the ligand concentration. The resulting plots were analyzed using the four-parameter curve-fitting algorithm described above.

### HPLC analysis of cellular and extracellular compartments

Cells were grown, seeded, and treated as described in the previous sections, however only with stock solutions containing 25 $\mu$ M of the desired ligand. After 24 hours, the 96-well plate was centrifuged at 1500 rpm (2300 x g) for 5 minutes. The media was removed and placed in microcentrifuge tubes (0.5mL high-clarity polypropylene natural microcentrifuge tubes). The plate was washed twice with DPBS with centrifuging steps between each wash. The washes showed no detectable amounts of standards by HPLC. 100 $\mu$ L of trypsin was added to each well and the plate was incubated for 30 minutes at room temperature. The plate was subjected to water bath-sonication for 10 minutes and cells were dislodged using a multi-pipetor and verified using a light microscope. The well contents were placed in microcentrifuge tubes. To both the extracellular and cellular mixes in microcentrifuge tubes was added 100 $\mu$ L acetonitrile and 15mg NaCl. They were then thoroughly vortexed and centrifuged at 3200rpm (4400 x g) for 5 minutes. The organic acetonitrile layer was collected and

analyzed by HPLC using a Shimadzu Model LC-20-AT liquid chromatograph equipped with an SPD-20-AT UV/VIS detector and a C18 AQ 5 $\mu$ m (4.6 x 250 mm) column (Grace, Deerfield, IL). The HPLC separation was afforded by using linear gradients formed between 0.04% triethylammonium (v/v) acetate (pH 7.4) and the indicated concentration of acetonitrile (MeCN): 0-1 min at 15% MeCN, 1-10 min at 15-100% MeCN, 10-14 min at 100% MeCN, and 14-15 min at 15% MeCN. Analysis of the eluate was carried out by absorbance at 254 nm. Concentrations were determined by relating the peak area to standard curves obtained using synthetic standards. The limit of detection (LOD) and limit of quantitation (LOQ) for the compounds was calculated using the relationships 3:1 and 10:1 signal to noise ratio, respectively. The LOD and LOQ for the compounds in this study were 0.03 nmol/100 $\mu$ L and 0.1nmol/100 $\mu$ L, respectively.

## APPENDIX

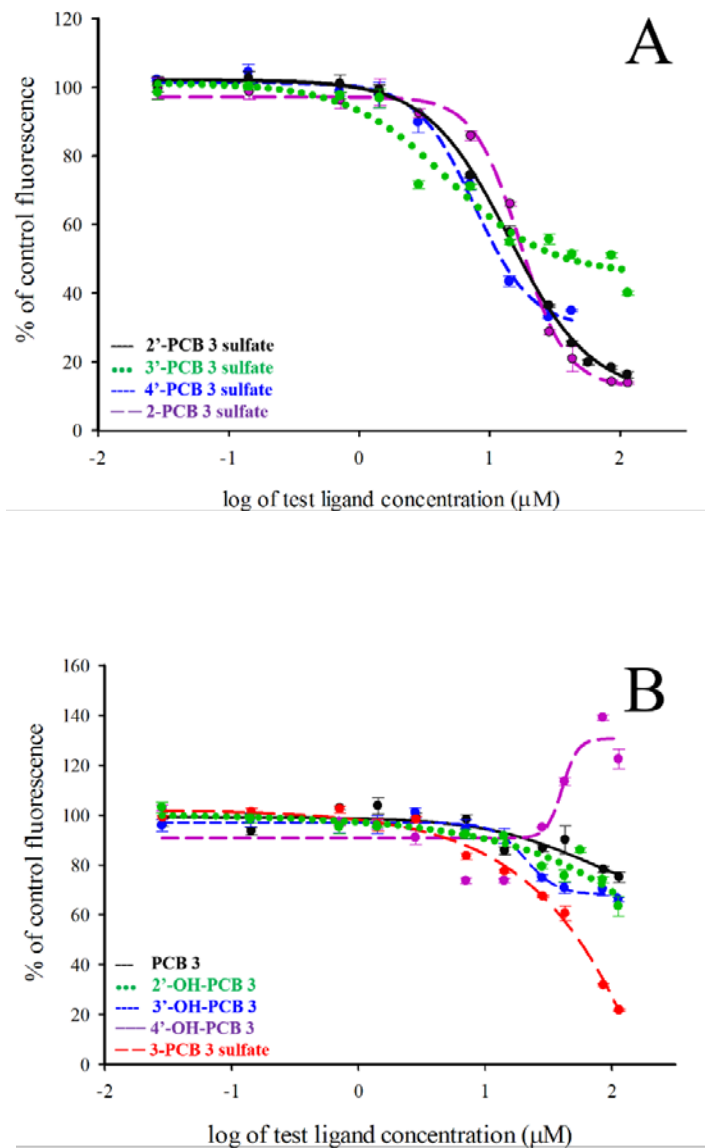


Figure A-1 Site I binding curves of monochlorinated LC-PCBs, OH-LC-PCBs, and LC-PCB sulfates plotted as percent of control fluorescence vs. increasing ligand concentration. A) ligands exhibiting dose dependent displacement of the fluorescent probe. B) ligands not exhibiting dose-dependent displacement of the fluorescent probe. Each experiment consists of 10μM HSA and 20μM DNSA. Data were fit to a sigmoidal dose response ligand-binding algorithm (SigmaPlot v.11.0, Systat Software, Chicago, IL) and EC<sub>50</sub> values are reported in Figure 3-7. Mean ± SE, n=3.

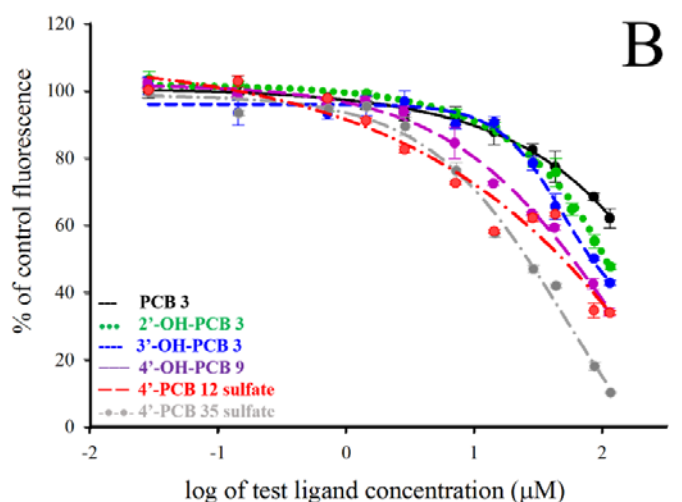
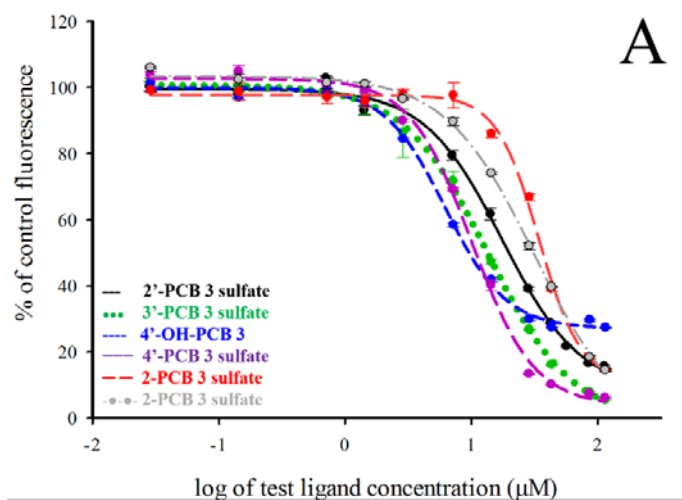


Figure A-2 Site II binding curves of LC-PCBs, OH-LC-PCBs, and LC-PCB sulfates plotted as percent of control fluorescence vs. increasing ligand concentration. A) monochlorinated compounds exhibiting dose dependent displacement of the fluorescent probe. B) all ligands not exhibiting dose-dependent displacement of the fluorescent probe from Site II. Each experiment consists of 10 $\mu$ M HSA and 5 $\mu$ M DP. Data were fit to a sigmoidal dose response ligand-binding algorithm (SigmaPlot v.11.0, Systat Software, Chicago, IL) and EC<sub>50</sub> values are reported in Figure 3-7. Mean  $\pm$  SE, n=3.



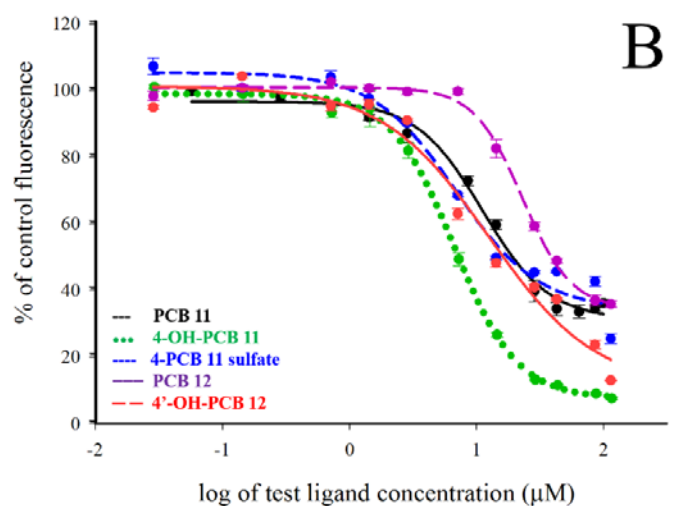
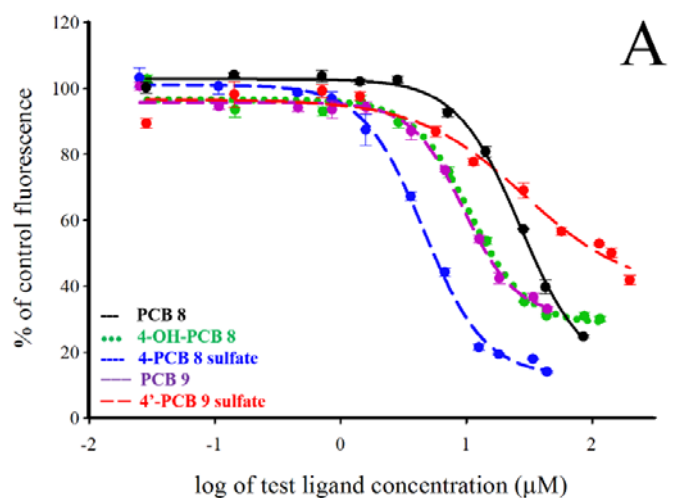


Figure A-3 Site II binding curves of dichlorinated LC-PCBs, OH-LC-PCBs, and LC-PCB sulfates plotted as percent of control fluorescence vs. increasing ligand concentration. A and B) ligands exhibiting dose dependent displacement of the fluorescent probe. Each experiment consists of 10 $\mu$ M HSA and 5 $\mu$ M DP. Data were fit to a sigmoidal dose response ligand-binding algorithm (SigmaPlot v.11.0, Systat Software, Chicago, IL) and EC<sub>50</sub> values are reported in Figure 3-7. Mean  $\pm$  SE, n=3.

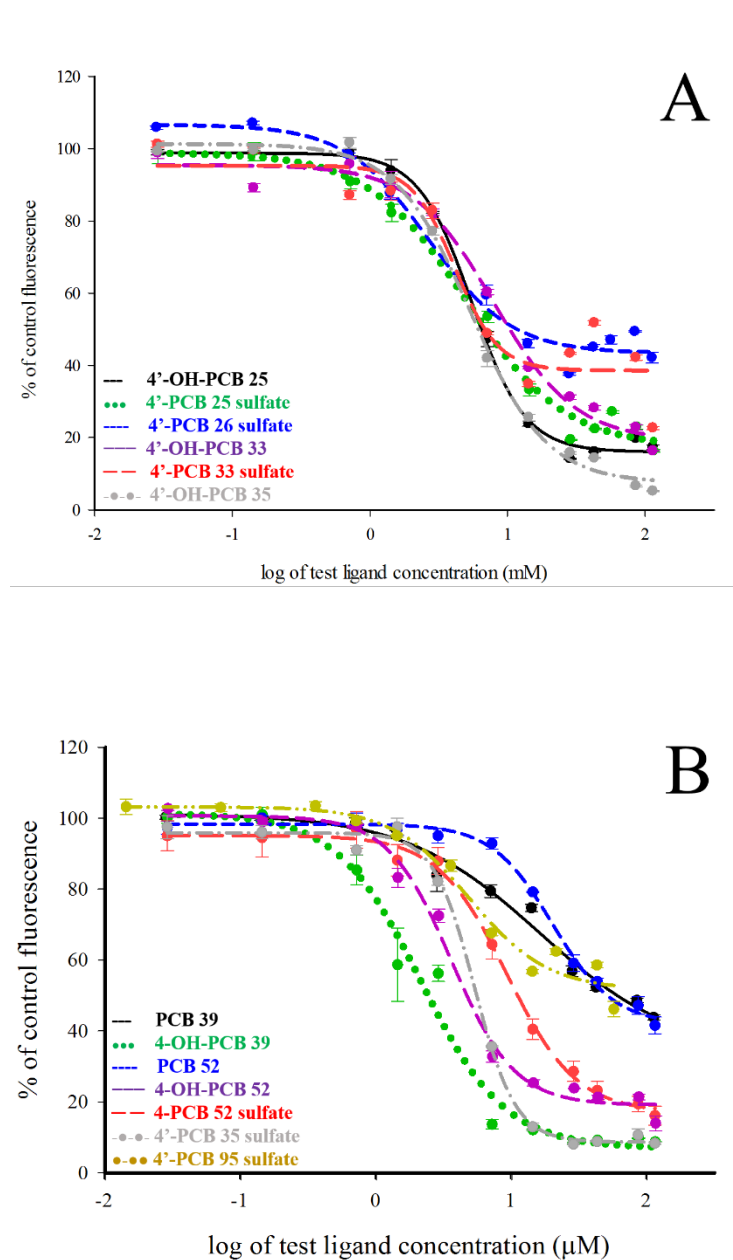


Figure A-4 Site II binding curves of tri-, tetra-, and pentachlorinated LC-PCBs, OH-LC-PCBs, and LC-PCB sulfates plotted as percent of control fluorescence vs. increasing ligand concentration. A and B) ligands exhibiting dose dependent displacement of the fluorescent probe. Each experiment consists of 10 $\mu$ M HSA and 5 $\mu$ M DP. Data were fit to a sigmoidal dose response ligand-binding algorithm (SigmaPlot v.11.0, Systat Software, Chicago, IL) and EC<sub>50</sub> values are reported in Figure 3-7. Mean  $\pm$  SE, n=3.

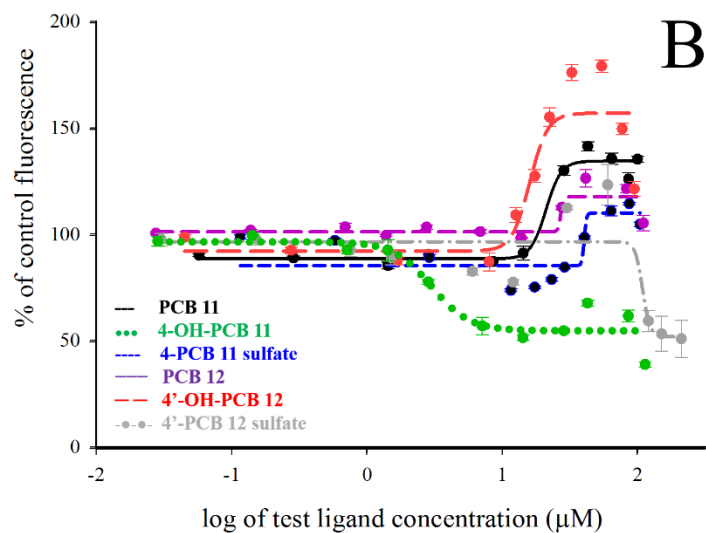
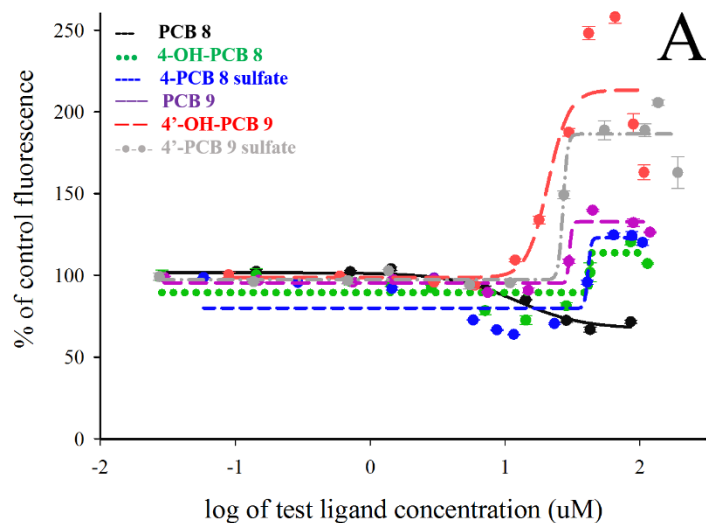


Figure A-5 Site I binding curves of dichlorinated LC-PCBs, OH-LC-PCBs, and LC-PCB sulfates plotted as percent of control fluorescence vs. increasing ligand concentration. A and B) ligands not exhibiting dose-dependent displacement of the fluorescent probe from Site I. Each experiment consists of 10 $\mu$ M HSA and 20 $\mu$ M DNSA. Data were fit to a sigmoidal dose response ligand-binding algorithm (SigmaPlot v.11.0, Systat Software, Chicago, IL) and EC<sub>50</sub> values are reported in Figure 3-7. Mean  $\pm$  SE, n=3.

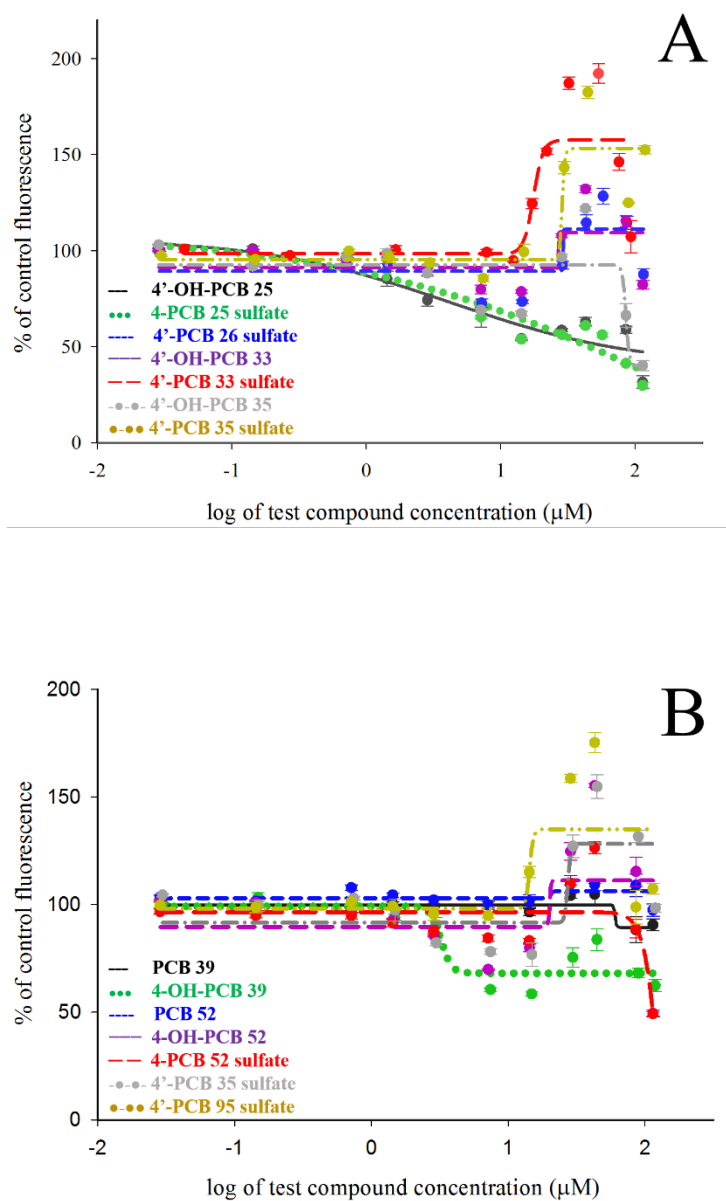


Figure A-6 Site I binding curves of tri-, tetra-, and pentachlorinated LC-PCBs, OH-LC-PCBs, and LC-PCB sulfates plotted as percent of control fluorescence vs. increasing ligand concentration. A and B) ligands not exhibiting dose-dependent displacement of the fluorescent probe from Site I. Each experiment consists of 10μM HSA and 20μM DNSA. Data were fit to a sigmoidal dose response ligand-binding algorithm (SigmaPlot v.11.0, Systat Software, Chicago, IL) and EC<sub>50</sub> values are reported in Figure 3-7. Mean ± SE, n=3.

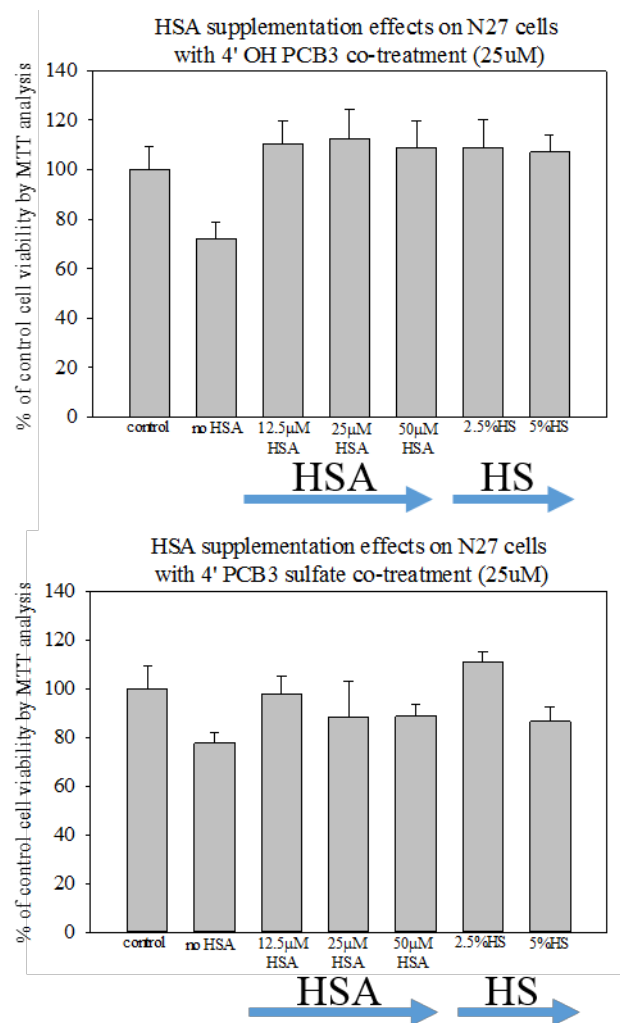


Figure A-7 The presence of human serum albumin (HSA) or horse serum (HS) supplementation in cell media mitigates the cytotoxic effects of both 4'-OH-PCB 3, and 4-PCB 3 sulfate in N27 cells. N27 cells treated with 25uM PCB metabolite were co-incubated with increasing amounts of HSA or horse serum. Data are reported as the percent of control cell viability by MTT analysis. n=3, (\* P<0.001 of control).

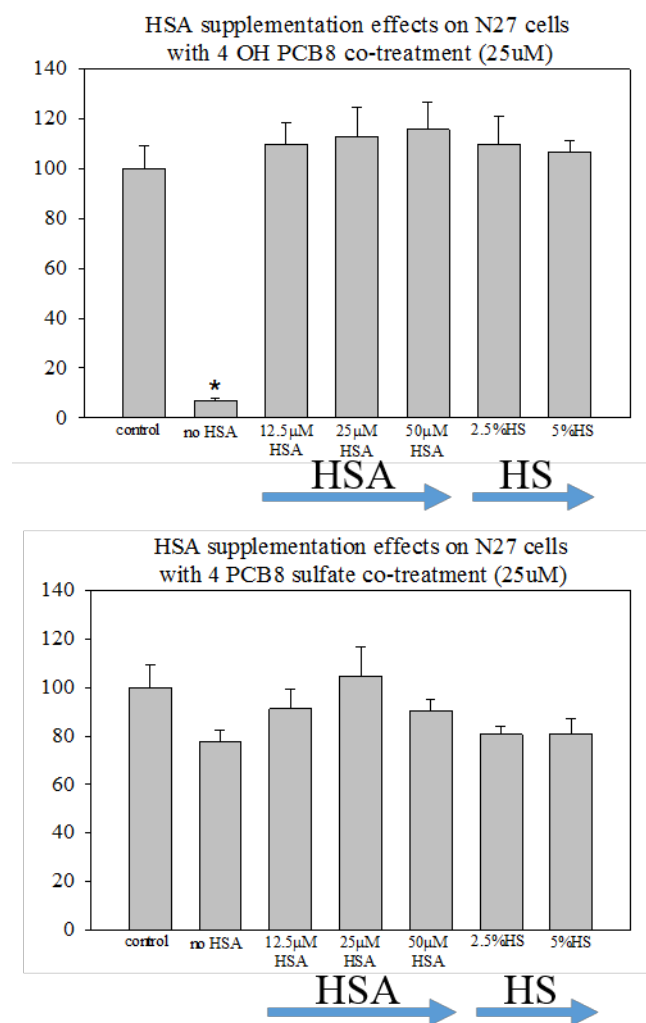


Figure A-8 The presence of human serum albumin (HSA) or horse serum (HS) supplementation in cell media mitigates the cytotoxic effects of both 4-OH-PCB 8, and 4-PCB 8 sulfate in N27 cells. N27 cells treated with 25µM PCB metabolite were co-incubated with increasing amounts of HSA or horse serum. Data are reported as the percent of control cell viability by MTT analysis. n=3, (\* P<0.001 of control).

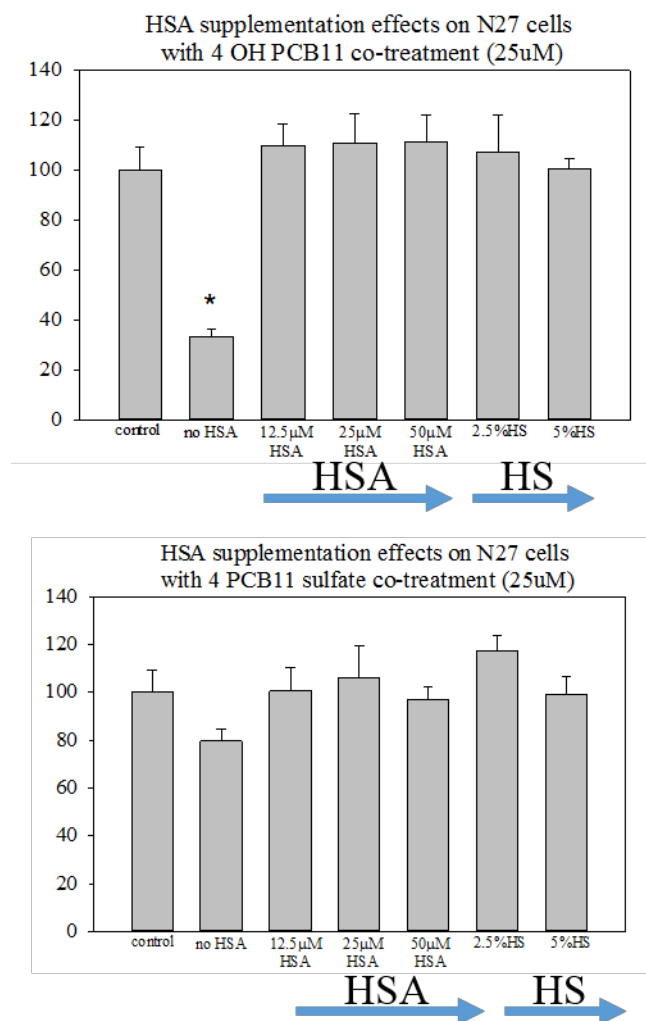


Figure A-9 The presence of human serum albumin (HSA) or horse serum (HS) supplementation in cell media mitigates the cytotoxic effects of both 4-OH-PCB 11, and 4-PCB 11 sulfate in N27 cells. N27 cells treated with 25µM PCB metabolite were co-incubated with increasing amounts of HSA or horse serum. Data are reported as the percent of control cell viability by MTT analysis. n=3, (\* P<0.001 of control).

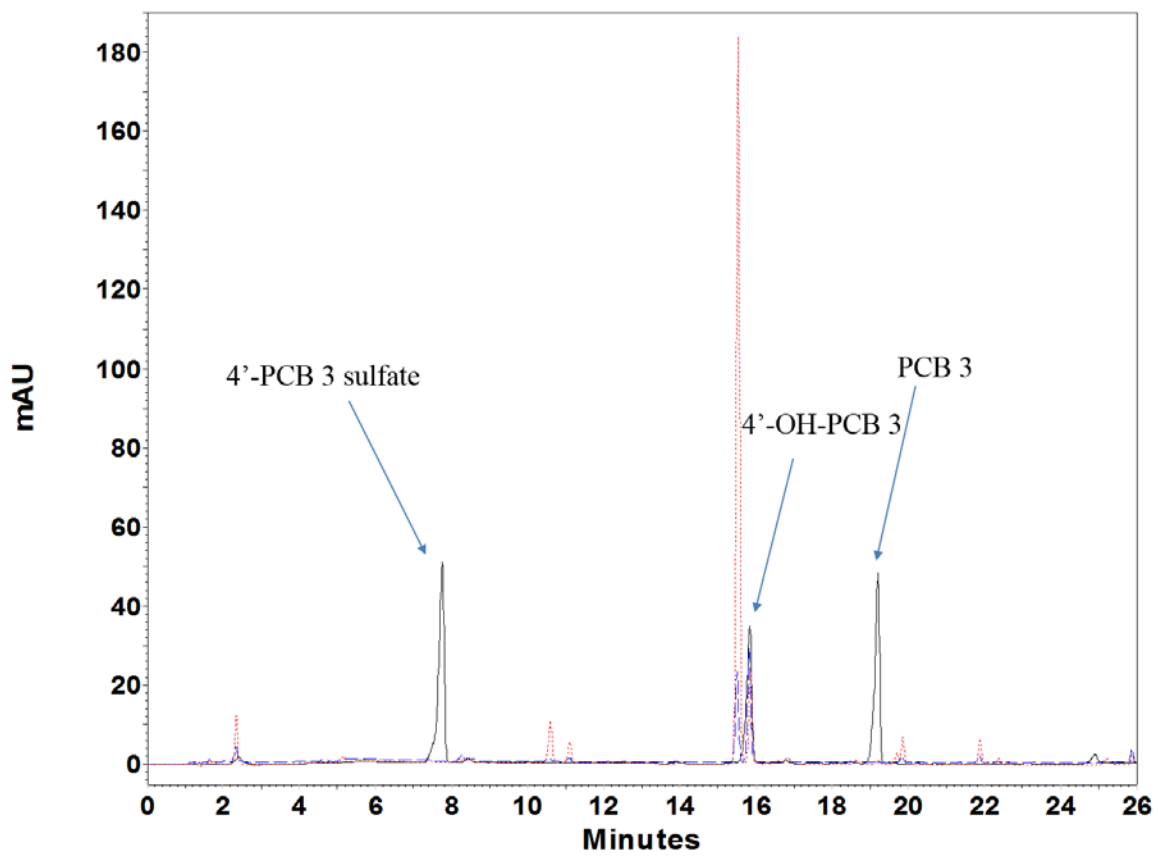


Figure A-10 Overlay of chromatograms from the HPLC analyses of extracellular media and cellular lysate extracts of N27 cells treated with 25 $\mu$ M 4'-OH-PCB 3 for 24 hours. Extracellular extract is represented in the blue dashed line. The lysate extract is represented in the dotted red line. Standards for the LC-PCB, the OH-LC-PCB, and the LC-PCB sulfate are represented in the solid black line. The extraction and HPLC conditions are described in detail in Chapter 6 Materials and Methods.



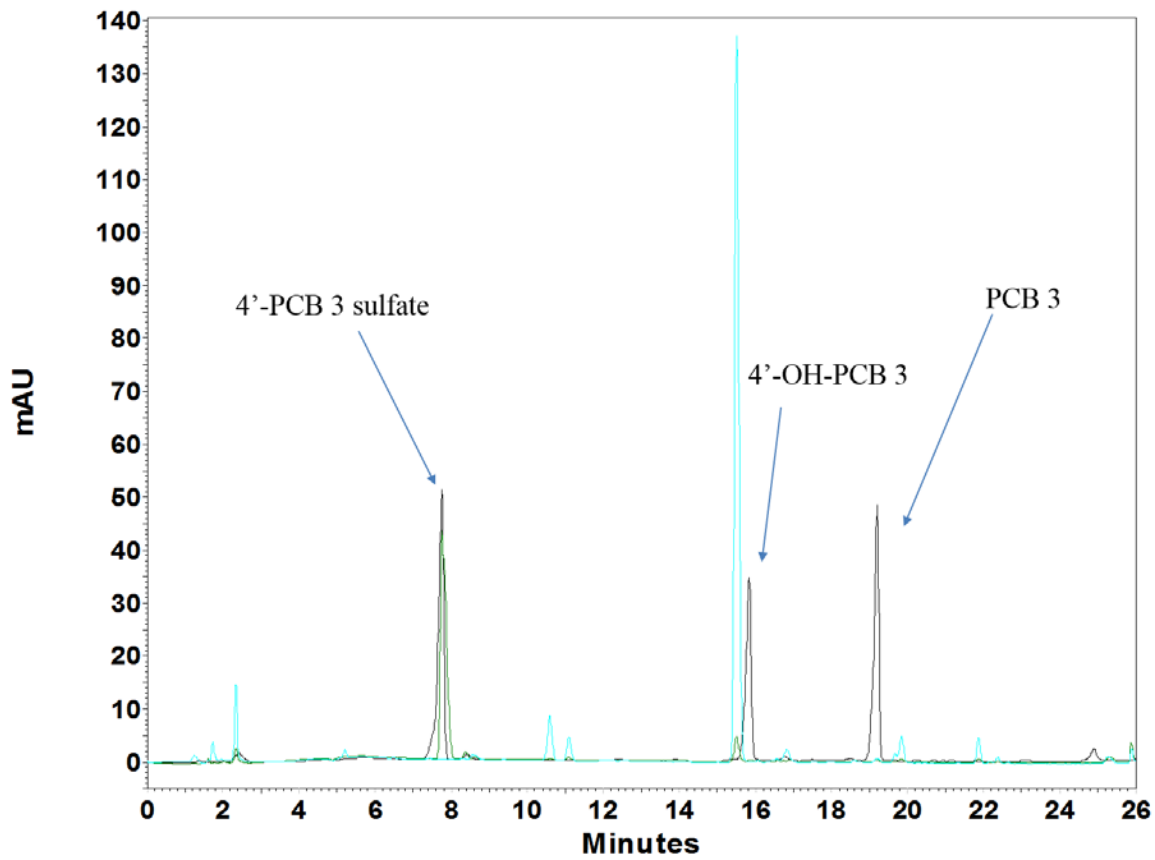


Figure A-11 Overlay of chromatograms from the HPLC analyses of extracellular media and cellular lysate extracts of N27 cells treated with  $25\mu\text{M}$  4'-PCB 3 sulfate for 24 hours. Extracellular extract is represented in the blue dashed line. The lysate extract is represented in the dotted red line. Standards for the LC-PCB, the OH-LC-PCB, and the LC-PCB sulfate are represented in the solid black line. The extraction and HPLC conditions are described in detail in Chapter 6 Materials and Methods.

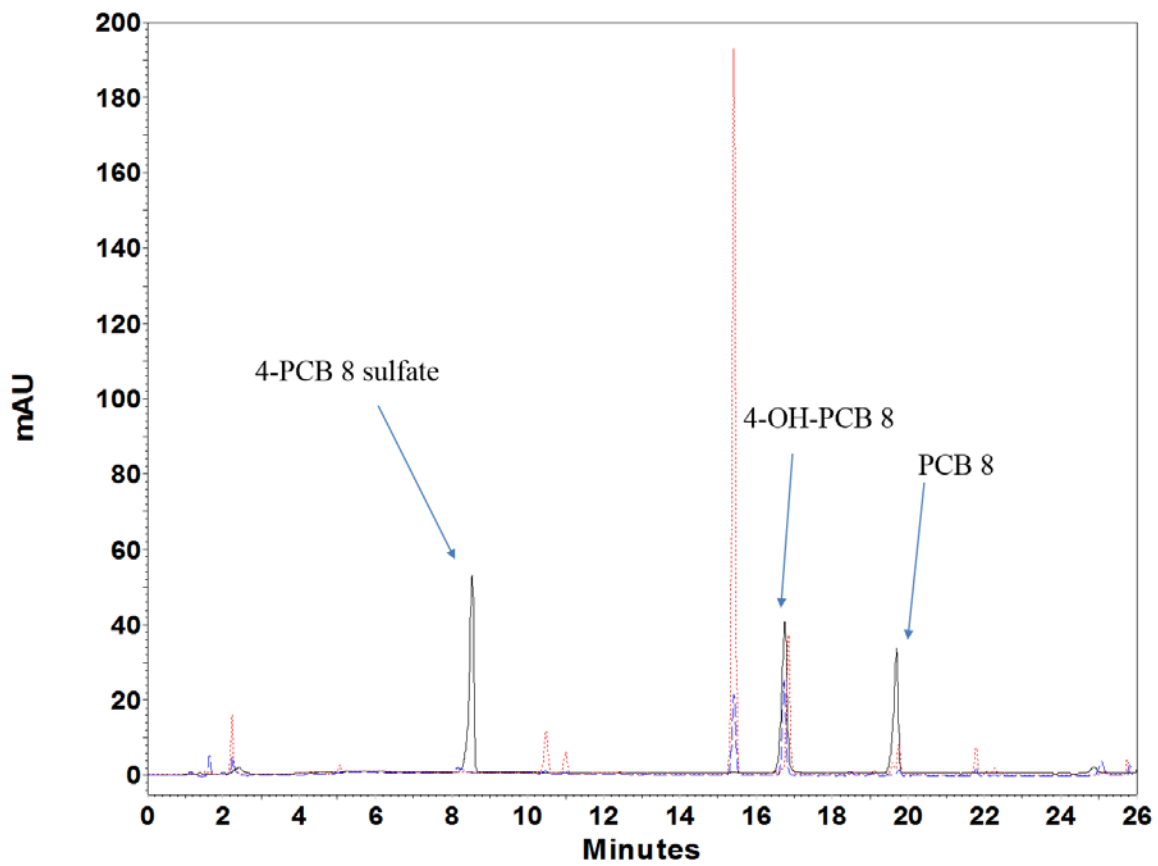


Figure A-12 Overlay of chromatograms from the HPLC analyses of extracellular media and cellular lysate extracts of N27 cells treated with 25 $\mu$ M 4-OH-PCB 8 for 24 hours. Extracellular extract is represented in the blue dashed line. The lysate extract is represented in the dotted red line. Standards for the LC-PCB, the OH-LC-PCB, and the LC-PCB sulfate are represented in the solid black line. The extraction and HPLC conditions are described in detail in Chapter 6 Materials and Methods.

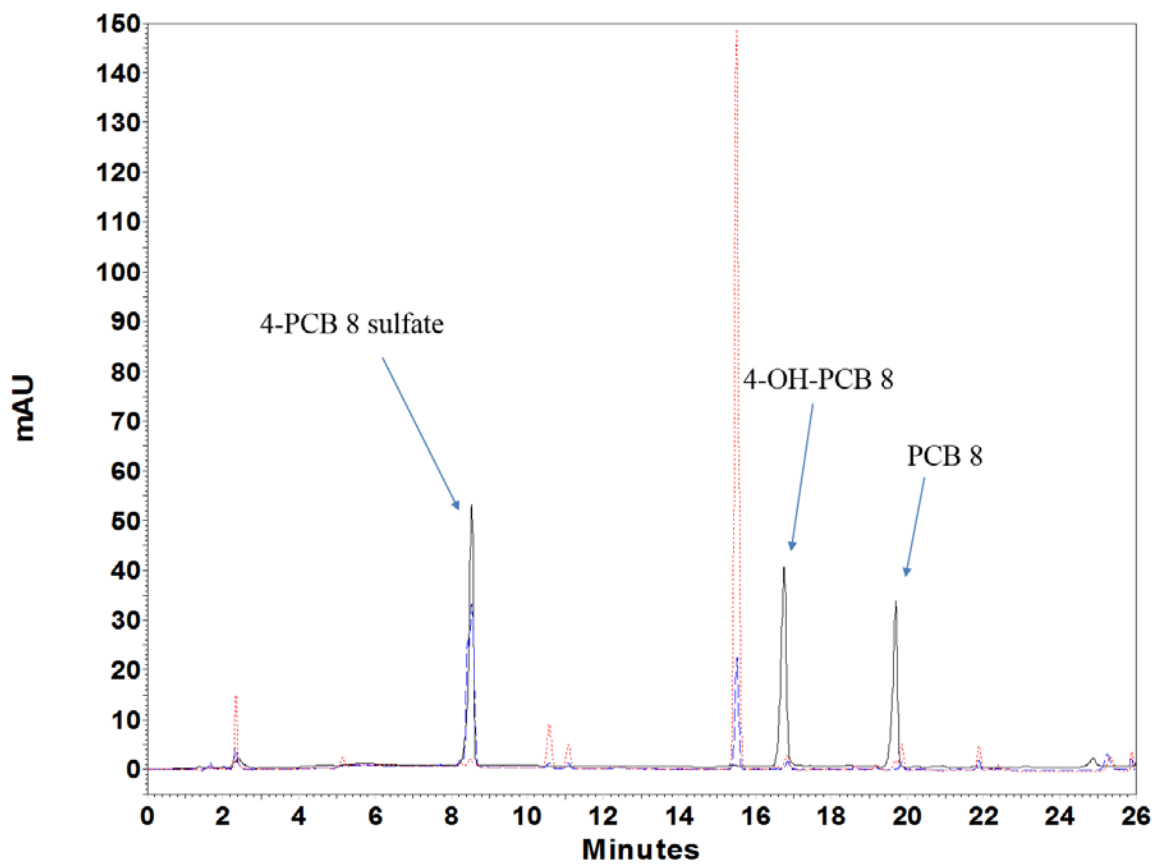


Figure A-13 Overlay of chromatograms from the HPLC analyses of extracellular media and cellular lysate extracts of N27 cells treated with 25 $\mu$ M 4-PCB 8 sulfate for 24 hours. Extracellular extract is represented in the blue dashed line. The lysate extract is represented in the dotted red line. Standards for the LC-PCB, the OH-LC-PCB, and the LC-PCB sulfate are represented in the solid black line. The extraction and HPLC conditions are described in detail in Chapter 6 Materials and Methods.

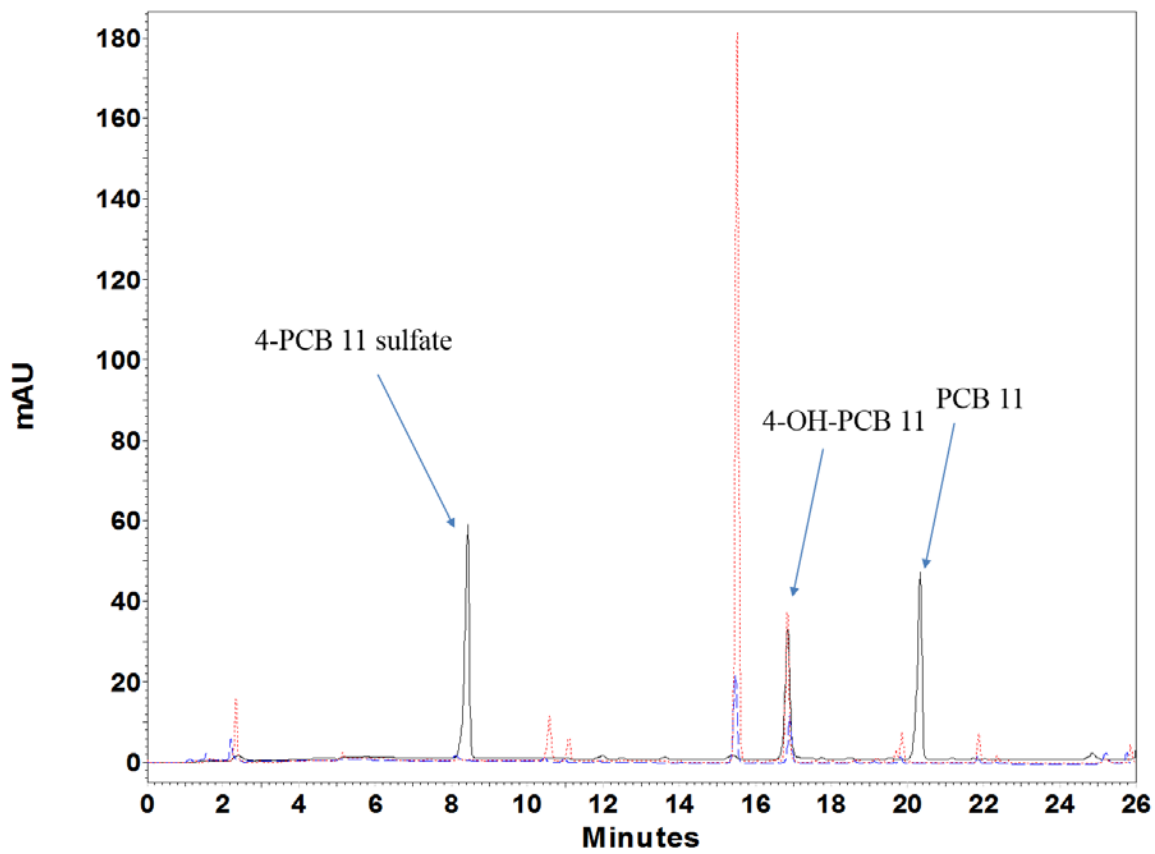


Figure A-14 Overlay of chromatograms from the HPLC analyses of extracellular media and cellular lysate extracts of N27 cells treated with 25 $\mu$ M 4-OH-PCB 11 for 24 hours. Extracellular extract is represented in the blue dashed line. The lysate extract is represented in the dotted red line. Standards for the LC-PCB, the OH-LC-PCB, and the LC-PCB sulfate are represented in the solid black line. The extraction and HPLC conditions are described in detail in Chapter 6 Materials and Methods.

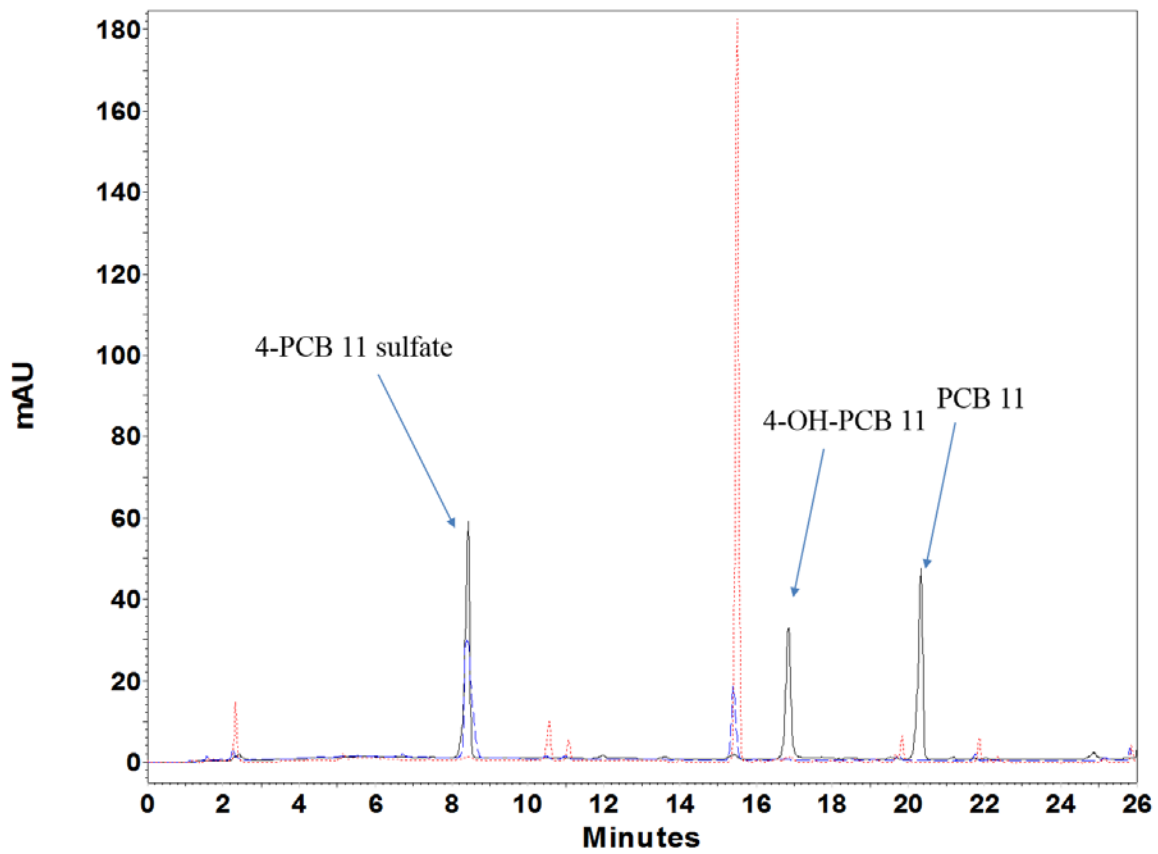


Figure A-15 Overlay of chromatograms from the HPLC analyses of extracellular media and cellular lysate extracts of N27 cells treated with 25 $\mu$ M 4-PCB 11 sulfate for 24 hours. Extracellular extract is represented in the blue dashed line. The lysate extract is represented in the dotted red line. Standards for the LC-PCB, the OH-LC-PCB, and the LC-PCB sulfate are represented in the solid black line. The extraction and HPLC conditions are described in detail in Chapter 6 Materials and Methods.

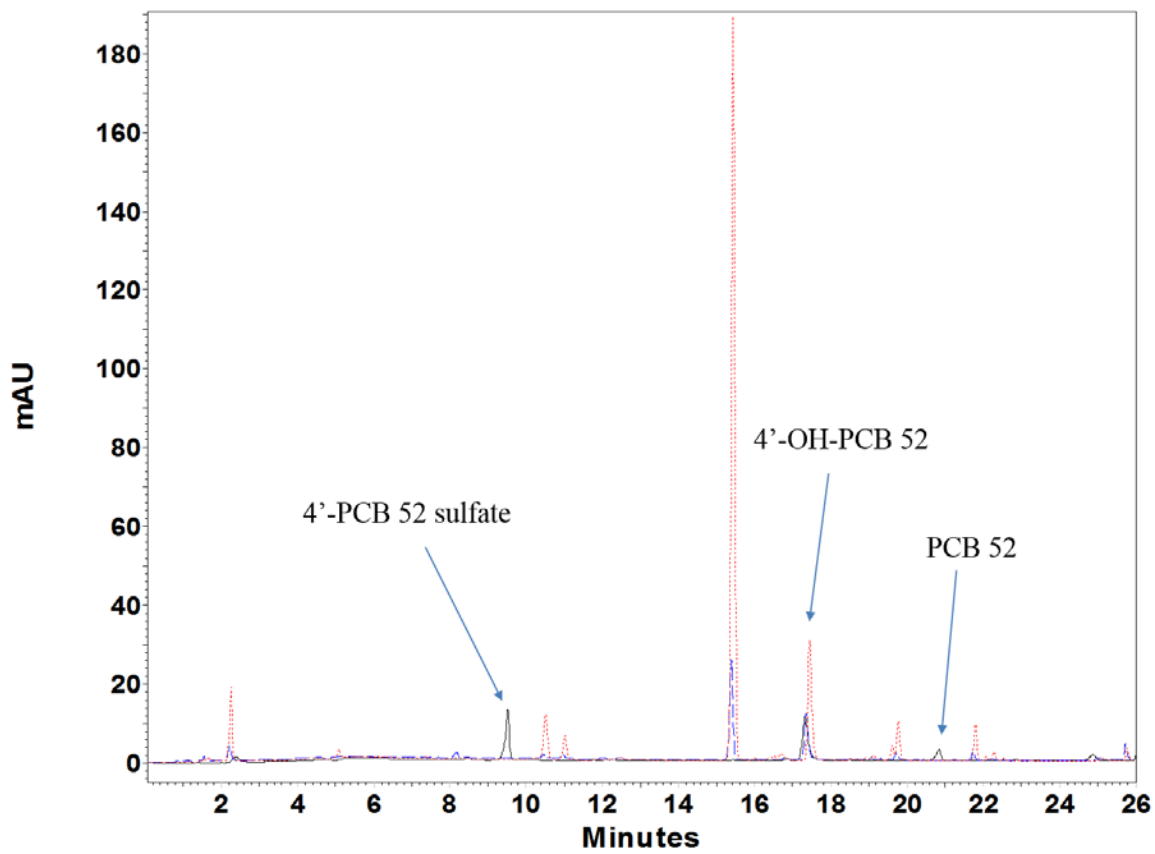


Figure A-16 Overlay of chromatograms from the HPLC analyses of extracellular media and cellular lysate extracts of N27 cells treated with  $25\mu\text{M}$  4-OH-PCB 52 sulfate for 24 hours. Extracellular extract is represented in the blue dashed line. The lysate extract is represented in the dotted red line. Standards for the LC-PCB, the OH-LC-PCB, and the LC-PCB sulfate are represented in the solid black line. The extraction and HPLC conditions are described in detail in Chapter 6 Materials and Methods.

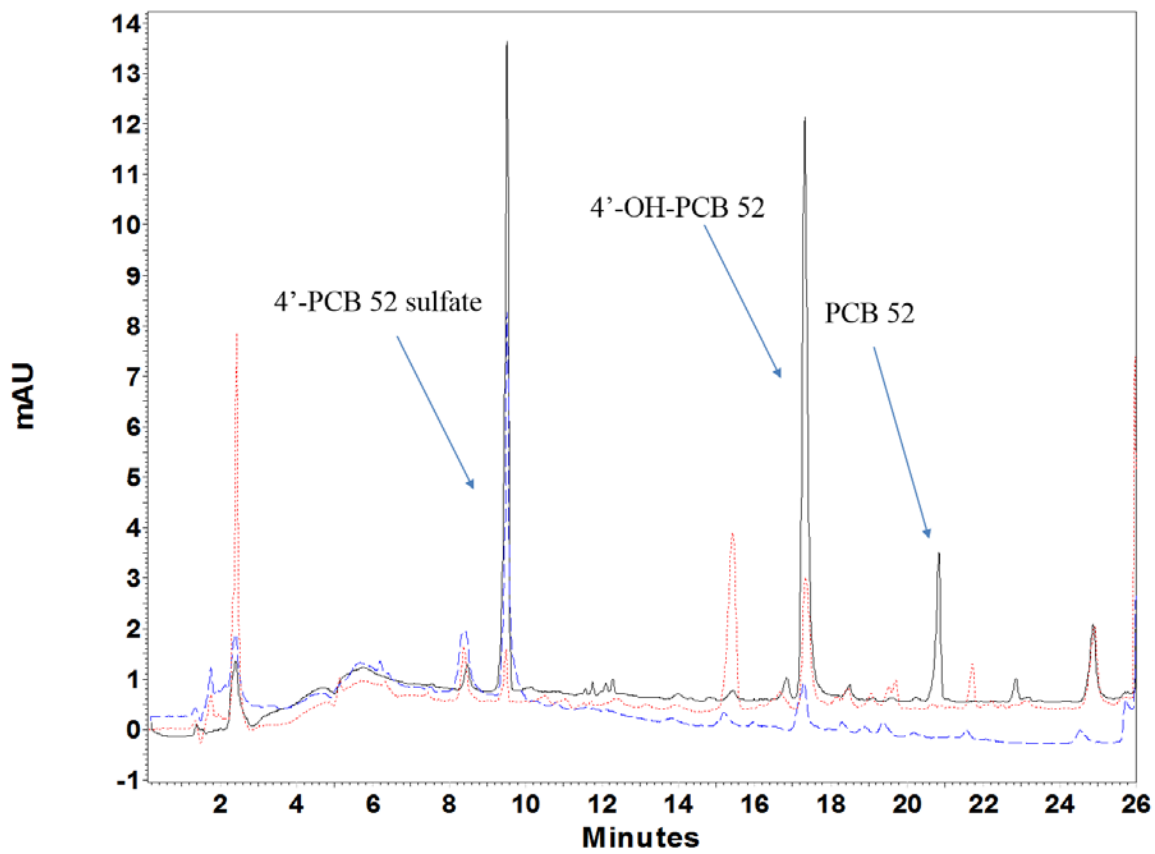


Figure A-17 Overlay of chromatograms from the HPLC analyses of extracellular media and cellular lysate extracts of N27 cells treated with 25 $\mu$ M 4-PCB 52 sulfate for 24 hours. Extracellular extract is represented in the blue dashed line. The lysate extract is represented in the dotted red line. Standards for the LC-PCB, the OH-LC-PCB, and the LC-PCB sulfate are represented in the solid black line. The extraction and HPLC conditions are described in detail in Chapter 6 Materials and Methods.

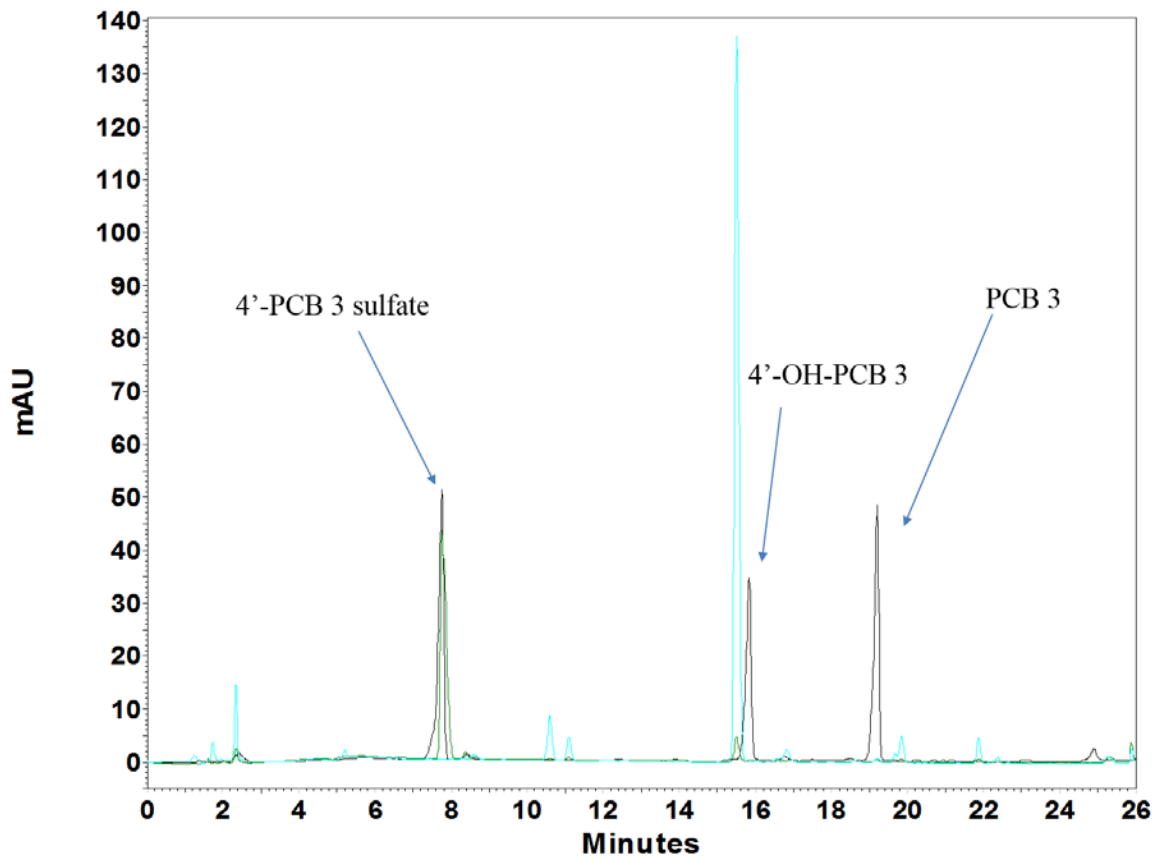


Figure A-18 Overlay of chromatograms from the HPLC analyses of extracellular media and cellular lysate extracts of SH-SY5Y cells treated with  $25\mu\text{M}$  4'-OH-PCB 3 for 24 hours. Extracellular extract is represented in the blue dashed line. The lysate extract is represented in the dotted red line. Standards for the LC-PCB, the OH-LC-PCB, and the LC-PCB sulfate are represented in the solid black line. The extraction and HPLC conditions are described in detail in Chapter 6 Materials and Methods.



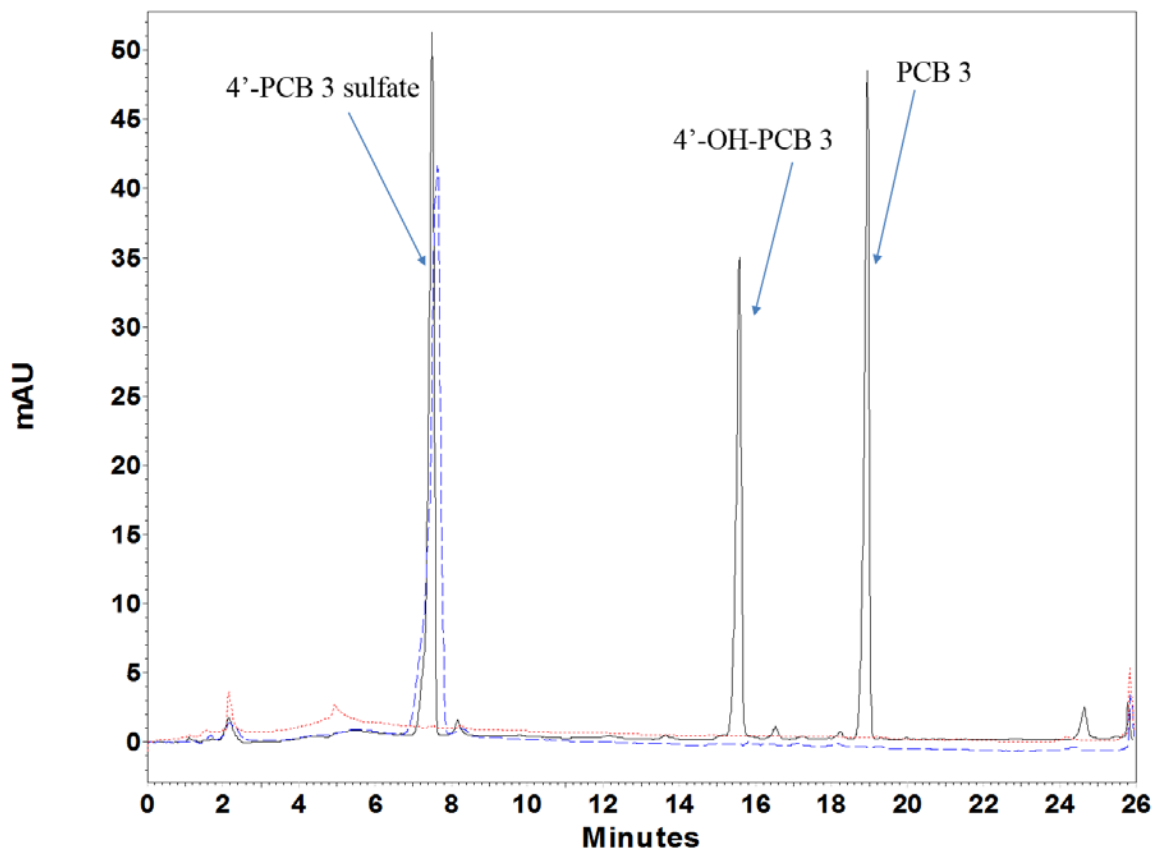


Figure A-19 Overlay of chromatograms from the HPLC analyses of extracellular media and cellular lysate extracts of SH-SY5Y cells treated with  $25\mu\text{M}$  4'-PCB 3 sulfate for 24 hours. Extracellular extract is represented in the blue dashed line. The lysate extract is represented in the dotted red line. Standards for the LC-PCB, the OH-LC-PCB, and the LC-PCB sulfate are represented in the solid black line. The extraction and HPLC conditions are described in detail in Chapter 6 Materials and Methods.

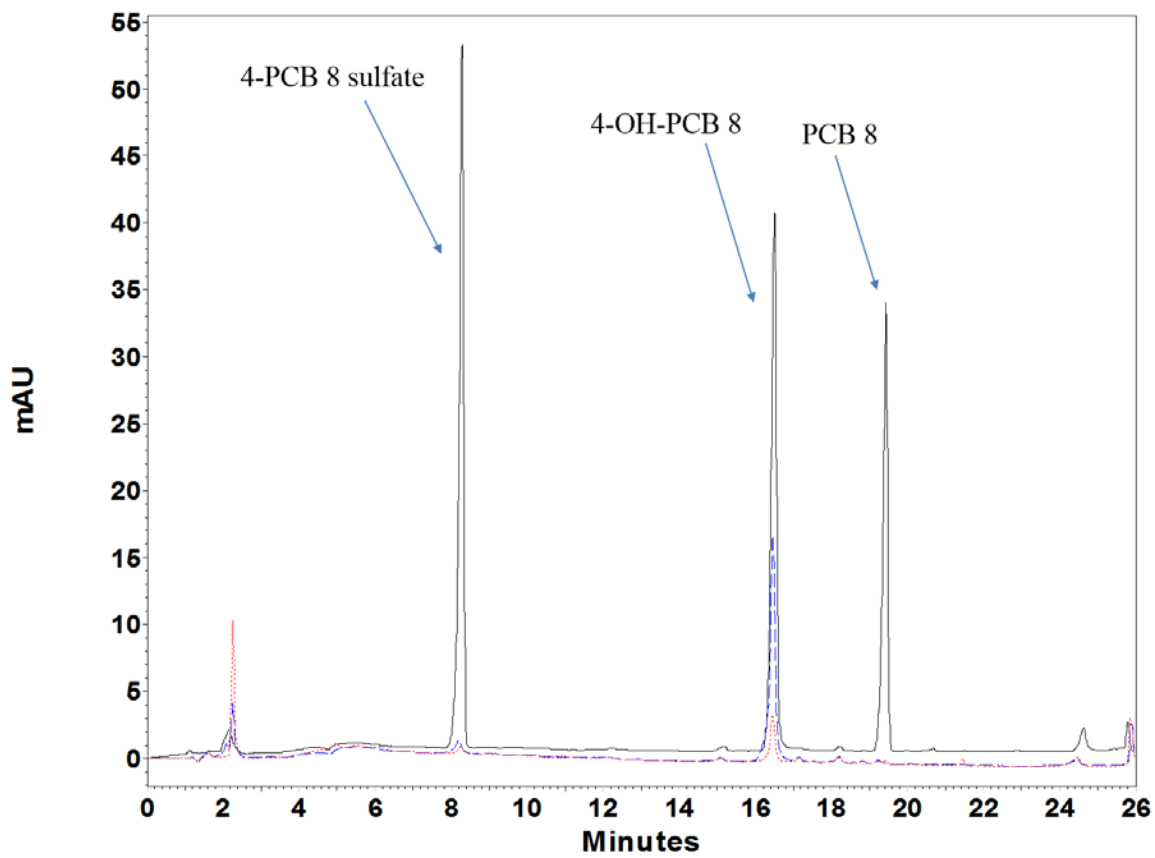


Figure A-20 Overlay of chromatograms from the HPLC analyses of extracellular media and cellular lysate extracts of SH-SY5Y cells treated with  $25\mu\text{M}$  4-OH-PCB 8 for 24 hours. Extracellular extract is represented in the blue dashed line. The lysate extract is represented in the dotted red line. Standards for the LC-PCB, the OH-LC-PCB, and the LC-PCB sulfate are represented in the solid black line. The extraction and HPLC conditions are described in detail in Chapter 6 Materials and Methods.

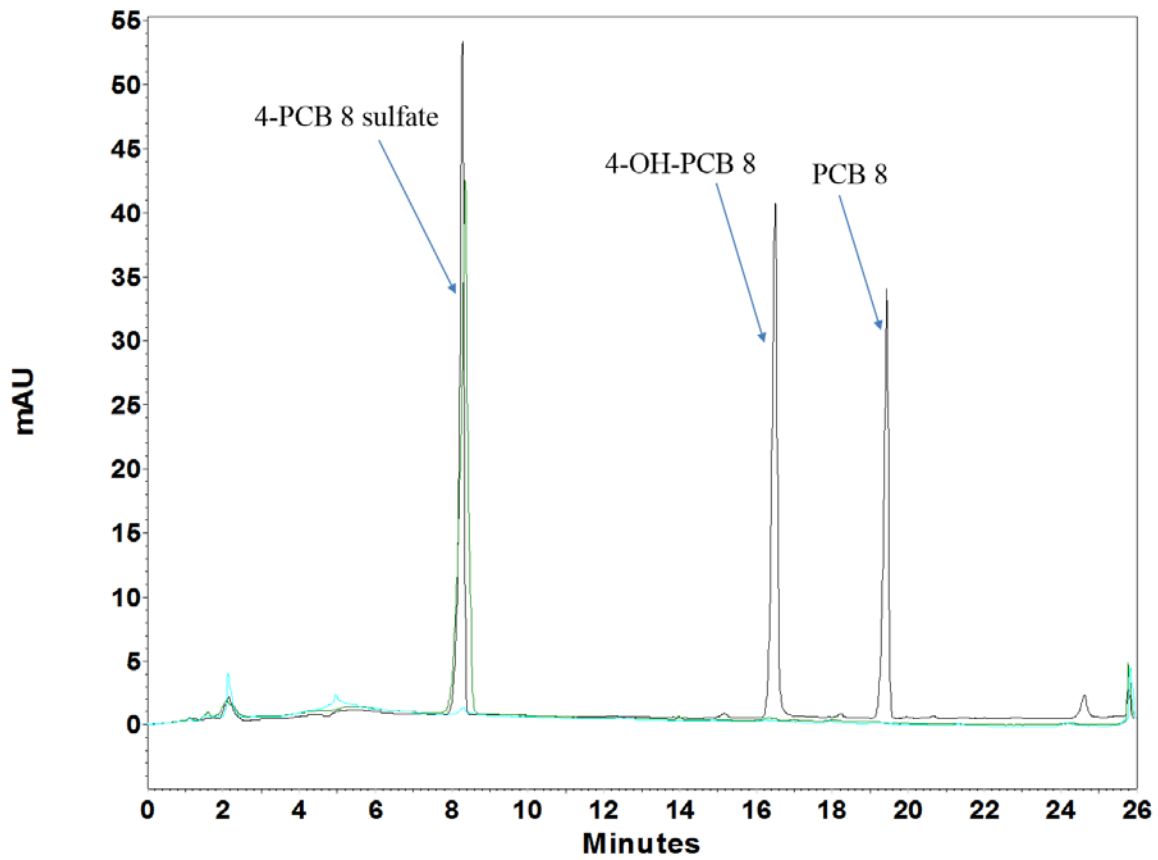


Figure A-21 Overlay of chromatograms from the HPLC analyses of extracellular media and cellular lysate extracts of SH-SY5Y cells treated with 25 $\mu$ M 4-PCB 8 sulfate for 24 hours. Extracellular extract is represented in the blue dashed line. The lysate extract is represented in the dotted red line. Standards for the LC-PCB, the OH-LC-PCB, and the LC-PCB sulfate are represented in the solid black line. The extraction and HPLC conditions are described in detail in Chapter 6 Materials and Methods.

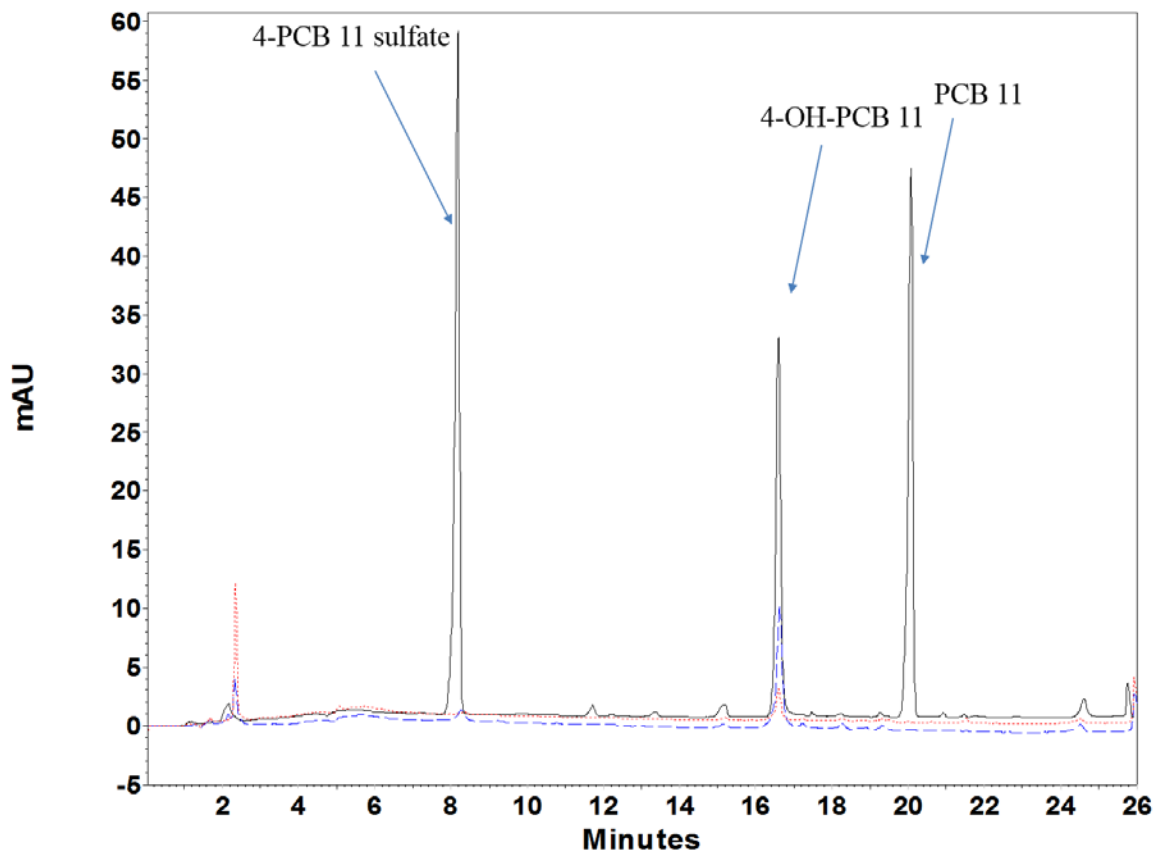


Figure A-22 Overlay of chromatograms from the HPLC analyses of extracellular media and cellular lysate extracts of SH-SY5Y cells treated with  $25\mu\text{M}$  4-OH-PCB 11 sulfate for 24 hours. Extracellular extract is represented in the blue dashed line. The lysate extract is represented in the dotted red line. Standards for the LC-PCB, the OH-LC-PCB, and the LC-PCB sulfate are represented in the solid black line. The extraction and HPLC conditions are described in detail in Chapter 6 Materials and Methods.

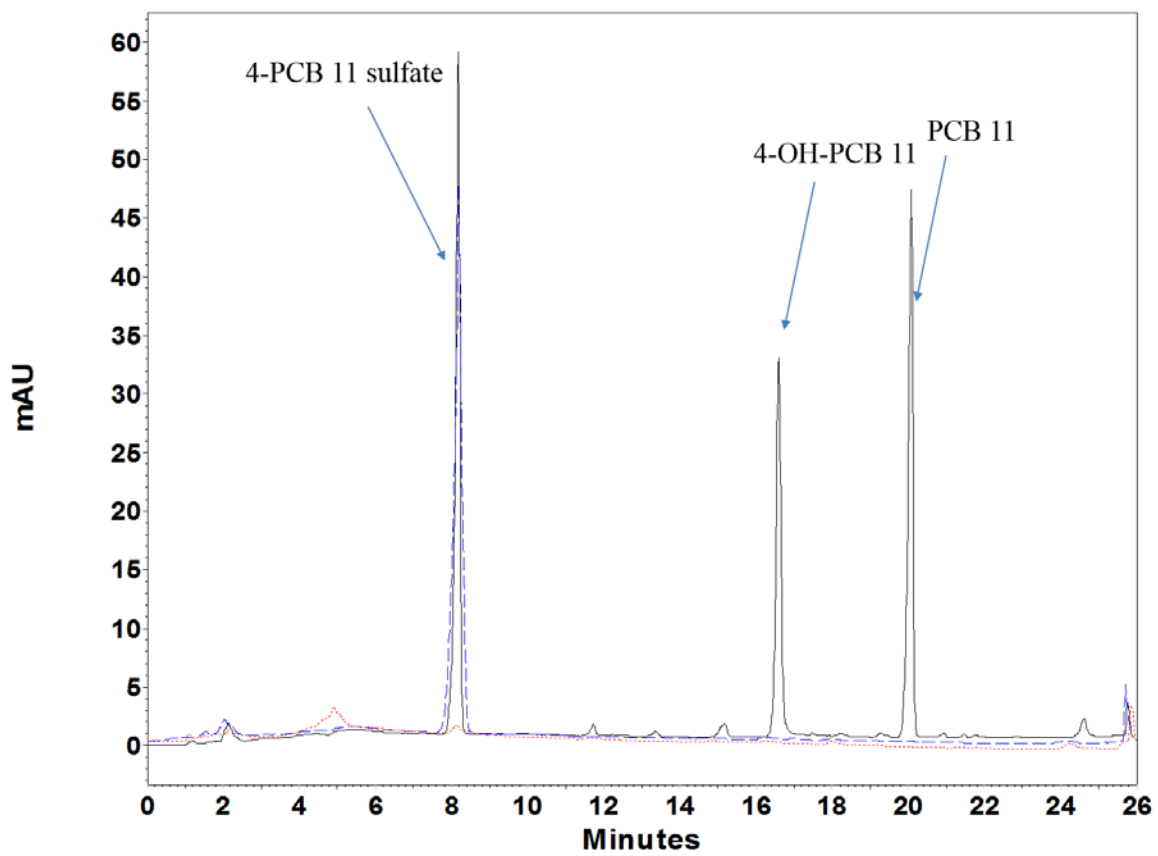


Figure A-23 Overlay of chromatograms from the HPLC analyses of extracellular media and cellular lysate extracts of SH-SY5Y cells treated with 25 $\mu$ M 4-PCB 11 sulfate for 24 hours. Extracellular extract is represented in the blue dashed line. The lysate extract is represented in the dotted red line. Standards for the LC-PCB, the OH-LC-PCB, and the LC-PCB sulfate are represented in the solid black line. The extraction and HPLC conditions are described in detail in Chapter 6 Materials and Methods.

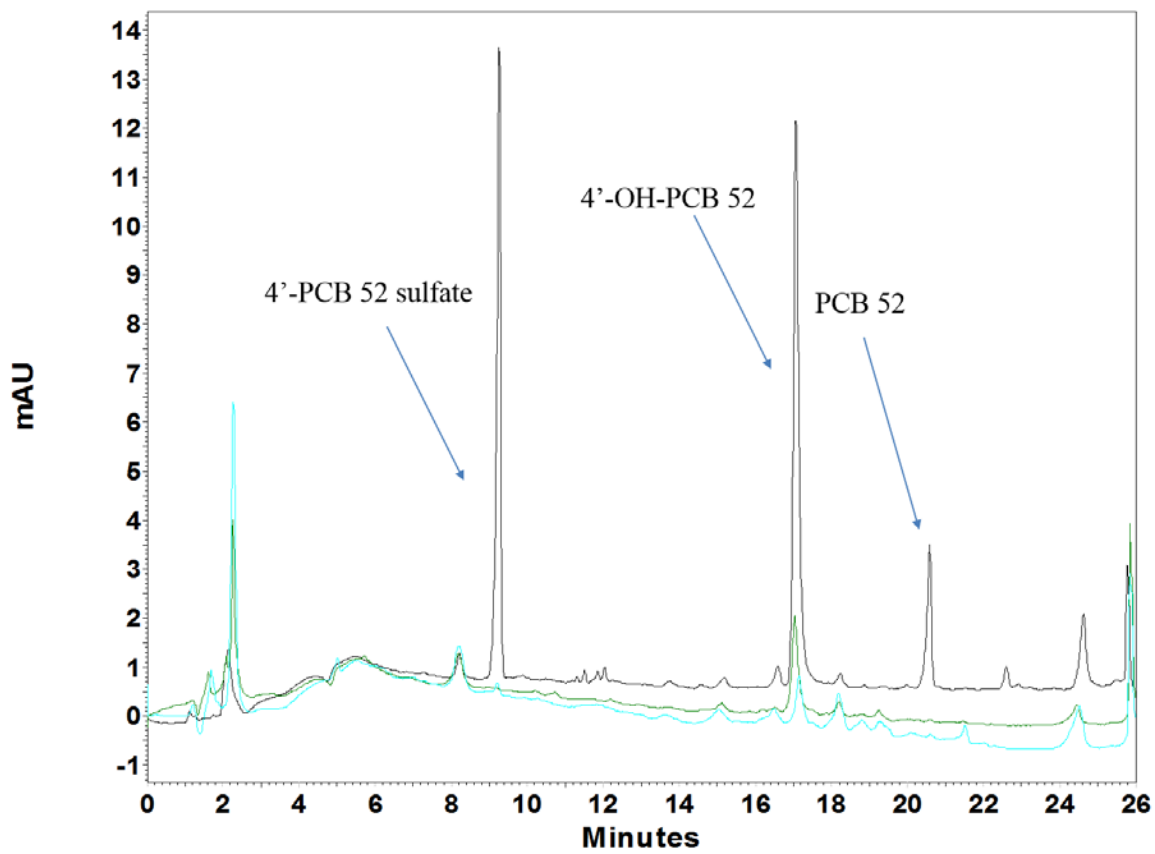


Figure A-24 Overlay of chromatograms from the HPLC analyses of extracellular media and cellular lysate extracts of SH-SY5Y cells treated with 25 $\mu$ M 4-OH-PCB 52 for 24 hours. Extracellular extract is represented in the blue dashed line. The lysate extract is represented in the dotted red line. Standards for the LC-PCB, the OH-LC-PCB, and the LC-PCB sulfate are represented in the solid black line. The extraction and HPLC conditions are described in detail in Chapter 6 Materials and Methods.

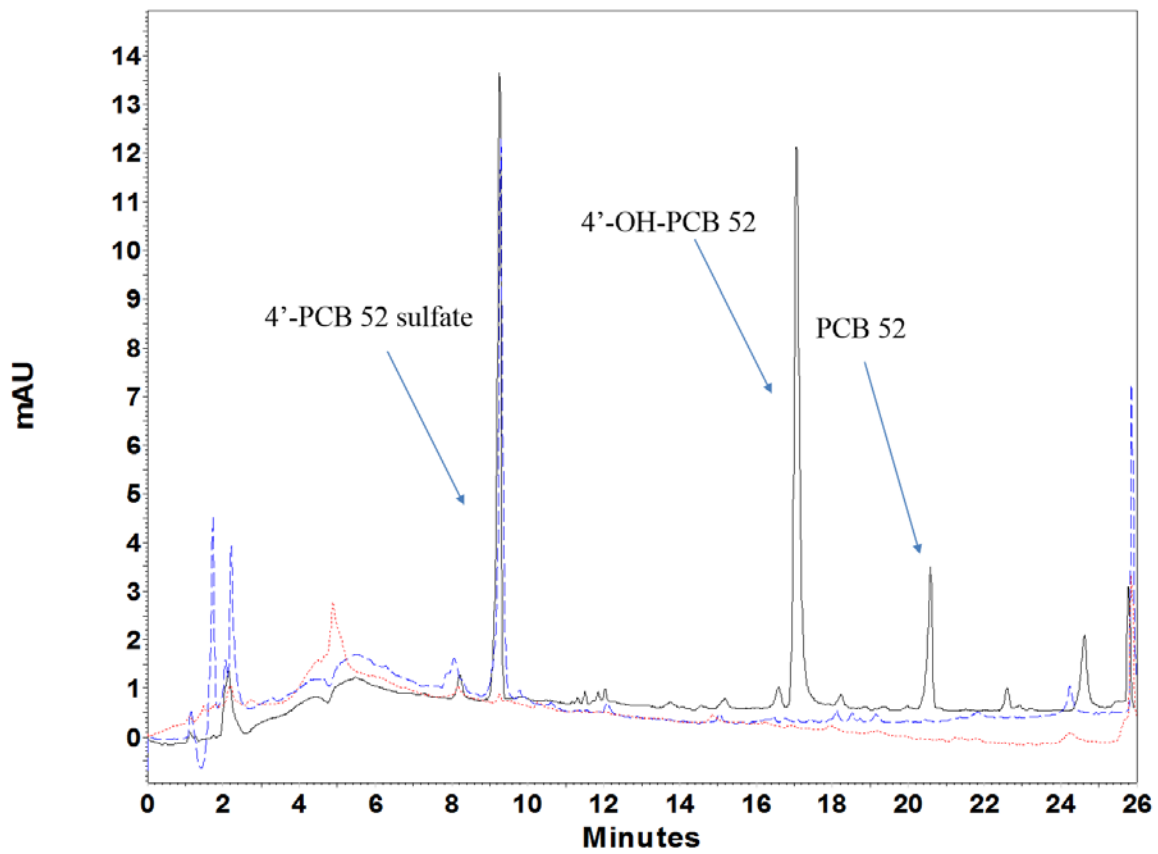


Figure A-25 Overlay of chromatograms from the HPLC analyses of extracellular media and cellular lysate extracts of SH-SY5Y cells treated with 25 $\mu$ M 4-PCB 52 sulfate for 24 hours. Extracellular extract is represented in the blue dashed line. The lysate extract is represented in the dotted red line. Standards for the LC-PCB, the OH-LC-PCB, and the LC-PCB sulfate are represented in the solid black line. The extraction and HPLC conditions are described in detail in Chapter 6 Materials and Methods.

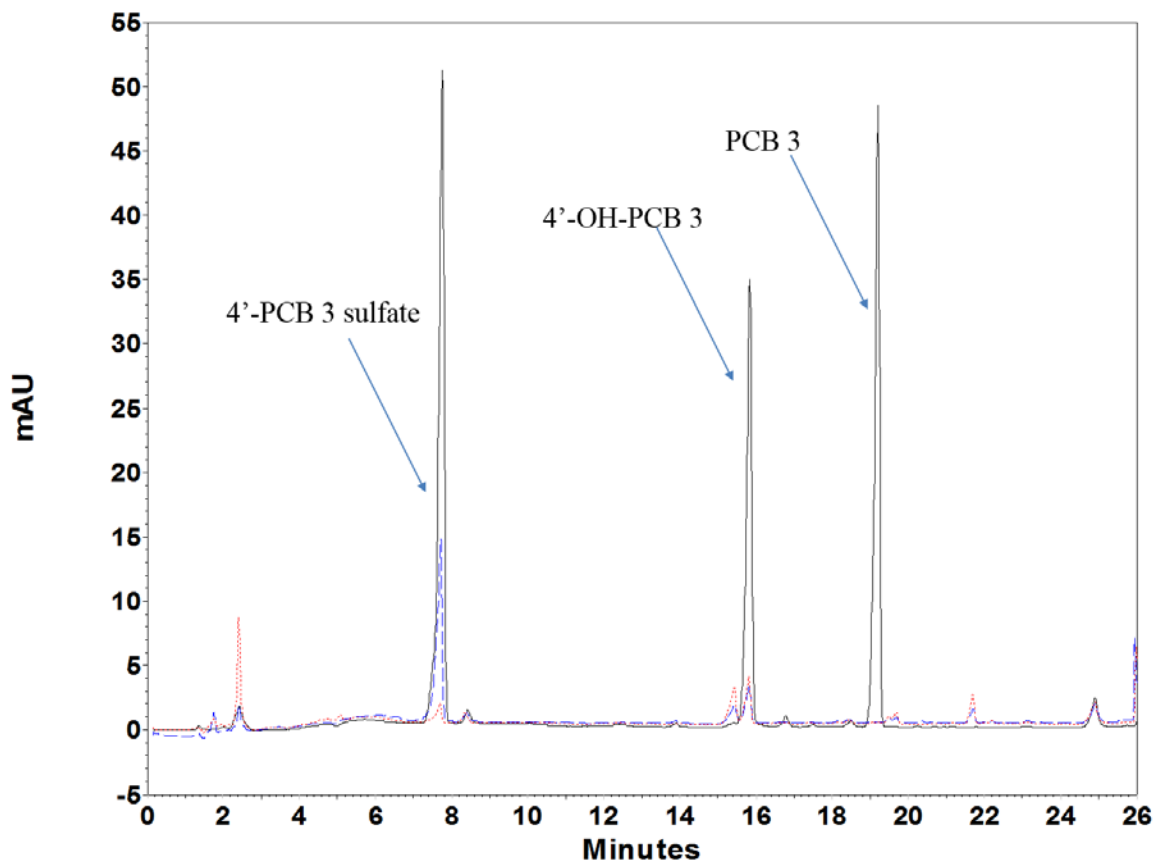


Figure A-26 Overlay of chromatograms from the HPLC analyses of extracellular media and cellular lysate extracts of HepG2 cells treated with  $25\mu\text{M}$  4'-OH-PCB 3 for 24 hours. Extracellular extract is represented in the blue dashed line. The lysate extract is represented in the dotted red line. Standards for the LC-PCB, the OH-LC-PCB, and the LC-PCB sulfate are represented in the solid black line. The extraction and HPLC conditions are described in detail in Chapter 6 Materials and Methods.



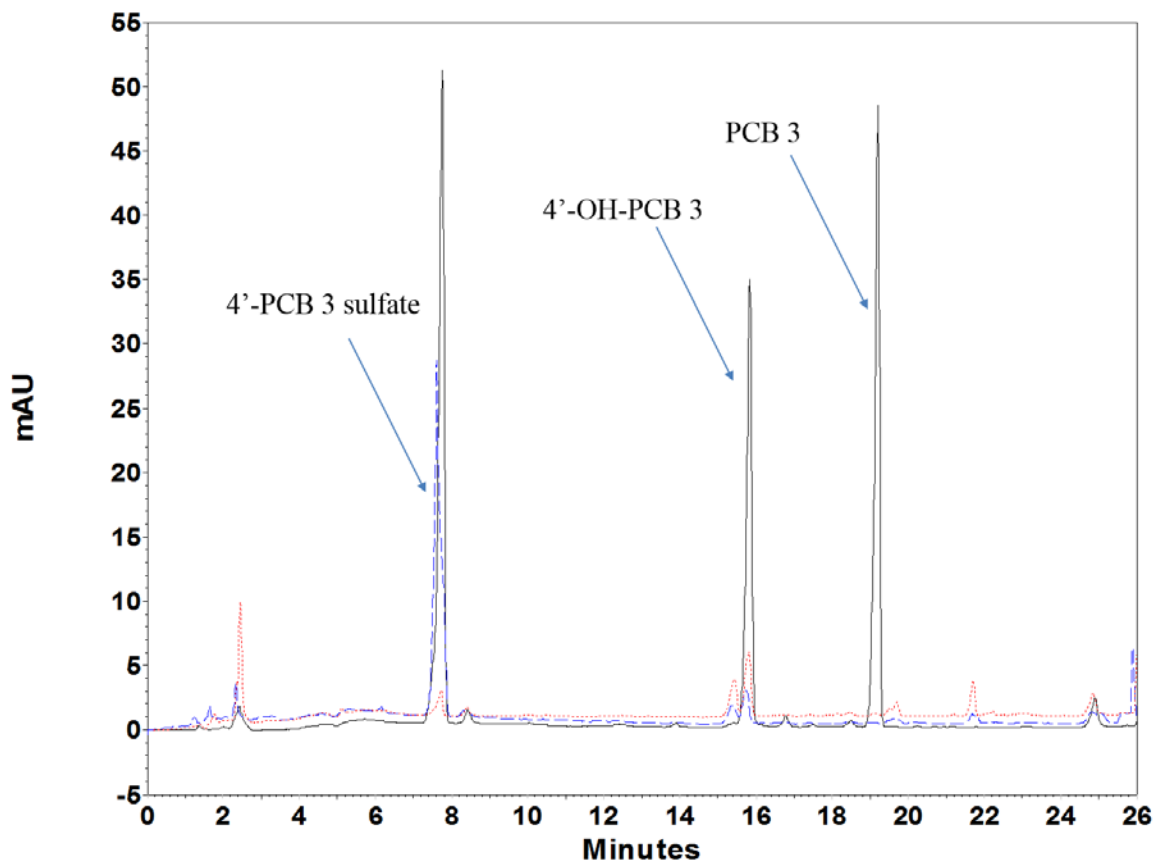


Figure A-27 Overlay of chromatograms from the HPLC analyses of extracellular media and cellular lysate extracts of HepG2 cells treated with 25 $\mu$ M 4'-PCB 3 sulfate for 24 hours. Extracellular extract is represented in the blue dashed line. The lysate extract is represented in the dotted red line. Standards for the LC-PCB, the OH-LC-PCB, and the LC-PCB sulfate are represented in the solid black line. The extraction and HPLC conditions are described in detail in Chapter 6 Materials and Methods.

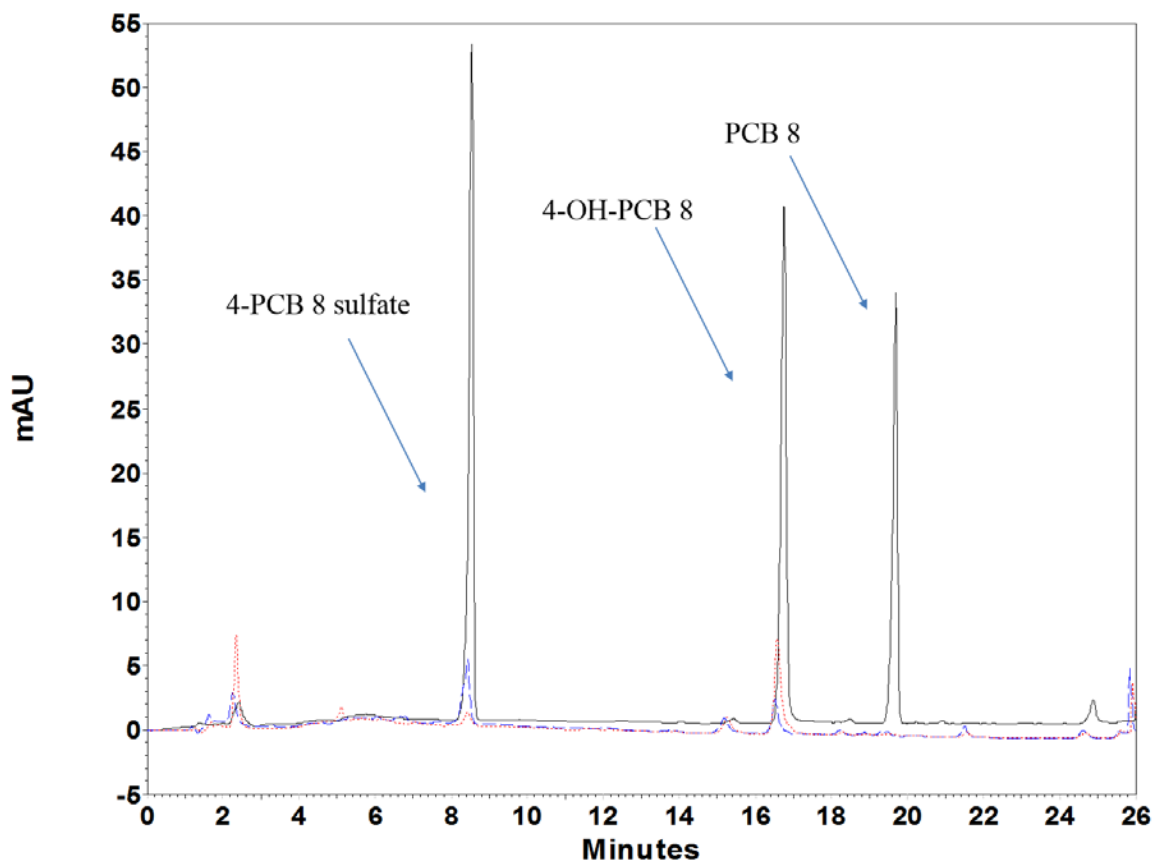


Figure A-28 Overlay of chromatograms from the HPLC analyses of extracellular media and cellular lysate extracts of HepG2 cells treated with  $25\mu\text{M}$  4-OH-PCB 8 for 24 hours. Extracellular extract is represented in the blue dashed line. The lysate extract is represented in the dotted red line. Standards for the LC-PCB, the OH-LC-PCB, and the LC-PCB sulfate are represented in the solid black line. The extraction and HPLC conditions are described in detail in Chapter 6 Materials and Methods.

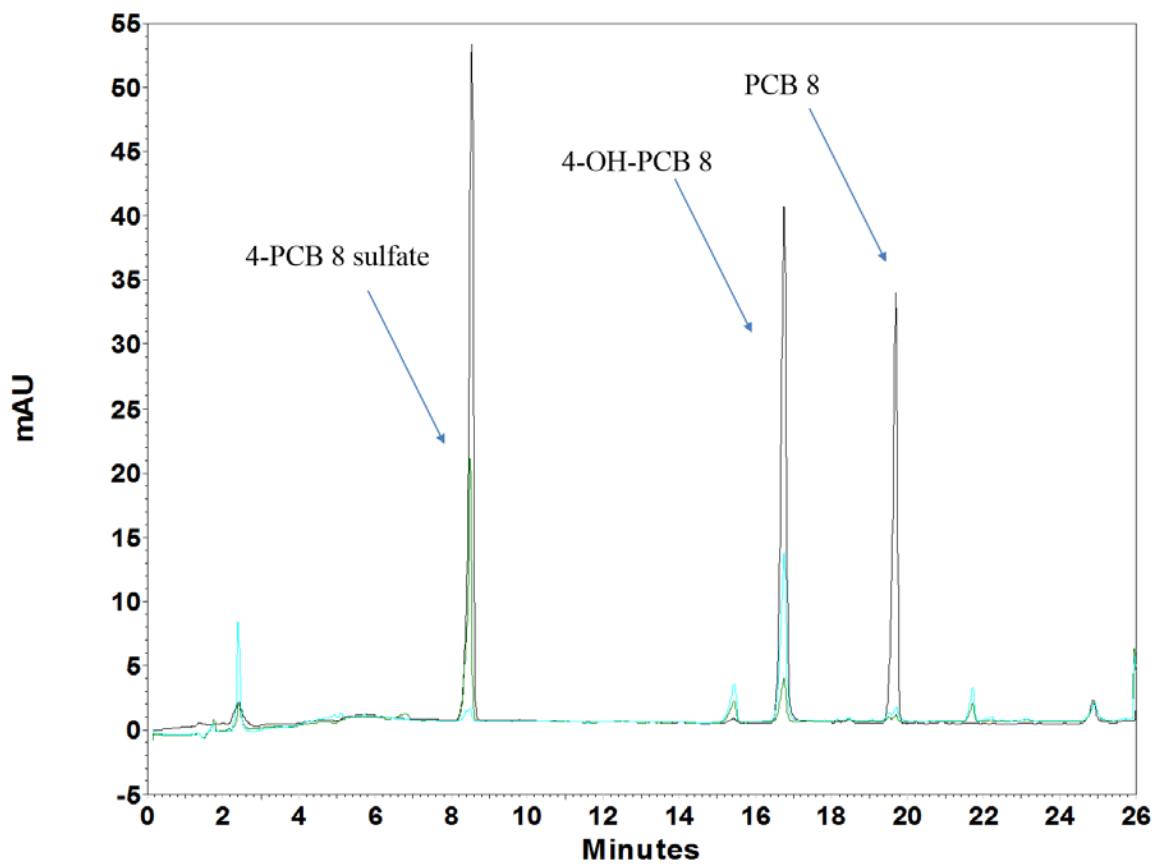


Figure A-29 Overlay of chromatograms from the HPLC analyses of extracellular media and cellular lysate extracts of HepG2 cells treated with 25 $\mu$ M 4-PCB 8 sulfate for 24 hours. Extracellular extract is represented in the blue dashed line. The lysate extract is represented in the dotted red line. Standards for the LC-PCB, the OH-LC-PCB, and the LC-PCB sulfate are represented in the solid black line. The extraction and HPLC conditions are described in detail in Chapter 6 Materials and Methods.

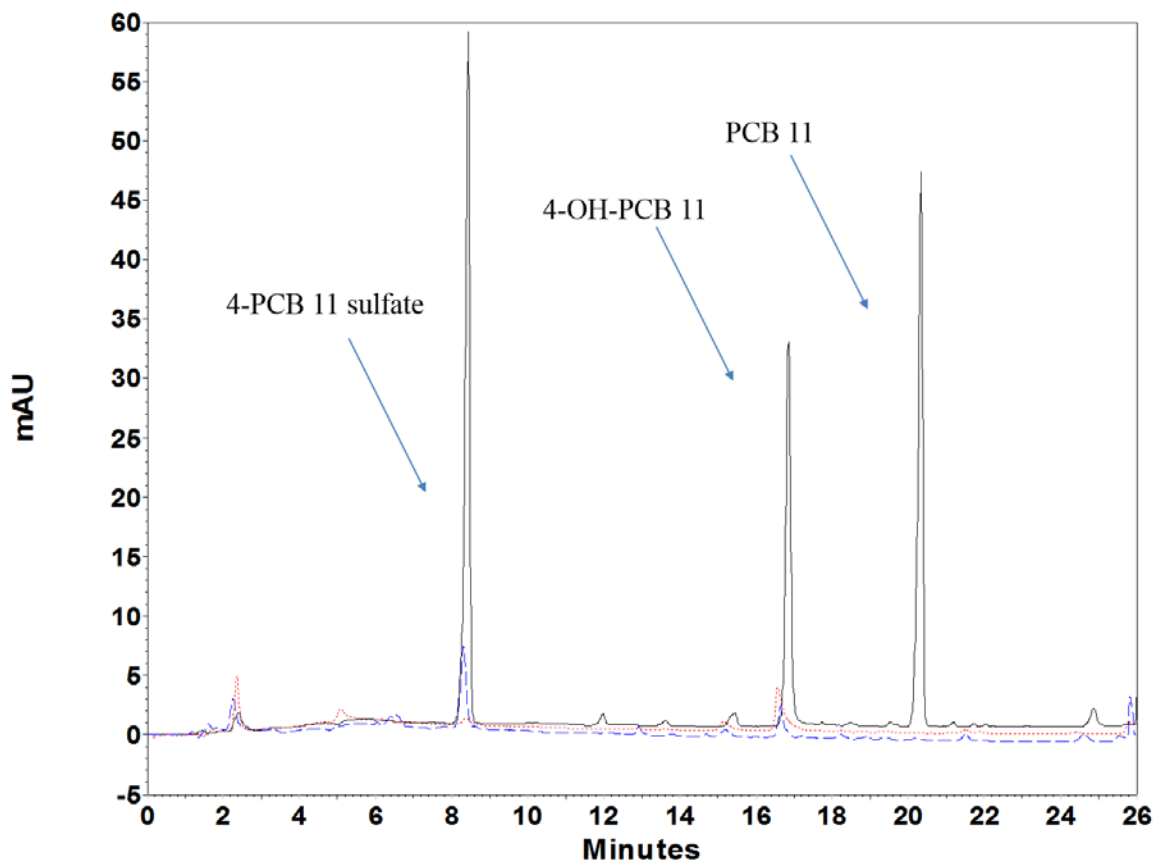


Figure A-30 Overlay of chromatograms from the HPLC analyses of extracellular media and cellular lysate extracts of HepG2 cells treated with 25 $\mu$ M 4-OH-PCB 11 for 24 hours. Extracellular extract is represented in the blue dashed line. The lysate extract is represented in the dotted red line. Standards for the LC-PCB, the OH-LC-PCB, and the LC-PCB sulfate are represented in the solid black line. The extraction and HPLC conditions are described in detail in Chapter 6 Materials and Methods.

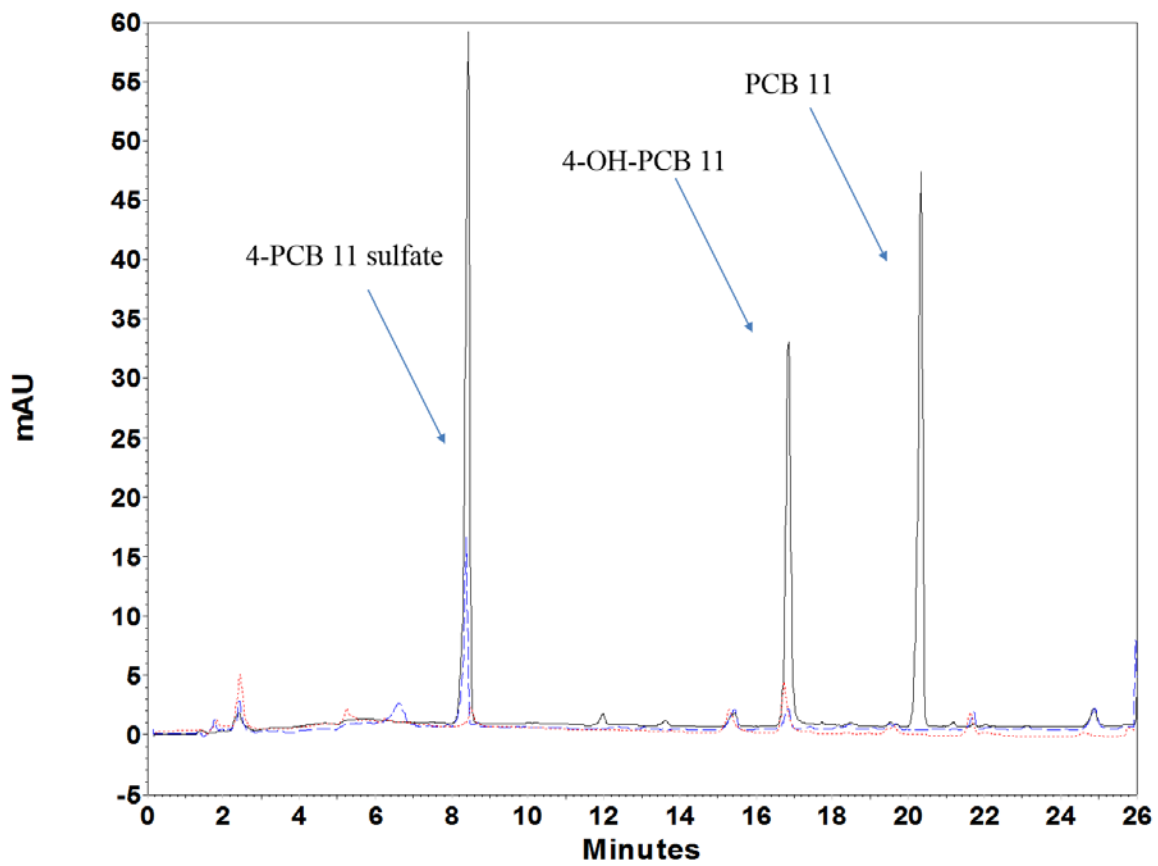


Figure A-31 Overlay of chromatograms from the HPLC analyses of extracellular media and cellular lysate extracts of HepG2 cells treated with 25 $\mu$ M 4-PCB 11 sulfate for 24 hours. Extracellular extract is represented in the blue dashed line. The lysate extract is represented in the dotted red line. Standards for the LC-PCB, the OH-LC-PCB, and the LC-PCB sulfate are represented in the solid black line. The extraction and HPLC conditions are described in detail in Chapter 6 Materials and Methods.

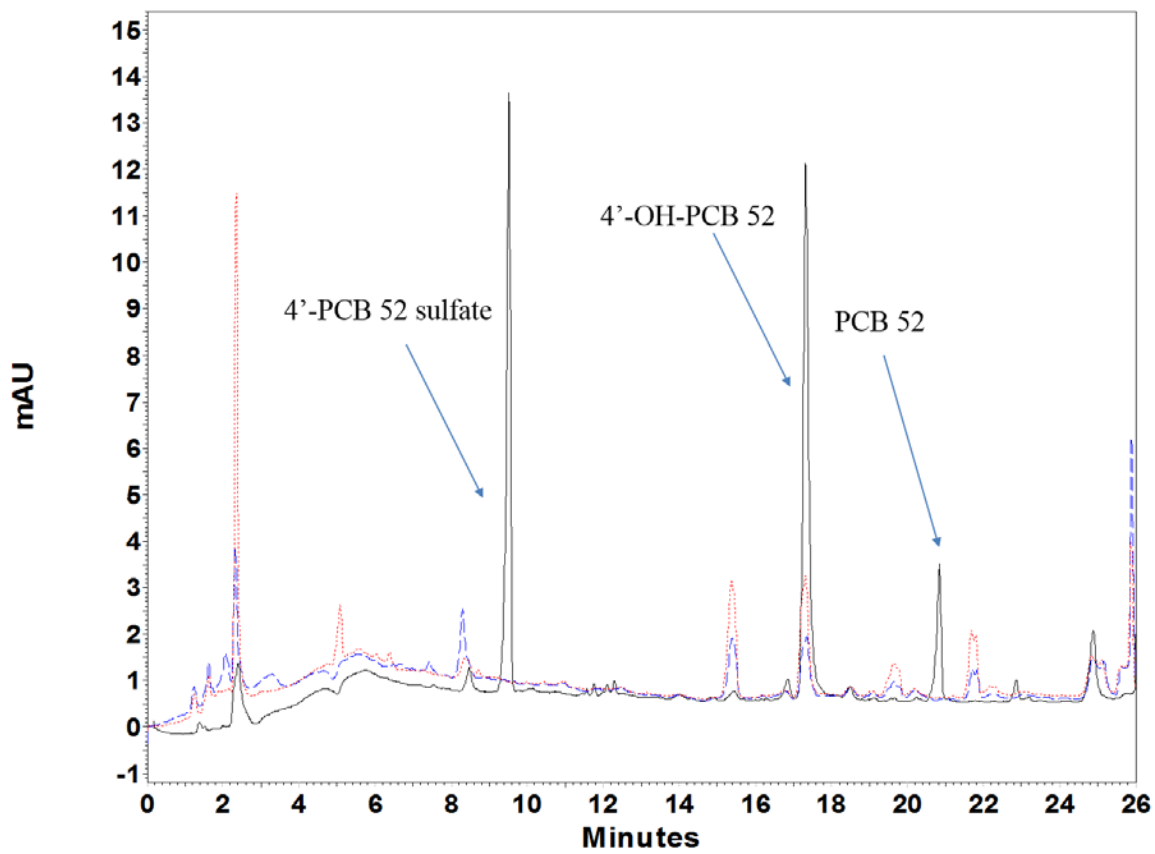


Figure A-32 Overlay of chromatograms from the HPLC analyses of extracellular media and cellular lysate extracts of HepG2 cells treated with  $25\mu\text{M}$  4-OH-PCB 52 for 24 hours. Extracellular extract is represented in the blue dashed line. The lysate extract is represented in the dotted red line. Standards for the LC-PCB, the OH-LC-PCB, and the LC-PCB sulfate are represented in the solid black line. The extraction and HPLC conditions are described in detail in Chapter 6 Materials and Methods.

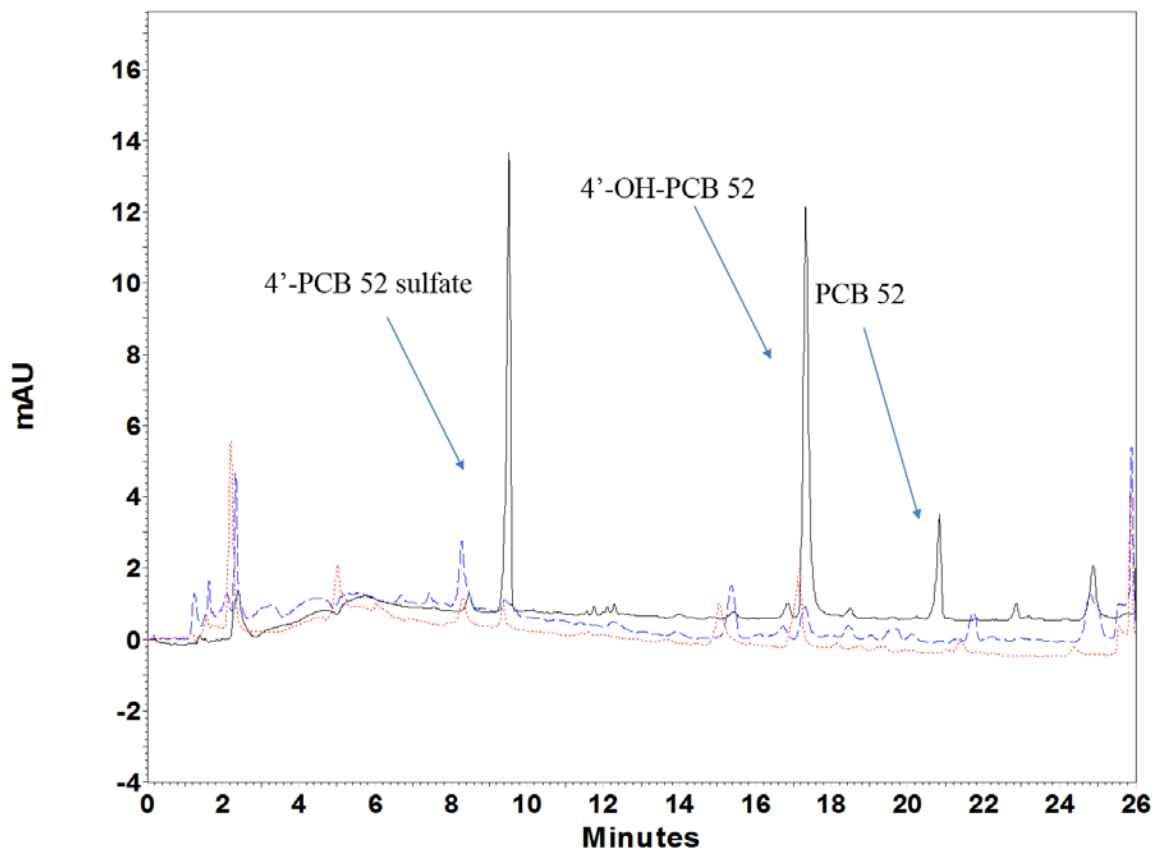


Figure A-33 Overlay of chromatograms from the HPLC analyses of extracellular media and cellular lysate extracts of HepG2 cells treated with 25 $\mu$ M 4-PCB 52 sulfate for 24 hours. Extracellular extract is represented in the blue dashed line. The lysate extract is represented in the dotted red line. Standards for the LC-PCB, the OH-LC-PCB, and the LC-PCB sulfate are represented in the solid black line. The extraction and HPLC conditions are described in detail in Chapter 6 Materials and Methods.

## REFERENCES

1. Robertson, L. W.; Hansen, L. G., *PCBs : recent advances in environmental toxicology and health effects*. University Press of Kentucky: Lexington, KY, 2001.
2. ATSDR, Toxicological profile for polychlorinated biphenyls (PCBs). *US Department of Health and Human Services, Public Health Service Agency for Toxic Substances and Disease Registry, Atlanta, GA, 2000*.
3. Ross, G., The public health implications of polychlorinated biphenyls (PCBs) in the environment. *Ecotoxicol. Environ. Saf.* **2004**, *59*, (3), 275-91.
4. Schmidt, H. S., G., Ueber Benziding ( $\alpha$ -Diamidodiphenyl). *Justus Liebigs Ann. Chem.* **1881**, *207*, 320-347.
5. Breivik, K.; Sweetman, A.; Pacyna, J. M.; Jones, K. C., Towards a global historical emission inventory for selected PCB congeners--a mass balance approach. 1. Global production and consumption. *Sci Total Environ* **2002**, *290*, (1-3), 181-98.
6. Erickson, M. D.; Kaley, R. G., 2nd, Applications of polychlorinated biphenyls. *Environ. Sci. Pollut. Res.* **2011**, *18*, (2), 135-51.
7. Lehmler, H. J.; Harrad, S. J.; Huhnerfuss, H.; Kania-Korwel, I.; Lee, C. M.; Lu, Z.; Wong, C. S., Chiral polychlorinated biphenyl transport, metabolism, and distribution: a review. *Environ Sci Technol* **2010**, *44*, (8), 2757-66.
8. Ballschmiter, K.; Zell, M., Analysis of polychlorinated biphenyls (PCB) by glass capillary gas chromatography. *Fresenius' Zeitschrift für analytische Chemie* **1980**, *302*, (1), 20-31.
9. Mills Iii, S. A.; Thal, D. I.; Barney, J., A summary of the 209 PCB congener nomenclature. *Chemosphere* **2007**, *68*, (9), 1603-1612.
10. Drinker, C. K., The Problem of Possible Systemic Effects From Certain Chlorinated Hydrocarbons. *J. Ind. Hyg. Toxicol.* **1937**, *19*, 283-311.
11. Carson, R.; Darling, L.; Darling, L., *Silent spring*. Houghton Mifflin ;Riverside Press: BostonCambridge, Mass., 1962; p x, 368 p.
12. Jensen, S., Report of a New Chemical Hazard. *NEW SCIENTIST* **1966**, *32*.
13. Borgå, K.; Fisk, A. T.; Hoekstra, P. F.; Muir, D. C. G., Biological and chemical factors of importance in the bioaccumulation and trophic transfer of persistent organochlorine contaminants in arctic marine food webs. *Environmental Toxicology and Chemistry* **2004**, *23*, (10), 2367-2385.
14. Borga, K.; Gabrielsen, G. W.; Skaare, J. U., Biomagnification of organochlorines along a Barents Sea food chain. *Environ Pollut* **2001**, *113*, (2), 187-98.
15. Weant, G. E.; McCormick, G. S.; Planning, U. S. E. P. A. O. o. A. Q.; Standards; Engineering-Science, i., *Nonindustrial Sources of Potentially Toxic Substances and Their Applicability to Source Apportionment Methods*. U.S. Environmental Protection Agency, Office of Air and Radiation , Office of Air Quality Planning and Standards: 1984.



16. Abramowicz, D. A., Aerobic and anaerobic PCB biodegradation in the environment. *Environ Health Perspect* **1995**, *103 Suppl 5*, 97-9.
17. Schecter, A.; Tiernan, T., Occupational exposure to polychlorinated dioxins, polychlorinated furans, polychlorinated biphenyls, and biphenylenes after an electrical panel and transformer accident in an office building in Binghamton, NY. *Environ Health Perspect* **1985**, *60*, 305-13.
18. Erdal, S.; Berman, L.; Hryhorczuk, D. O., Multimedia emissions inventory of polychlorinated biphenyls for the U.S. Great Lakes states. *J Air Waste Manag Assoc* **2008**, *58*, (8), 1022-32.
19. Kluesner, D. W. Hudson River PCBs: Background and Site Information. <http://www3.epa.gov/hudson/background.htm> (January 22nd),
20. Eschenroeder, A. Q.; Doyle, C. P.; Faeder, E. J., Health risks of PCB spills from electrical equipment. *Risk Anal* **1986**, *6*, (2), 213-21.
21. Nisbet, I. C.; Sarofim, A. F., Rates and Routes of Transport of PCBs in the Environment. *Environ Health Perspect* **1972**, *1*, 21-38.
22. Swain, W. R., Chlorinated Organic Residues in Fish, Water, and Precipitation from the Vicinity of Isle Royale, Lake Superior. *Journal of Great Lakes Research* **1978**, *4*, (3-4), 398-407.
23. Palmer, P. M.; Wilson, L. R.; Casey, A. C.; Wagner, R. E., Occurrence of PCBs in raw and finished drinking water at seven public water systems along the Hudson River. *Environ Monit Assess* **2011**, *175*, (1-4), 487-99.
24. Pavlova, P. A.; Schmid, P.; Bogdal, C.; Steinlin, C.; Jenk, T. M.; Schwikowski, M., Polychlorinated biphenyls in glaciers. 1. Deposition history from an Alpine ice core. *Environ Sci Technol* **2014**, *48*, (14), 7842-8.
25. Wierda, M. R.; Leith, K. F.; Grubb, T. G.; Sikarskie, J. G.; Best, D. A.; Bowerman, W., Using bald eagles to track spatial (1999-2008) and temporal (1987-1992, 1999-2003, and 2004-2008) trends of contaminants in Michigan's aquatic ecosystems. *Environ Toxicol Chem* **2015**.
26. Quiroz, R.; Popp, P.; Barra, R., Analysis of PCB levels in snow from the Aconcagua Mountain (Southern Andes) using the stir bar sorptive extraction. *Environmental Chemistry Letters* **2008**, *7*, (3), 283-288.
27. Kiviranta, H.; Vartiainen, T.; Verta, M.; Tuomisto, J. T.; Tuomisto, J., High fish-specific dioxin concentrations in Finland. *Lancet* **2000**, *355*, (9218), 1883-5.
28. Sharma, B. M.; Nizzetto, L.; Bharat, G. K.; Tayal, S.; Melymuk, L.; Sanka, O.; Pribylova, P.; Audy, O.; Larssen, T., Melting Himalayan glaciers contaminated by legacy atmospheric depositions are important sources of PCBs and high-molecular-weight PAHs for the Ganges floodplain during dry periods. *Environ Pollut* **2015**, *206*, 588-96.
29. Rodenburg, L. A.; Du, S.; Xiao, B.; Fennell, D. E., Source apportionment of polychlorinated biphenyls in the New York/New Jersey Harbor. *Chemosphere* **2011**, *83*, (6), 792-8.

30. Davis, J. A.; Hetzel, F.; Oram, J. J.; McKee, L. J., Polychlorinated biphenyls (PCBs) in San Francisco Bay. *Environ Res* **2007**, *105*, (1), 67-86.
31. Barron, M. G., Bioconcentration. Will water-borne organic chemicals accumulate in aquatic animals? *Environ. Sci. Technol.* **1990**, *24*, (11), 1612-1618.
32. Hope, B.; Scatolini, S.; Titus, E.; Cotter, J., Distribution patterns of polychlorinated biphenyl congeners in water, sediment and biota from Midway Atoll (North Pacific Ocean). *Mar. Pollut. Bull.* **1997**, *34*, (7), 548-563.
33. Elliott, K. H.; Cesh, L. S.; Dooley, J. A.; Letcher, R. J.; Elliott, J. E., PCBs and DDE, but not PBDEs, increase with trophic level and marine input in nestling bald eagles. *Sci. Total Environ.* **2009**, *407*, (12), 3867-75.
34. Gutleb, A. C.; Cenijn, P.; Velzen, M.; Lie, E.; Ropstad, E.; Skaare, J. U.; Malmberg, T.; Bergman, A.; Gabrielsen, G. W.; Legler, J., In vitro assay shows that PCB metabolites completely saturate thyroid hormone transport capacity in blood of wild polar bears (*Ursus maritimus*). *Environ. Sci. Technol.* **2010**, *44*, (8), 3149-54.
35. Hung, H.; Kallenborn, R.; Breivik, K.; Su, Y.; Brorstrom-Lunden, E.; Olafsdottir, K.; Thorlacius, J. M.; Leppanen, S.; Bossi, R.; Skov, H.; Mano, S.; Patton, G. W.; Stern, G.; Sverko, E.; Fellin, P., Atmospheric monitoring of organic pollutants in the Arctic under the Arctic Monitoring and Assessment Programme (AMAP): 1993-2006. *Sci Total Environ* **2010**, *408*, (15), 2854-73.
36. Wania, F.; Mackay, D., Peer reviewed: tracking the distribution of persistent organic pollutants. *Environ Sci Technol* **1996**, *30*, (9), 390A-6A.
37. Macdonal, R. W.; Barrie, L. A.; Bidleman, T. F.; Diamond, M. L.; Gregor, D. J.; Semkin, R. G.; Strachan, W. M.; Li, Y. F.; Wania, F.; Alae, M.; Alexeeva, L. B.; Backus, S. M.; Bailey, R.; Bewers, J. M.; Gobeil, C.; Halsall, C. J.; Harner, T.; Hoff, J. T.; Jantunen, L. M.; Lockhart, W. L.; Mackay, D.; Muir, D. C.; Pudykiewicz, J.; Reimer, K. J.; Smith, J. N.; Stern, G. A., Contaminants in the Canadian Arctic: 5 years of progress in understanding sources, occurrence and pathways. *Sci Total Environ* **2000**, *254*, (2-3), 93-234.
38. Carpenter, D. O.; DeCaprio, A. P.; O'Hehir, D.; Akhtar, F.; Johnson, G.; Scudato, R. J.; Apatiki, L.; Kava, J.; Gologergen, J.; Miller, P. K.; Eckstein, L., Polychlorinated biphenyls in serum of the Siberian Yupik people from St. Lawrence Island, Alaska. *Int J Circumpolar Health* **2005**, *64*, (4), 322-35.
39. Verreault, J.; Muir, D. C.; Norstrom, R. J.; Stirling, I.; Fisk, A. T.; Gabrielsen, G. W.; Derocher, A. E.; Evans, T. J.; Dietz, R.; Sonne, C.; Sandala, G. M.; Gebbink, W.; Riget, F. F.; Born, E. W.; Taylor, M. K.; Nagy, J.; Letcher, R. J., Chlorinated hydrocarbon contaminants and metabolites in polar bears (*Ursus maritimus*) from Alaska, Canada, East Greenland, and Svalbard: 1996-2002. *Sci Total Environ* **2005**, *351-352*, 369-90.
40. Sonne, C., Health effects from long-range transported contaminants in Arctic top predators: An integrated review based on studies of polar bears and relevant model species. *Environ Int* **2010**, *36*, (5), 461-91.
41. Letcher, R. J.; Bustnes, J. O.; Dietz, R.; Jenssen, B. M.; Jorgensen, E. H.; Sonne, C.; Verreault, J.; Vijayan, M. M.; Gabrielsen, G. W., Exposure and effects assessment of

- persistent organohalogen contaminants in arctic wildlife and fish. *Sci Total Environ* **2010**, *408*, (15), 2995-3043.
42. Gabrielsen, K. M.; Krokstad, J. S.; Villanger, G. D.; Blair, D. A.; Obregon, M. J.; Sonne, C.; Dietz, R.; Letcher, R. J.; Jenssen, B. M., Thyroid hormones and deiodinase activity in plasma and tissues in relation to high levels of organohalogen contaminants in East Greenland polar bears (*Ursus maritimus*). *Environ Res* **2015**, *136*, 413-23.
  43. Bustnes, J. O.; Hanssen, S. A.; Folstad, I.; Erikstad, K. E.; Hasselquist, D.; Skaare, J. U., Immune function and organochlorine pollutants in Arctic breeding glaucous gulls. *Arch Environ Contam Toxicol* **2004**, *47*, (4), 530-41.
  44. Ayotte, P.; Dewailly, E.; Ryan, J. J.; Bruneau, S.; Lebel, G., PCBs and dioxin-like compounds in plasma of adult Inuit living in Nunavik (Arctic Quebec). *Chemosphere* **1997**, *34*, (5-7), 1459-68.
  45. Dewailly, E.; Ryan, J. J.; Laliberte, C.; Bruneau, S.; Weber, J. P.; Gingras, S.; Carrier, G., Exposure of remote maritime populations to coplanar PCBs. *Environ Health Perspect* **1994**, *102 Suppl 1*, 205-9.
  46. Dewailly, E.; Ayotte, P.; Bruneau, S.; Laliberte, C.; Muir, D. C.; Norstrom, R. J., Inuit exposure to organochlorines through the aquatic food chain in arctic quebec. *Environ Health Perspect* **1993**, *101*, (7), 618-20.
  47. Korrick, S. A.; Altshul, L., High breast milk levels of polychlorinated biphenyls (PCBs) among four women living adjacent to a PCB-contaminated waste site. *Environ Health Perspect* **1998**, *106*, (8), 513-8.
  48. Hsu, S. T.; Ma, C. I.; Hsu, S. K.; Wu, S. S.; Hsu, N. H.; Yeh, C. C.; Wu, S. B., Discovery and epidemiology of PCB poisoning in Taiwan: a four-year followup. *Environ Health Perspect* **1985**, *59*, 5-10.
  49. Yu, M. L.; Guo, Y. L.; Hsu, C. C.; Rogan, W. J., Increased mortality from chronic liver disease and cirrhosis 13 years after the Taiwan "yucheng" ("oil disease") incident. *Am J Ind Med* **1997**, *31*, (2), 172-5.
  50. Li, M. C.; Chen, P. C.; Tsai, P. C.; Furue, M.; Onozuka, D.; Hagihara, A.; Uchi, H.; Yoshimura, T.; Guo, Y. L., Mortality after exposure to polychlorinated biphenyls and polychlorinated dibenzofurans: a meta-analysis of two highly exposed cohorts. *Int J Cancer* **2015**, *137*, (6), 1427-32.
  51. Furue, M.; Uenotsuchi, T.; Urabe, K.; Ishikawa, T.; Kuwabara, M., Overview of Yusho. *Journal of Dermatological Science Supplement* **2005**, *1*, (1), S3-S10.
  52. Lai, T. J.; Guo, Y. L.; Guo, N. W.; Hsu, C. C., Effect of prenatal exposure to polychlorinated biphenyls on cognitive development in children: a longitudinal study in Taiwan. *Br J Psychiatry Suppl* **2001**, *40*, s49-52.
  53. Chen, Y. C.; Guo, Y. L.; Hsu, C. C.; Rogan, W. J., Cognitive development of Yu-Cheng ("oil disease") children prenatally exposed to heat-degraded PCBs. *JAMA* **1992**, *268*, (22), 3213-8.
  54. Wimmerova, S.; Watson, A.; Drobna, B.; Sovcikova, E.; Weber, R.; Lancz, K.; Patayova, H.; Richterova, D.; Kostiakova, V.; Jureckova, D.; Zavacky, P.; Stremy, M.; Jusko, T. A.;

- Murinova, L. P.; Hertz-Picciotto, I.; Trnovec, T., The spatial distribution of human exposure to PCBs around a former production site in Slovakia. *Environ Sci Pollut R* **2015**, *22*, (19), 14405-14415.
55. Fernandez-Rodriguez, M.; Arrebola, J. P.; Artacho-Cordon, F.; Amaya, E.; Aragones, N.; Llorca, J.; Perez-Gomez, B.; Ardanaz, E.; Kogevinas, M.; Castano-Vinyals, G.; Pollan, M.; Olea, N., Levels and predictors of persistent organic pollutants in an adult population from four Spanish regions. *Sci Total Environ* **2015**, *538*, 152-61.
  56. Pieters, R.; Focant, J. F., Dioxin, furan and PCB serum levels in a South African Tswana population: comparing the polluting effects of using different cooking and heating fuels. *Environ Int* **2014**, *66*, 71-8.
  57. Wang, Y.; Xu, M.; Jin, J.; He, S.; Li, M.; Sun, Y., Concentrations and relationships between classes of persistent halogenated organic compounds in pooled human serum samples and air from Laizhou Bay, China. *Sci Total Environ* **2014**, *482-483*, 276-82.
  58. Ljunggren, S. A.; Helmfrid, I.; Salihovic, S.; van Bavel, B.; Wingren, G.; Lindahl, M.; Karlsson, H., Persistent organic pollutants distribution in lipoprotein fractions in relation to cardiovascular disease and cancer. *Environ Int* **2014**, *65*, 93-9.
  59. Serdar, B.; LeBlanc, W. G.; Norris, J. M.; Dickinson, L. M., Potential effects of polychlorinated biphenyls (PCBs) and selected organochlorine pesticides (OCPs) on immune cells and blood biochemistry measures: a cross-sectional assessment of the NHANES 2003-2004 data. *Environ. Health* **2014**, *13*, 114.
  60. Kumar, J.; Lind, P. M.; Salihovic, S.; van Bavel, B.; Ekdahl, K. N.; Nilsson, B.; Lind, L.; Ingelsson, E., Influence of persistent organic pollutants on the complement system in a population-based human sample. *Environ. Int.* **2014**, *71*, 94-100.
  61. Bell, M. R., Endocrine-disrupting actions of PCBs on brain development and social and reproductive behaviors. *Curr. Opin. Pharmacol.* **2014**, *19*, 134-44.
  62. Ulbrich, B.; Stahlmann, R., Developmental toxicity of polychlorinated biphenyls (PCBs): a systematic review of experimental data. *Arch. Toxicol.* **2004**, *78*, (5), 252-68.
  63. Schantz, S. L.; Widholm, J. J.; Rice, D. C., Effects of PCB exposure on neuropsychological function in children. *Environ. Health Perspect.* **2003**, *111*, (3), 357-576.
  64. Verner, M. A.; Hart, J. E.; Sagiv, S. K.; Bellinger, D. C.; Altshul, L. M.; Korrick, S. A., Measured prenatal and estimated postnatal levels of polychlorinated biphenyls (PCBs) and ADHD-related behaviors in 8-year-old children. *Environ. Health Perspect.* **2015**, *123*, (9), 888-94.
  65. Robertson, L. W.; Ludewig, G., Polychlorinated Biphenyl (PCB) carcinogenicity with special emphasis on airborne PCBs. *Gefahrstoffe, Reinhaltung der Luft = Air quality control / Herausgeber, BIA und KRdL im VDI und DIN* **2011**, *71*, (1-2), 25-32.
  66. Lauby-Secretan, B.; Loomis, D.; Grosse, Y.; El Ghissassi, F.; Bouvard, V.; Benbrahim-Tallaa, L.; Guha, N.; Baan, R.; Mattock, H.; Straif, K., International Agency for Research on Cancer Monograph Working Group, IARC, Lyon France: Carcinogenicity of polychlorinated biphenyls and polybrominated biphenyls. *Lancet Oncol.* **2013**, *14*, (4), 287-8.

67. Engel, L. S.; Lan, Q.; Rothman, N., Polychlorinated biphenyls and non-Hodgkin lymphoma. *Cancer Epidemiol Biomarkers Prev* **2007**, *16*, (3), 373-6.
68. Engel, L. S.; Laden, F.; Andersen, A.; Strickland, P. T.; Blair, A.; Needham, L. L.; Barr, D. B.; Wolff, M. S.; Helzlsouer, K.; Hunter, D. J.; Lan, Q.; Cantor, K. P.; Comstock, G. W.; Brock, J. W.; Bush, D.; Hoover, R. N.; Rothman, N., Polychlorinated biphenyl levels in peripheral blood and non-Hodgkin's lymphoma: a report from three cohorts. *Cancer research* **2007**, *67*, (11), 5545-52.
69. Kushi, L. H.; Finnegan, J.; Martinson, B.; Rightmyer, J.; Vachon, C.; Yochum, L., Polychlorinated Biphenyls, Chlordanes, and the Etiology of Non-Hodgkin's Lymphoma. *Epidemiology* **1997**, *8*, (6), 689-690.
70. Hardell, L.; van Bavel, B.; Lindström, G.; Carlberg, M.; Dreifaldt, A. C.; Wijkström, H.; Starkhammar, H.; Eriksson, M.; Hallquist, A.; Kolmert, T., Increased concentrations of polychlorinated biphenyls, hexachlorobenzene, and chlordanes in mothers of men with testicular cancer. *Environ. Health Perspect.* **2003**, *111*, (7), 930-934.
71. Zhang, Y.; Wise, J. P.; Holford, T. R.; Xie, H.; Boyle, P.; Zahm, S. H.; Rusiecki, J.; Zou, K.; Zhang, B.; Zhu, Y.; Owens, P. H.; Zheng, T., Serum Polychlorinated Biphenyls, Cytochrome P-450 1A1 Polymorphisms, and Risk of Breast Cancer in Connecticut Women. *American Journal of Epidemiology* **2004**, *160*, (12), 1177-1183.
72. Golden, R.; Kimbrough, R., Weight of evidence evaluation of potential human cancer risks from exposure to polychlorinated biphenyls: an update based on studies published since 2003. *Critical reviews in toxicology* **2009**, *39*, (4), 299-331.
73. Bosetti, C.; Negri, E.; Fattore, E.; La Vecchia, C., Occupational exposure to polychlorinated biphenyls and cancer risk. *Eur J Cancer Prev* **2003**, *12*, (4), 251-5.
74. National Research Council (U.S.). Committee on the Assessment of Polychlorinated Biphenyls in the Environment., *Polychlorinated biphenyls : a report*. National Academy of Sciences: Washington, 1979; p xiv, 182 p.
75. Frederiksen, M.; Meyer, H. W.; Ebbelohj, N. E.; Gunnarsen, L., Polychlorinated biphenyls (PCBs) in indoor air originating from sealants in contaminated and uncontaminated apartments within the same housing estate. *Chemosphere* **2012**, *89*, (4), 473-9.
76. Liebl, B.; Schettgen, T.; Kerscher, G.; Broding, H. C.; Otto, A.; Angerer, J.; Drexler, H., Evidence for increased internal exposure to lower chlorinated polychlorinated biphenyls (PCB) in pupils attending a contaminated school. *Int. J. Hyg. Environ. Health* **2004**, *207*, (4), 315-24.
77. Meyer, H. W.; Frederiksen, M.; Goen, T.; Ebbelohj, N. E.; Gunnarsen, L.; Brauer, C.; Kolarik, B.; Muller, J.; Jacobsen, P., Plasma polychlorinated biphenyls in residents of 91 PCB-contaminated and 108 non-contaminated dwellings-an exposure study. *Int J Hyg Environ Health* **2013**, *216*, (6), 755-62.
78. Pedersen, E. B.; Ebbelohj, N. E.; Goen, T.; Meyer, H. W.; Jacobsen, P., Exposure to 27 polychlorinated biphenyls in the indoor environment of a workplace: a controlled bio-monitoring study. *Int Arch Occup Environ Health* **2016**, *89*, (1), 43-7.

79. Awasthi, A. K.; Zeng, X.; Li, J., Environmental pollution of electronic waste recycling in India: A critical review. *Environmental Pollution* **2016**, *211*, 259-270.
80. Zheng, J.; Yu, L. H.; Chen, S. J.; Hu, G. C.; Chen, K. H.; Yan, X.; Luo, X. J.; Zhang, S.; Yu, Y. J.; Yang, Z. Y.; Mai, B. X., Polychlorinated Biphenyls (PCBs) in Human Hair and Serum from E-Waste Recycling Workers in Southern China: Concentrations, Chiral Signatures, Correlations, and Source Identification. *Environ Sci Technol* **2016**.
81. Wittsiepe, J.; Fobil, J. N.; Till, H.; Burchard, G. D.; Wilhelm, M.; Feldt, T., Levels of polychlorinated dibenzo-p-dioxins, dibenzofurans (PCDD/Fs) and biphenyls (PCBs) in blood of informal e-waste recycling workers from Agbogbloshie, Ghana, and controls. *Environ Int* **2015**, *79*, 65-73.
82. Hu, D.; Hornbuckle, K. C., Inadvertent polychlorinated biphenyls in commercial paint pigments. *Environ Sci Technol* **2010**, *44*, (8), 2822-7.
83. Nyberg, E.; Danielsson, S.; Eriksson, U.; Faxneld, S.; Miller, A.; Bignert, A., Spatio-temporal trends of PCBs in the Swedish freshwater environment 1981-2012. *Ambio* **2014**, *43 Suppl 1*, 45-57.
84. Carpenter, D. O., Exposure to and health effects of volatile PCBs. *Rev. Environ. Health* **2015**, *30*, (2), 81-92.
85. Egsmose, E. L.; Brauner, E. V.; Frederiksen, M.; Morck, T. A.; Siersma, V. D.; Hansen, P. W.; Nielsen, F.; Grandjean, P.; Knudsen, L. E., Associations between plasma concentrations of PCB 28 and possible indoor exposure sources in Danish school children and mothers. *Environ Int* **2016**, *87*, 13-9.
86. Liebl, B.; Schettgen, T.; Kerscher, G.; Broding, H.-C.; Otto, A.; Angerer, J.; Drexler, H., Evidence for increased internal exposure to lower chlorinated polychlorinated biphenyls (PCB) in pupils attending a contaminated school. *Int. J. Hyg. Environ. Health* **2004**, *207*, (4), 315-324.
87. Persoon, C.; Peters, T. M.; Kumar, N.; Hornbuckle, K. C., Spatial distribution of airborne polychlorinated biphenyls in Cleveland, Ohio and Chicago, Illinois. *Environ. Sci. Technol.* **2010**, *44*, (8), 2797-802.
88. Zhang, X.; Diamond, M. L.; Robson, M.; Harrad, S., Sources, emissions, and fate of polybrominated diphenyl ethers and polychlorinated biphenyls indoors in Toronto, Canada. *Environ Sci Technol* **2011**, *45*, (8), 3268-74.
89. Hu, D.; Lehmler, H. J.; Martinez, A.; Wang, K.; Hornbuckle, K. C., Atmospheric PCB congeners across Chicago. *Atmos. Environ.* **2010**, *44*, (12), 1550-1557.
90. Hu, D.; Martinez, A.; Hornbuckle, K. C., Discovery of non-aro-chlor PCB (3,3'-dichlorobiphenyl) in Chicago air. *Environ Sci Technol* **2008**, *42*, (21), 7873-7.
91. Vorkamp, K., An overlooked environmental issue? A review of the inadvertent formation of PCB-11 and other PCB congeners and their occurrence in consumer products and in the environment. *Sci Total Environ* **2016**, *541*, 1463-76.
92. Hu, D.; Martinez, A.; Hornbuckle, K. C., Sedimentary Records of Non-Arochlor and Arochlor PCB mixtures in the Great Lakes. *J. Great Lakes Res.* **2011**, *37*, (2), 359-364.

93. Koh, W. X.; Hornbuckle, K. C.; Thorne, P. S., Human Serum from Urban and Rural Adolescents and Their Mothers Shows Exposure to Polychlorinated Biphenyls Not Found in Commercial Mixtures. *Environ Sci Technol* **2015**, *49*, (13), 8105-12.
94. Hu, D.; Hornbuckle, K. C., Inadvertent polychlorinated biphenyls in commercial paint pigments. *Environ. Sci. Technol.* **2010**, *44*, (8), 2822-7.
95. Rodenburg, L. A.; Guo, J.; Du, S.; Cavallo, G. J., Evidence for unique and ubiquitous environmental sources of 3,3'-dichlorobiphenyl (PCB 11). *Environ Sci Technol* **2010**, *44*, (8), 2816-21.
96. Shang, H.; Li, Y.; Wang, T.; Wang, P.; Zhang, H.; Zhang, Q.; Jiang, G., The presence of polychlorinated biphenyls in yellow pigment products in China with emphasis on 3,3'-dichlorobiphenyl (PCB 11). *Chemosphere* **2014**, *98*, 44-50.
97. Basu, I.; Arnold, K. A.; Venier, M.; Hites, R. A., Partial pressures of PCB-11 in air from several Great Lakes sites. *Environ Sci Technol* **2009**, *43*, (17), 6488-92.
98. Hu, X.; Adamcakova-Dodd, A.; Thorne, P. S., The fate of inhaled (14)C-labeled PCB11 and its metabolites in vivo. *Environ. Int.* **2014**, *63*, 92-100.
99. Norstrom, K.; Czub, G.; McLachlan, M. S.; Hu, D.; Thorne, P. S.; Hornbuckle, K. C., External exposure and bioaccumulation of PCBs in humans living in a contaminated urban environment. *Environ Int* **2010**, *36*, (8), 855-61.
100. Palmer, P. M.; Belanger, E. E.; Wilson, L. R.; Hwang, S. A.; Narang, R. S.; Gomez, M. I.; Cayo, M. R.; Durocher, L. A.; Fitzgerald, E. F., Outdoor air PCB concentrations in three communities along the Upper Hudson River, New York. *Arch Environ Contam Toxicol* **2008**, *54*, (3), 363-71.
101. Fitzgerald, E. F.; Shrestha, S.; Palmer, P. M.; Wilson, L. R.; Belanger, E. E.; Gomez, M. I.; Cayo, M. R.; Hwang, S. A., Polychlorinated biphenyls (PCBs) in indoor air and in serum among older residents of upper Hudson River communities. *Chemosphere* **2011**, *85*, (2), 225-31.
102. Fitzgerald, E. F.; Belanger, E. E.; Gomez, M. I.; Cayo, M.; McCaffrey, R. J.; Seegal, R. F.; Jansing, R. L.; Hwang, S.-a.; Hicks, H. E., Polychlorinated Biphenyl Exposure and Neuropsychological Status among Older Residents of Upper Hudson River Communities. *Environ. Health Perspect.* **2008**, *116*, (2), 209-215.
103. Zhu, Y.; Mapuskar, K. A.; Marek, R. F.; Xu, W.; Lehmler, H. J.; Robertson, L. W.; Hornbuckle, K. C.; Spitz, D. R.; Aykin-Burns, N., A new player in environmentally induced oxidative stress: polychlorinated biphenyl congener, 3,3'-dichlorobiphenyl (PCB11). *Toxicol Sci* **2013**, *136*, (1), 39-50.
104. Grimm, F. A.; Hu, D.; Kania-Korwel, I.; Lehmler, H. J.; Ludewig, G.; Hornbuckle, K. C.; Duffel, M. W.; Bergman, A.; Robertson, L. W., Metabolism and metabolites of polychlorinated biphenyls. *Crit. Rev. Toxicol.* **2015**, *45*, (3), 245-72.
105. Hansen, L. G., *Identification of steady state and episodic PCB congeners from multiple pathway exposures*. The University Press of Kentucky: Lexington, Kentucky, US, 2001.

106. Quinete, N.; Schettgen, T.; Bertram, J.; Kraus, T., Occurrence and distribution of PCB metabolites in blood and their potential health effects in humans: a review. *Environ. Sci. Pollut. Res. Int.* **2014**, *21*, (20), 11951-72.
107. Quinete, N.; Schettgen, T.; Bertram, J.; Kraus, T., Analytical approaches for the determination of PCB metabolites in blood: a review. *Anal. Bioanal. Chem.* **2014**, *406*, (25), 6151-64.
108. Safe, S., Toxicology, structure-function relationship, and human and environmental health impacts of polychlorinated biphenyls: progress and problems. *Environ Health Perspect* **1993**, *100*, 259-68.
109. Marek, R. F.; Thorne, P. S.; DeWall, J.; Hornbuckle, K. C., Variability in PCB and OH-PCB serum levels in children and their mothers in urban and rural U.S. communities. *Environ. Sci. Technol.* **2014**, *48*, (22), 13459-67.
110. Schafer, P.; Muller, M.; Kruger, A.; Steinberg, C. E.; Menzel, R., Cytochrome P450-dependent metabolism of PCB52 in the nematode *Caenorhabditis elegans*. *Arch. Biochem. Biophys.* **2009**, *488*, (1), 60-8.
111. Ueno, D.; Darling, C.; Alaei, M.; Campbell, L.; Pacepavicius, G.; Teixeira, C.; Muir, D., Detection of hydroxylated polychlorinated biphenyls (OH-PCBs) in the abiotic environment: surface water and precipitation from Ontario, Canada. *Environ Sci Technol* **2007**, *41*, (6), 1841-8.
112. Marek, R. F.; Martinez, A.; Hornbuckle, K. C., Discovery of hydroxylated polychlorinated biphenyls (OH-PCBs) in sediment from a lake Michigan waterway and original commercial aroclors. *Environ Sci Technol* **2013**, *47*, (15), 8204-10.
113. Koh, W. X.; Hornbuckle, K. C.; Marek, R. F.; Wang, K.; Thorne, P. S., Hydroxylated polychlorinated biphenyls in human sera from adolescents and their mothers living in two U.S. Midwestern communities. *Chemosphere* **2016**, *147*, 389-95.
114. Marek, R. F.; Thorne, P. S.; Wang, K.; Dewall, J.; Hornbuckle, K. C., PCBs and OH-PCBs in serum from children and mothers in urban and rural U.S. communities. *Environ Sci Technol* **2013**, *47*, (7), 3353-61.
115. Soechitram, S. D.; Athanasiadou, M.; Hovander, L.; Bergman, Å.; Sauer, P. J. J., Fetal Exposure to PCBs and Their Hydroxylated Metabolites in a Dutch Cohort. *Environ. Health Perspect.* **2004**, *112*, (11), 1208-1212.
116. Park, J. S.; Bergman, A.; Linderholm, L.; Athanasiadou, M.; Kocan, A.; Petrik, J.; Drobna, B.; Trnovec, T.; Charles, M. J.; Hertz-Picciotto, I., Placental transfer of polychlorinated biphenyls, their hydroxylated metabolites and pentachlorophenol in pregnant women from eastern Slovakia. *Chemosphere* **2008**, *70*, (9), 1676-84.
117. Berghuis, S. A.; Soechitram, S. D.; Sauer, P. J. J.; Bos, A. F., Prenatal Exposure to Polychlorinated Biphenyls and Their Hydroxylated Metabolites is Associated with Neurological Functioning in 3-Month-Old Infants. *Toxicological Sciences* **2014**, *142*, (2), 455-462.
118. Park, H. Y.; Park, J. S.; Sovcikova, E.; Kocan, A.; Linderholm, L.; Bergman, A.; Trnovec, T.; Hertz-Picciotto, I., Exposure to hydroxylated polychlorinated biphenyls



- (OH-PCBs) in the prenatal period and subsequent neurodevelopment in eastern Slovakia. *Environ Health Perspect* **2009**, *117*, (10), 1600-6.
119. Spencer, W. A.; Lehmler, H. J.; Robertson, L. W.; Gupta, R. C., Oxidative DNA adducts after Cu(2+)-mediated activation of dihydroxy PCBs: role of reactive oxygen species. *Free Radic. Biol. Med.* **2009**, *46*, (10), 1346-52.
  120. Xu, D.; Li, L.; Liu, L.; Dong, H.; Deng, Q.; Yang, X.; Song, E.; Song, Y., Polychlorinated biphenyl quinone induces mitochondrial-mediated and caspase-dependent apoptosis in HepG2 cells. *Environ. Toxicol.* **2015**, *30*, (9), 1063-72.
  121. Ludewig, G.; Lehmann, L.; Esch, H.; Robertson, L. W., Metabolic Activation of PCBs to Carcinogens in Vivo - A Review. *Environ. Toxicol. Pharmacol.* **2008**, *25*, (2), 241-6.
  122. Flor, S.; Ludewig, G., Polyploidy-induction by dihydroxylated monochlorobiphenyls: structure-activity-relationships. *Environ. Int.* **2010**, *36*, (8), 962-9.
  123. Lin, P. H.; Sangaiah, R.; Ranasinghe, A.; Upton, P. B.; La, D. K.; Gold, A.; Swenberg, J. A., Formation of quinonoid-derived protein adducts in the liver and brain of Sprague-Dawley rats treated with 2,2',5, 5'-tetrachlorobiphenyl. *Chem Res Toxicol* **2000**, *13*, (8), 710-8.
  124. Zhao, S.; Narang, A.; Ding, X.; Eadon, G., Characterization and quantitative analysis of DNA adducts formed from lower chlorinated PCB-derived quinones. *Chem Res Toxicol* **2004**, *17*, (4), 502-11.
  125. Letcher, R. J. K.-W., E.; Bergman, A., *Methyl Sulfone and Hydroxylated Metabolites of Polychlorinated Biphenyls*. Springer-Verlag: Berlin, 2000; Vol. 3, p 317-57.
  126. Ekuase, E. J.; Liu, Y.; Lehmler, H. J.; Robertson, L. W.; Duffel, M. W., Structure-activity relationships for hydroxylated polychlorinated biphenyls as inhibitors of the sulfation of dehydroepiandrosterone catalyzed by human hydroxysteroid sulfotransferase SULT2A1. *Chem Res Toxicol* **2011**, *24*, (10), 1720-8.
  127. Kester, M. H.; Bulduk, S.; van Toor, H.; Tibboel, D.; Meinel, W.; Glatt, H.; Falany, C. N.; Coughtrie, M. W.; Schuur, A. G.; Brouwer, A.; Visser, T. J., Potent inhibition of estrogen sulfotransferase by hydroxylated metabolites of polyhalogenated aromatic hydrocarbons reveals alternative mechanism for estrogenic activity of endocrine disrupters. *J. Clin. Endocrinol. Metab.* **2002**, *87*, (3), 1142-50.
  128. Liu, Y.; Apak, T. I.; Lehmler, H. J.; Robertson, L. W.; Duffel, M. W., Hydroxylated polychlorinated biphenyls are substrates and inhibitors of human hydroxysteroid sulfotransferase SULT2A1. *Chem. Res. Toxicol.* **2006**, *19*, (11), 1420-5.
  129. Grimm, F. A.; Lehmler, H. J.; He, X.; Robertson, L. W.; Duffel, M. W., Sulfated metabolites of polychlorinated biphenyls are high-affinity ligands for the thyroid hormone transport protein transthyretin. *Environ. Health Perspect.* **2013**, *121*, (6), 657-62.
  130. Grimm, F. A.; Lehmler, H. J.; He, X.; Robertson, L. W.; Duffel, M. W., Modulating inhibitors of transthyretin fibrillogenesis via sulfation: polychlorinated biphenyl sulfates as models. *Chem. Biol. Interact.* **2015**, *228*, 1-8.

131. Dhakal, K.; He, X.; Lehmler, H. J.; Teesch, L. M.; Duffel, M. W.; Robertson, L. W., Identification of sulfated metabolites of 4-chlorobiphenyl (PCB3) in the serum and urine of male rats. *Chem Res Toxicol* **2012**, *25*, (12), 2796-804.
132. Grimm, F. A.; He, X.; Teesch, L. M.; Lehmler, H. J.; Robertson, L. W.; Duffel, M. W., Tissue Distribution, Metabolism, and Excretion of 3,3'-Dichloro-4'-sulfooxy-biphenyl in the Rat. *Environ. Sci. Technol.* **2015**, *49*, (13), 8087-95.
133. Baker, M. E., Albumin, steroid hormones and the origin of vertebrates. *J Endocrinol* **2002**, *175*, (1), 121-7.
134. Ahn, S. M.; Byun, K.; Cho, K.; Kim, J. Y.; Yoo, J. S.; Kim, D.; Paek, S. H.; Kim, S. U.; Simpson, R. J.; Lee, B., Human microglial cells synthesize albumin in brain. *PLoS one* **2008**, *3*, (7), e2829.
135. Kragh-Hansen, U.; Chuang, V. T.; Otagiri, M., Practical aspects of the ligand-binding and enzymatic properties of human serum albumin. *Biol. Pharm. Bull.* **2002**, *25*, (6), 695-704.
136. Muller, W. E.; Wollert, U., Human serum albumin as a 'silent receptor' for drugs and endogenous substances. *Pharmacology* **1979**, *19*, (2), 59-67.
137. Peters, T. J., *All About Albumin. Biochemistry, Genetics, and Medical Applications.* Academic Press: San Diego, 1996.
138. DUNN, J. F.; NISULA, B. C.; RODBARD, D., Transport of Steroid Hormones: Binding of 21 Endogenous Steroids to Both Testosterone-Binding Globulin and Corticosteroid-Binding Globulin in Human Plasma. *The Journal of Clinical Endocrinology & Metabolism* **1981**, *53*, (1), 58-68.
139. Watkins, S.; Madison, J.; Galliano, M.; Minchiotti, L.; Putnam, F. W., Analbuminemia: three cases resulting from different point mutations in the albumin gene. *Proc Natl Acad Sci U S A* **1994**, *91*, (20), 9417-21.
140. Nicholson, J. P.; Wolmarans, M. R.; Park, G. R., The role of albumin in critical illness. *Br J Anaesth* **2000**, *85*, (4), 599-610.
141. Mathiesen, L.; Rytting, E.; Mose, T.; Knudsen, L. E., Transport of benzo[alpha]pyrene in the dually perfused human placenta perfusion model: effect of albumin in the perfusion medium. *Basic Clin. Pharmacol. Toxicol.* **2009**, *105*, (3), 181-7.
142. Nanovskaya, T. N.; Patrikeeva, S.; Hemauer, S.; Fokina, V.; Mattison, D.; Hankins, G. D.; Ahmed, M. S., Effect of albumin on transplacental transfer and distribution of rosiglitazone and glyburide. *J. Matern. Fetal Neonatal Med.* **2008**, *21*, (3), 197-207.
143. Nanovskaya, T. N.; Bowen, R. S.; Patrikeeva, S. L.; Hankins, G. D.; Ahmed, M. S., Effect of plasma proteins on buprenorphine transfer across dually perfused placental lobule. *J. Matern. Fetal Neonatal Med.* **2009**, *22*, (8), 646-53.
144. Nanovskaya, T. N.; Nekhayeva, I.; Hankins, G. D.; Ahmed, M. S., Effect of human serum albumin on transplacental transfer of glyburide. *Biochem Pharmacol* **2006**, *72*, (5), 632-9.

145. Kragh-Hansen, U., Molecular and practical aspects of the enzymatic properties of human serum albumin and of albumin–ligand complexes. *Biochimica et Biophysica Acta (BBA) - General Subjects* **2013**, 1830, (12), 5535-5544.
146. Sogorb, M. A.; Vilanova, E., Serum albumins and detoxication of anti-cholinesterase agents. *Chemico-Biological Interactions* **2010**, 187, (1–3), 325-329.
147. Berman, H. M.; Westbrook, J.; Feng, Z.; Gilliland, G.; Bhat, T. N.; Weissig, H.; Shindyalov, I. N.; Bourne, P. E., The Protein Data Bank. *Nucleic Acids Res* **2000**, 28, (1), 235-42.
148. Ghuman, J.; Zunszain, P. A.; Petitpas, I.; Bhattacharya, A. A.; Otagiri, M.; Curry, S., Structural basis of the drug-binding specificity of human serum albumin. *J. Mol. Biol.* **2005**, 353, (1), 38-52.
149. Dockal, M.; Chang, M.; Carter, D. C.; Ruker, F., Five recombinant fragments of human serum albumin-tools for the characterization of the warfarin binding site. *Protein Sci* **2000**, 9, (8), 1455-65.
150. Diana, F. J.; Veronich, K.; Kapoor, A. L., Binding of nonsteroidal anti-inflammatory agents and their effect on binding of racemic warfarin and its enantiomers to human serum albumin. *J Pharm Sci* **1989**, 78, (3), 195-9.
151. Witiak, D. T.; Whitehouse, M. W., Species differences in the albumin binding of 2,4,6-trinitrobenzaldehyde, chlorophenoxyacetic acids, 2-(4'-hydroxybenzeneazo)benzoic acid and some other acidic drugs--the unique behavior of rat plasma albumin. *Biochem Pharmacol* **1969**, 18, (5), 971-7.
152. Ghuman, J.; Zunszain, P. A.; Petitpas, I.; Bhattacharya, A. A.; Otagiri, M.; Curry, S., Structural basis of the drug-binding specificity of human serum albumin. *J Mol Biol* **2005**, 353, (1), 38-52.
153. Chakrabarti, S. K., Cooperativity of warfarin binding with human serum albumin induced by free fatty acid anion. *Biochem Pharmacol* **1978**, 27, (5), 739-43.
154. Dobretsov, G. E.; Syreishchikova, T. I.; Smolina, N. V.; Uzbekov, M. G., Effects of fatty acids on human serum albumin binding centers. *Bull Exp Biol Med* **2012**, 153, (3), 323-6.
155. Hackett, M. J.; Joolakanti, S.; Hartranft, M. E.; Guley, P. C.; Cho, M. J., A dicarboxylic fatty acid derivative of paclitaxel for albumin-assisted drug delivery. *J Pharm Sci* **2012**, 101, (9), 3292-304.
156. Kratz, F., A clinical update of using albumin as a drug vehicle - a commentary. *Journal of controlled release : official journal of the Controlled Release Society* **2014**, 190, 331-6.
157. Mohammed, A.; Eklund, A.; Ostlund-Lindqvist, A. M.; Slanina, P., Distribution of toxaphene, DDT, and PCB among lipoprotein fractions in rat and human plasma. *Arch Toxicol* **1990**, 64, (7), 567-71.
158. Borlakoglu, J. T.; Welch, V. A.; Wilkins, J. P.; Dils, R. R., Transport and cellular uptake of polychlorinated biphenyls (PCBs)--I. Association of individual PCB isomers and congeners with plasma lipoproteins and proteins in the pigeon. *Biochem Pharmacol* **1990**, 40, (2), 265-72.

159. Guo, Y. L.; Emmett, E. A.; Pellizzari, E. D.; Rohde, C. A., Influence of serum cholesterol and albumin on partitioning of PCB congeners between human serum and adipose tissue. *Toxicology and applied pharmacology* **1987**, *87*, (1), 48-56.
160. Kihlstrom, I., Influence of albumin concentration in the foetal circulation on the placental transfer of 2,2',4,4',5,5'-hexachlorobiphenyl in the guinea pig. *Acta pharmacologica et toxicologica* **1982**, *50*, (4), 300-4.
161. Borlak, J.; Dangers, M.; Thum, T., Aroclor 1254 modulates gene expression of nuclear transcription factors: implications for albumin gene transcription and protein synthesis in rat hepatocyte cultures. *Toxicology and applied pharmacology* **2002**, *181*, (2), 79-88.
162. Lee, S. K.; Hamer, D.; Bedwell, C. L.; Lohitnavy, M.; Yang, R. S. H., Effect of PCBs on the lactational transfer of methyl mercury in mice: PBPK modeling. *Environ. Toxicol. Pharmacol.* **2009**, *27*, (1), 75-83.
163. Fang, S.; Li, H.; Liu, T.; Xuan, H.; Li, X.; Zhao, C., Molecular interaction of PCB180 to human serum albumin: insights from spectroscopic and molecular modelling studies. *J. Mol. Model.* **2014**, *20*, (4), 2098.
164. Rownicka-Zubik, J.; Sulkowski, L.; Toborek, M., Interactions of PCBs with human serum albumin: in vitro spectroscopic study. *Spectrochim. Acta. A Mol. Biomol. Spectrosc.* **2014**, *124*, 632-7.
165. Han, C.; Fang, S.; Cao, H.; Lu, Y.; Ma, Y.; Wei, D.; Xie, X.; Liu, X.; Li, X.; Fei, D.; Zhao, C., Molecular interaction of PCB153 to human serum albumin: insights from spectroscopic and molecular modeling studies. *J. Hazard. Mater.* **2013**, *248-249*, 313-21.
166. Jacobson, J. L. J., S.W., *Developmental effects of PCBs in the Fish Eater Cohort Studies*. Lexington, Kentucky, US, 2001.
167. Jacobson, J. L.; Jacobson, S. W., Dose-response in perinatal exposure to polychlorinated biphenyls (PCBs): the Michigan and North Carolina cohort studies. *Toxicology and industrial health* **1996**, *12*, (3-4), 435-45.
168. Grandjean, P.; Weihe, P.; Burse, V. W.; Needham, L. L.; Storr-Hansen, E.; Heinzow, B.; Debes, F.; Murata, K.; Simonsen, H.; Ellefsen, P.; Budtz-Jorgensen, E.; Keiding, N.; White, R. F., Neurobehavioral deficits associated with PCB in 7-year-old children prenatally exposed to seafood neurotoxicants. *Neurotoxicol Teratol* **2001**, *23*, (4), 305-17.
169. Walkowiak, J.; Wiener, J. A.; Fastabend, A.; Heinzow, B.; Kramer, U.; Schmidt, E.; Steingruber, H. J.; Wundram, S.; Winneke, G., Environmental exposure to polychlorinated biphenyls and quality of the home environment: effects on psychodevelopment in early childhood. *Lancet* **2001**, *358*, (9293), 1602-7.
170. Berghuis, S. A.; Bos, A. F.; Sauer, P. J.; Roze, E., Developmental neurotoxicity of persistent organic pollutants: an update on childhood outcome. *Arch Toxicol* **2015**, *89*, (5), 687-709.
171. Jurewicz, J.; Polanska, K.; Hanke, W., Chemical exposure early in life and the neurodevelopment of children--an overview of current epidemiological evidence. *Ann Agric Environ Med* **2013**, *20*, (3), 465-86.

172. Polanska, K.; Jurewicz, J.; Hanke, W., Review of current evidence on the impact of pesticides, polychlorinated biphenyls and selected metals on attention deficit / hyperactivity disorder in children. *Int J Occup Med Environ Health* **2013**, *26*, (1), 16-38.
173. Berghuis, S. A.; Soechitram, S. D.; Hitzert, M. M.; Sauer, P. J.; Bos, A. F., Prenatal exposure to polychlorinated biphenyls and their hydroxylated metabolites is associated with motor development of three-month-old infants. *Neurotoxicology* **2013**, *38*, 124-30.
174. Gore, A. C.; Chappell, V. A.; Fenton, S. E.; Flaws, J. A.; Nadal, A.; Prins, G. S.; Toppari, J.; Zoeller, R. T., Executive Summary to EDC-2: The Endocrine Society's Second Scientific Statement on Endocrine-Disrupting Chemicals. *Endocr Rev* **2015**, *36*, (6), 593-602.
175. Fonnum, F.; Mariussen, E., Mechanisms involved in the neurotoxic effects of environmental toxicants such as polychlorinated biphenyls and brominated flame retardants. *J. Neurochem.* **2009**, *111*, (6), 1327-47.
176. Lee, D. W.; Opanashuk, L. A., Polychlorinated biphenyl mixture aroclor 1254-induced oxidative stress plays a role in dopaminergic cell injury. *Neurotoxicology* **2004**, *25*, (6), 925-39.
177. Tan, Y.; Chen, C. H.; Lawrence, D.; Carpenter, D. O., Ortho-substituted PCBs kill cells by altering membrane structure. *Toxicol Sci* **2004**, *80*, (1), 54-9.
178. Tan, Y.; Song, R.; Lawrence, D.; Carpenter, D. O., Ortho-substituted but not coplanar PCBs rapidly kill cerebellar granule cells. *Toxicol Sci* **2004**, *79*, (1), 147-56.
179. Pessah, I. N.; Cherednichenko, G.; Lein, P. J., Minding the calcium store: Ryanodine receptor activation as a convergent mechanism of PCB toxicity. *Pharmacol Ther* **2010**, *125*, (2), 260-85.
180. Shimokawa, N.; Miyazaki, W.; Iwasaki, T.; Koibuchi, N., Low dose hydroxylated PCB induces c-Jun expression in PC12 cells. *Neurotoxicology* **2006**, *27*, (2), 176-83.
181. Adornetto, A.; Pagliara, V.; Renzo, G. D.; Arcone, R., Polychlorinated biphenyls impair dibutyryl cAMP-induced astrocytic differentiation in rat C6 glial cell line. *FEBS Open Bio* **2013**, *3*, 459-66.
182. Kodavanti, P. R.; Ward, T. R.; Derr-Yellin, E. C.; McKinney, J. D.; Tilson, H. A., Increased [<sup>3</sup>H]phorbol ester binding in rat cerebellar granule cells and inhibition of <sup>45</sup>Ca(2+) buffering in rat cerebellum by hydroxylated polychlorinated biphenyls. *Neurotoxicology* **2003**, *24*, (2), 187-98.
183. Dreiem, A.; Rykken, S.; Lehmler, H. J.; Robertson, L. W.; Fonnum, F., Hydroxylated polychlorinated biphenyls increase reactive oxygen species formation and induce cell death in cultured cerebellar granule cells. *Toxicology and applied pharmacology* **2009**, *240*, (2), 306-13.
184. Lilienthal, H.; Heikkinen, P.; Andersson, P. L.; van der Ven, L. T.; Viluksela, M., Dopamine-dependent behavior in adult rats after perinatal exposure to purity-controlled polychlorinated biphenyl congeners (PCB52 and PCB180). *Toxicol Lett* **2014**, *224*, (1), 32-9.

185. Chou, S. M.; Miike, T.; Payne, W. M.; Davis, G. J., Neuropathology of "spinning syndrome" induced by prenatal intoxication with a PCB in mice. *Ann N Y Acad Sci* **1979**, *320*, 373-95.
186. Seegal, R. F.; Bush, B.; Shain, W., Lightly chlorinated ortho-substituted PCB congeners decrease dopamine in nonhuman primate brain and in tissue culture. *Toxicology and applied pharmacology* **1990**, *106*, (1), 136-44.
187. Corrigan, F. M.; Murray, L.; Wyatt, C. L.; Shore, R. F., Diorthosubstituted polychlorinated biphenyls in caudate nucleus in Parkinson's disease. *Exp Neurol* **1998**, *150*, (2), 339-42.
188. Langeveld, W. T.; Meijer, M.; Westerink, R. H., Differential effects of 20 non-dioxin-like PCBs on basal and depolarization-evoked intracellular calcium levels in PC12 cells. *Toxicol Sci* **2012**, *126*, (2), 487-96.
189. Angus, W. G.; Contreras, M. L., Effects of polychlorinated biphenyls on dopamine release from PC12 cells. *Toxicol Lett* **1996**, *89*, (3), 191-9.
190. Steenland, K.; Hein, M. J.; Cassinelli, R. T., 2nd; Prince, M. M.; Nilsen, N. B.; Whelan, E. A.; Waters, M. A.; Ruder, A. M.; Schnorr, T. M., Polychlorinated biphenyls and neurodegenerative disease mortality in an occupational cohort. *Epidemiology* **2006**, *17*, (1), 8-13.
191. Prince, M. M.; Hein, M. J.; Ruder, A. M.; Waters, M. A.; Laber, P. A.; Whelan, E. A., Update: cohort mortality study of workers highly exposed to polychlorinated biphenyls (PCBs) during the manufacture of electrical capacitors, 1940-1998. *Environmental Health* **2006**, *5*, (1), 1-10.
192. Hatcher-Martin, J. M.; Gearing, M.; Steenland, K.; Levey, A. I.; Miller, G. W.; Pennell, K. D., Association between polychlorinated biphenyls and Parkinson's disease neuropathology. *Neurotoxicology* **2012**, *33*, (5), 1298-304.
193. Tilson, H. A.; Kodavanti, P. R., The neurotoxicity of polychlorinated biphenyls. *Neurotoxicology* **1998**, *19*, (4-5), 517-25.
194. Lyng, G. D.; Snyder-Keller, A.; Seegal, R. F., Dopaminergic development of prenatal ventral mesencephalon and striatum in organotypic co-cultures. *Brain Res* **2007**, *1133*, (1), 1-9.
195. Seegal, R. F.; Bush, B.; Brosch, K. O., Sub-chronic exposure of the adult rat to Aroclor 1254 yields regionally-specific changes in central dopaminergic function. *Neurotoxicology* **1991**, *12*, (1), 55-65.
196. Seegal, R. F.; Bush, B.; Brosch, K. O., Comparison of effects of Aroclors 1016 and 1260 on non-human primate catecholamine function. *Toxicology* **1991**, *66*, (2), 145-63.
197. Betarbet, R.; Sherer, T. B.; MacKenzie, G.; Garcia-Osuna, M.; Panov, A. V.; Greenamyre, J. T., Chronic systemic pesticide exposure reproduces features of Parkinson's disease. *Nature neuroscience* **2000**, *3*, (12), 1301-6.
198. Landrigan, P. J.; Sonawane, B.; Butler, R. N.; Trasande, L.; Callan, R.; Droller, D., Early environmental origins of neurodegenerative disease in later life. *Environ Health Perspect* **2005**, *113*, (9), 1230-3.

199. Baran, H.; Jellinger, K., Human brain phenolsulfotransferase. Regional distribution in Parkinson's disease. *J. Neural Transm. Park. Dis. Dement. Sect.* **1992**, *4*, 267-76.
200. Richardson, S. J.; Wijayagunaratne, R. C.; D'Souza, D. G.; Darras, V. M.; Van Herck, S. L. J., Transport of thyroid hormones via the choroid plexus into the brain: the roles of transthyretin and thyroid hormone transmembrane transporters. *Front. Neurosci.* **2015**, *9*, 66.
201. Fasano, M.; Curry, S.; Terreno, E.; Galliano, M.; Fanali, G.; Narciso, P.; Notari, S.; Ascenzi, P., The extraordinary ligand binding properties of human serum albumin. *IUBMB Life* **2005**, *57*, (12), 787-96.
202. Mizuma, T.; Komori, M.; Ueno, M.; Horikoshi, I., Sulphate conjugation enhances reversible binding of drug to human serum albumin. *J. Pharm. Pharmacol.* **1991**, *43*, (6), 446-8.
203. Seelbach, M.; Chen, L.; Powell, A.; Choi, Y. J.; Zhang, B.; Hennig, B.; Toborek, M., Polychlorinated biphenyls disrupt blood-brain barrier integrity and promote brain metastasis formation. *Environ Health Perspect* **2010**, *118*, (4), 479-84.
204. Himmelfarb, J.; McMonagle, E.; McMenamin, E., Plasma protein thiol oxidation and carbonyl formation in chronic renal failure. *Kidney Int* **2000**, *58*, (6), 2571-8.
205. He, X. M.; Carter, D. C., Atomic structure and chemistry of human serum albumin. *Nature* **1992**, *358*, (6383), 209-15.
206. Bertucci, C.; Domenici, E., Reversible and covalent binding of drugs to human serum albumin: methodological approaches and physiological relevance. *Curr Med Chem* **2002**, *9*, (15), 1463-81.
207. Chen, Y. M.; Guo, L. H., Combined fluorescence and electrochemical investigation on the binding interaction between organic acid and human serum albumin. *J Environ Sci (China)* **2009**, *21*, (3), 373-9.
208. Cao, J.; Guo, L. H.; Wan, B.; Wei, Y., In vitro fluorescence displacement investigation of thyroxine transport disruption by bisphenol A. *J Environ Sci (China)* **2011**, *23*, (2), 315-21.
209. Simard, J. R.; Zunszain, P. A.; Hamilton, J. A.; Curry, S., Location of high and low affinity fatty acid binding sites on human serum albumin revealed by NMR drug-competition analysis. *J Mol Biol* **2006**, *361*, (2), 336-51.
210. Sudlow, G.; Birkett, D. J.; Wade, D. N., The characterization of two specific drug binding sites on human serum albumin. *Mol. Pharmacol.* **1975**, *11*, (6), 824-32.
211. Chen, Y. M.; Guo, L. H., Fluorescence study on site-specific binding of perfluoroalkyl acids to human serum albumin. *Arch. Toxicol.* **2009**, *83*, (3), 255-61.
212. Quazi, S.; Yokogoshi, H.; Yoshida, A., Effect of dietary fiber on hypercholesterolemia induced by dietary PCB or cholesterol in rats. *J Nutr* **1983**, *113*, (6), 1109-18.
213. Emmett, E. A., Polychlorinated biphenyl exposure and effects in transformer repair workers. *Environ Health Perspect* **1985**, *60*, 185-92.

214. Borlakoglu, J. T.; Welch, V. A.; Edwards-Webb, J. D.; Dils, R. R., Transport and cellular uptake of polychlorinated biphenyls (PCBs)--II. Changes in vivo in plasma lipoproteins and proteins of pigeons in response to PCBs, and a proposed model for the transport and cellular uptake of PCBs. *Biochem Pharmacol* **1990**, *40*, (2), 273-81.
215. Ucan-Marin, F.; Arukwe, A.; Mortensen, A. S.; Gabrielsen, G. W.; Letcher, R. J., Recombinant albumin and transthyretin transport proteins from two gull species and human: chlorinated and brominated contaminant binding and thyroid hormones. *Environ Sci Technol* **2010**, *44*, (1), 497-504.
216. Aki, H.; Yamamoto, M., Thermodynamic characterization of drug binding to human serum albumin by isothermal titration microcalorimetry. *J. Pharm. Sci.* **1994**, *83*, (12), 1712-6.
217. Goncharov, N. V.; Belinskaia, D. A.; Razygraev, A. V.; Ukolov, A. I., [On the Enzymatic Activity of Albumin]. *Bioorg. Khim.* **2015**, *41*, (2), 131-44.
218. Baraka-Vidot, J.; Planesse, C.; Meilhac, O.; Militello, V.; van den Elsen, J.; Bourdon, E.; Rondeau, P., Glycation alters ligand binding, enzymatic, and pharmacological properties of human albumin. *Biochemistry* **2015**, *54*, (19), 3051-62.
219. Dhakal, K.; Uwimana, E.; Adamcakova-Dodd, A.; Thorne, P. S.; Lehmler, H. J.; Robertson, L. W., Disposition of phenolic and sulfated metabolites after inhalation exposure to 4-chlorobiphenyl (PCB3) in female rats. *Chem. Res. Toxicol.* **2014**, *27*, (8), 1411-20.
220. Dhakal, K.; Adamcakova-Dodd, A.; Lehmler, H. J.; Thorne, P. S.; Robertson, L. W., Sulfate conjugates are urinary markers of inhalation exposure to 4-chlorobiphenyl (PCB3). *Chem. Res. Toxicol.* **2013**, *26*, (6), 853-5.
221. Doolittle, R. F., The Evolution of the Vertebrate Plasma-Proteins. *Biol. Bull.* **1987**, *172*, (3), 269-283.
222. Earhart, A. D.; Patrikeeva, S.; Wang, X.; Abdelrahman, D. R.; Hankins, G. D.; Ahmed, M. S.; Nanovskaya, T., Transplacental transfer and metabolism of bupropion. *J. Matern. Fetal Neonatal Med.* **2010**, *23*, (5), 409-16.
223. Kodavanti, P. R., Neurotoxicity of persistent organic pollutants: possible mode(s) of action and further considerations. *Dose-response : a publication of International Hormesis Society* **2005**, *3*, (3), 273-305.
224. Tanner, C. M.; Ottman, R.; Goldman, S. M.; Ellenberg, J.; Chan, P.; Mayeux, R.; Langston, J. W., Parkinson disease in twins: an etiologic study. *JAMA* **1999**, *281*, (4), 341-6.
225. Siddiqi, S. H.; Abraham, N. K.; Geiger, C. L.; Karimi, M.; Perlmutter, J. S.; Black, K. J., The Human Experience with Intravenous Levodopa. *Frontiers in Pharmacology* **2015**, *6*, 307.
226. Jagmag, S. A.; Tripathi, N.; Shukla, S. D.; Maiti, S.; Khurana, S., Evaluation of Models of Parkinson's Disease. *Front Neurosci* **2015**, *9*, 503.



227. Schantz, S. L., Developmental neurotoxicity of PCBs in humans: what do we know and where do we go from here? *Neurotoxicol Teratol* **1996**, *18*, (3), 217-27; discussion 229-76.
228. Rossignol, D. A.; Genuis, S. J.; Frye, R. E., Environmental toxicants and autism spectrum disorders: a systematic review. *Translational psychiatry* **2014**, *4*, e360.
229. Safe, S.; Bandiera, S.; Sawyer, T.; Robertson, L.; Safe, L.; Parkinson, A.; Thomas, P. E.; Ryan, D. E.; Reik, L. M.; Levin, W.; Denomme, M. A.; Fujita, T., PCBs: structure–function relationships and mechanism of action. *Environ. Health Perspect.* **1985**, *60*, 47-56.
230. Seegal, R. F.; Bush, B.; Brosch, K. O., Decreases in dopamine concentrations in adult, non-human primate brain persist following removal from polychlorinated biphenyls. *Toxicology* **1994**, *86*, (1-2), 71-87.
231. Shain, W.; Bush, B.; Seegal, R., Neurotoxicity of polychlorinated biphenyls: structure-activity relationship of individual congeners. *Toxicology and applied pharmacology* **1991**, *111*, (1), 33-42.
232. Lyng, G. D.; Snyder-Keller, A.; Seegal, R. F., Polychlorinated biphenyl-induced neurotoxicity in organotypic cocultures of developing rat ventral mesencephalon and striatum. *Toxicol Sci* **2007**, *97*, (1), 128-39.
233. Lee, D. W.; Notter, S. A.; Thiruchelvam, M.; Dever, D. P.; Fitzpatrick, R.; Kostyniak, P. J.; Cory-Slechta, D. A.; Opanashuk, L. A., Subchronic polychlorinated biphenyl (Aroclor 1254) exposure produces oxidative damage and neuronal death of ventral midbrain dopaminergic systems. *Toxicol Sci* **2012**, *125*, (2), 496-508.
234. Richardson, J. R.; Miller, G. W., Acute exposure to aroclor 1016 or 1260 differentially affects dopamine transporter and vesicular monoamine transporter 2 levels. *Toxicol Lett* **2004**, *148*, (1-2), 29-40.
235. Caudle, W. M.; Richardson, J. R.; Delea, K. C.; Guillot, T. S.; Wang, M.; Pennell, K. D.; Miller, G. W., Polychlorinated biphenyl-induced reduction of dopamine transporter expression as a precursor to Parkinson's disease-associated dopamine toxicity. *Toxicol Sci* **2006**, *92*, (2), 490-9.
236. Steenland, K.; Hein, M. J.; Cassinelli, R. T.; Prince, M. M.; Nilsen, N. B.; Whelan, E. A.; Waters, M. A.; Ruder, A. M.; Schnorr, T. M., Polychlorinated biphenyls and neurodegenerative disease mortality in an occupational cohort. *Epidemiology* **2006**, *17*.
237. Wooten, G. F.; Currie, L. J.; Bovbjerg, V. E.; Lee, J. K.; Patrie, J., Are men at greater risk for Parkinson's disease than women? *J. Neurol. Neurosurg. Psychiatry* **2004**, *75*, (4), 637-9.
238. Ruder, A. M.; Hein, M. J.; Hopf, N. B.; Waters, M. A., Mortality among 24,865 workers exposed to polychlorinated biphenyls (PCBs) in three electrical capacitor manufacturing plants: a ten-year update. *Int J Hyg Environ Health* **2014**, *217*, (2-3), 176-87.
239. Kasten, M.; Heinzow, B.; Vieregge, P.; Klein, C., Reply to: "polychlorinated biphenyls in prospectively collected serum and Parkinson's disease risk". *Mov Disord* **2013**, *28*, (9), 1317.

240. Weisskopf, M. G.; Knekt, P.; O'Reilly, E. J.; Lyytinen, J.; Reunanen, A.; Laden, F.; Altshul, L.; Ascherio, A., Polychlorinated biphenyls in prospectively collected serum and Parkinson's disease risk. *Mov Disord* **2012**, *27*, (13), 1659-65.
241. Hisada, A.; Shimodaira, K.; Okai, T.; Watanabe, K.; Takemori, H.; Takasuga, T.; Koyama, M.; Watanabe, N.; Suzuki, E.; Shirakawa, M.; Noda, Y.; Komine, Y.; Ariki, N.; Kato, N.; Yoshinaga, J., Associations between levels of hydroxylated PCBs and PCBs in serum of pregnant women and blood thyroid hormone levels and body size of neonates. *Int J Hyg Environ Health* **2014**, *217*, (4-5), 546-53.
242. Londono, M.; Shimokawa, N.; Miyazaki, W.; Iwasaki, T.; Koibuchi, N., Hydroxylated PCB induces Ca<sup>2+</sup> oscillations and alterations of membrane potential in cultured cortical cells. *J Appl Toxicol* **2010**, *30*, (4), 334-42.
243. Wayman, G. A.; Bose, D. D.; Yang, D.; Lesiak, A.; Bruun, D.; Impey, S.; Ledoux, V.; Pessah, I. N.; Lein, P. J., PCB-95 modulates the calcium-dependent signaling pathway responsible for activity-dependent dendritic growth. *Environ Health Perspect* **2012**, *120*, (7), 1003-9.
244. Wayman, G. A.; Yang, D.; Bose, D. D.; Lesiak, A.; Ledoux, V.; Bruun, D.; Pessah, I. N.; Lein, P. J., PCB-95 promotes dendritic growth via ryanodine receptor-dependent mechanisms. *Environ Health Perspect* **2012**, *120*, (7), 997-1002.
245. Prasad, K. N.; Erika, C.; Susan, K.; Edwards-Prasad, J.; Curt, F.; Vernadakis, A., Establishment and Characterization of Immortalized Clonal Cell Lines from Fetal Rat Mesencephalic Tissue. *In Vitro Cellular & Developmental Biology. Animal* **1994**, *30A*, (9), 596-603.
246. Peng, J.; Mao, X. O.; Stevenson, F. F.; Hsu, M.; Andersen, J. K., The herbicide paraquat induces dopaminergic nigral apoptosis through sustained activation of the JNK pathway. *J Biol Chem* **2004**, *279*, (31), 32626-32.
247. Xie, H. R.; Hu, L. S.; Li, G. Y., SH-SY5Y human neuroblastoma cell line: in vitro cell model of dopaminergic neurons in Parkinson's disease. *Chinese medical journal* **2010**, *123*, (8), 1086-92.
248. Cheung, Y. T.; Lau, W. K.; Yu, M. S.; Lai, C. S.; Yeung, S. C.; So, K. F.; Chang, R. C., Effects of all-trans-retinoic acid on human SH-SY5Y neuroblastoma as in vitro model in neurotoxicity research. *Neurotoxicology* **2009**, *30*, (1), 127-35.
249. Lopes, F. M.; Schröder, R.; Júnior, M. L. C. d. F.; Zanotto-Filho, A.; Müller, C. B.; Pires, A. S.; Meurer, R. T.; Colpo, G. D.; Gelain, D. P.; Kapczinski, F.; Moreira, J. C. F.; Fernandes, M. d. C.; Klamt, F., Comparison between proliferative and neuron-like SH-SY5Y cells as an in vitro model for Parkinson disease studies. *Brain Res.* **2010**, *1337*, 85-94.
250. Westerink, W. M.; Schoonen, W. G., Phase II enzyme levels in HepG2 cells and cryopreserved primary human hepatocytes and their induction in HepG2 cells. *Toxicol In Vitro* **2007**, *21*, (8), 1592-602.
251. De, S.; Ghosh, S.; Chatterjee, R.; Chen, Y. Q.; Moses, L.; Kesari, A.; Hoffman, E. P.; Dutta, S. K., PCB congener specific oxidative stress response by microarray analysis using human liver cell line. *Environ Int* **2010**, *36*, (8), 907-17.

252. Ghosh, S.; De, S.; Chen, Y.; Sutton, D. C.; Ayorinde, F. O.; Dutta, S. K., Polychlorinated biphenyls (PCB-153) and (PCB-77) absorption in human liver (HepG2) and kidney (HK2) cells in vitro: PCB levels and cell death. *Environ Int* **2010**, *36*, (8), 893-900.
253. Berridge, M. V.; Herst, P. M.; Tan, A. S., Tetrazolium dyes as tools in cell biology: new insights into their cellular reduction. *Biotechnol Annu Rev* **2005**, *11*, 127-52.
254. Bergmeyer, H. U., *Methods of enzymatic analysis*. 2d English ed.; Verlag Chemie; Academic Press: Weinheim, New York, 1974; Vol. 3.
255. Cutler, R. W.; Deuel, R. K.; Barlow, C. F., Albumin exchange between plasma and cerebrospinal fluid. *Arch Neurol* **1967**, *17*, (3), 261-70.
256. Li, X.; Parkin, S.; Duffel, M. W.; Robertson, L. W.; Lehmler, H. J., An efficient approach to sulfate metabolites of polychlorinated biphenyls. *Environ. Int.* **2010**, *36*, (8), 843-8.
257. Lehmler, H. J.; Robertson, L. W., Synthesis of hydroxylated PCB metabolites with the Suzuki-coupling. *Chemosphere* **2001**, *45*, (8), 1119-27.
258. Lehmler, H. J.; He, X.; Li, X.; Duffel, M. W.; Parkin, S., Effective synthesis of sulfate metabolites of chlorinated phenols. *Chemosphere* **2013**, *93*, (9), 1965-71.
259. Costa, L. G.; Fattori, V.; Giordano, G.; Vitalone, A., An in vitro approach to assess the toxicity of certain food contaminants: methylmercury and polychlorinated biphenyls. *Toxicology* **2007**, *237*, (1-3), 65-76.
260. Eriksson, P.; Fredriksson, A., Developmental neurotoxicity of four ortho-substituted polychlorinated biphenyls in the neonatal mouse. *Environmental toxicology and pharmacology* **1996**, *1*, (3), 155-65.
261. Sudlow, G.; Birkett, D. J.; Wade, D. N., Spectroscopic techniques in the study of protein binding: the use of 1-anilino-8-naphthalenesulphonate as a fluorescent probe for the study of the binding of iophenoxic and iopanoic acids to human serum albumin. *Mol. Pharmacol.* **1973**, *9*, (5), 649-57.
262. van Meerloo, J.; Kaspers, G. J.; Cloos, J., Cell sensitivity assays: the MTT assay. *Methods Mol. Biol.* **2011**, *731*, 237-45.